plant designs with economic evaluations are available.[19,20] Moreover, three units of a coal-to-MeOH plant (the shift converter, acid-gas removal unit and MeOH converter) are fairly well-proven processes. Among the second-generation gasifiers, the Texaco gasifier is commercially proven and is in operation in several plants. Shell is building a 200-400 TPD of coal unit using a dry feed system to the gasifier. Other coal-gasification systems of interest have been reviewed.[21]

5.1-2I. Methanol and Higher Oxygenated Compounds as Fuels

Chemicals from MeOH, though now important, will probably be made from excess MeOH or SG manufactured primarily for fuel use. Methanol is used as a gasoline extender, as a neat fuel for automobiles, in the synthesis of methyl tert-butyl ether (MTBE) which is an octane extender, as a turbine fuel, and as a source of CO and H_2 for the synthesis of transportation fuel. Alcohols were used as transportation fuels in the early part of the 20th century until cheap gasoline made its appearance. BY 1937, some 70,000 tons of synthetic MeOH were used in vehicles in Germany. Methanol has been and still is used in racing cars because of increased power obtainable compared to gasoline. Blends of ethanol in gasoline have been in commercial use in Cuba, South Africa and South America for some years. A number of surveys and reviews have been published on the use of alcohols as automotive fuels.[22-25]

Europe's dependence on imported petroleum, coupled with the 1973 embargo, led Germany to sponsor a comprehensive study on the use of MeOH and H_2 as fuels. Studies on MeOH as an additive to gasoline have continued since 1975, often with US government support.[26] In 1976, the Swedish Methanol Development Co. sponsored the first international meeting on MeOH at the Royal Swedish Academy.[27] Methanol may ultimately be made from remote sources of NG, from coal, and eventually from renewable resources.

Electric utilities have been interested in MeOH as a fuel on a large scale for peak loads in turbines. Methanol and ethanol are already in use as gasoline additives. The use of neat MeOH will probably be limited initially to fleets in selected regions; hundreds of cars are being tested on neat MeOH in California. Gasohol, a blend of 10% ethanol and 90% gasoline, has been used in Nebraska for many years and has been sold

throughout the US. Over a million cars are fueled by neat ethanol or 10 to 20% ethanol-gasoline mixtures in Brazil.

Methanol differs from a typical gasoline component such as isooctane in that it is a polar molecule with oxygen constituting half of its weight; it thus picks up water easily. It is an attractive gasoline additive. It has a higher octane rating than isooctane and is manufactured all over the world from SG that is obtainable from almost any organic resource. Phase separation (caused by water pick-up), possible corrosion of some engine parts and volatility considerations rule out the use of straight MeOH or gasoline mixed with large amounts of MeOH (>5%), except for cars that are specially built for use of these fuels. Arco received EPA approval for a MeOH plus cosolvent mixture with gasoline and sold the product in parts of New York State and in Pennsylvania until about 1985. Arco's additive consisted of 4.75% MeOH and 4.75% TBA (tert-butyl alcohol) in 90.5% unleaded gasoline. Blending 5% MeOH and 5% cosolvent into all gasoline used in the US could reduce crude oil imports by over 200 million BPY. However, no suitable distribution system exists for such a blend.

Two other points are pertinent. Emissions from the MEOH-cosolvent-gasoline blends are lower than from straight gasoline. Also, the cosolvent is not limited to TBA; other alcohols and ethers may be used as cosolvents.

It is possible that MeOH-gasoline blends will serve as a bridge between straight gasoline and straight MeOH. EPA has lowered the allowable addition of tetraethyllead to gasoline to 0.1 gram per gallon; octane enhancement by added alcohols and ethers may therefore become necessary to retain octane ratings.

But the MeOH-gasoline blending picture is complex. It has been stated[28] that coal-based processes for the synthesis of MeOH will eventually win out but NG will have the edge for a long time to come.

A rapidly growing use of MeOH as a fuel is in the synthesis of methyl tert-butyl ether (MTBE). This ether was approved by EPA in 1979 as an octane enhancer for unleaded gasoline at concentrations of 7% or less by volume. MTBE capacity in the US grew from zero in 1970 to 2.18 million metric tons in 1985 and its projected growth seems to be limited only by the availability of isobutene.

The MTBE-gasoline blend provides a number of advantages over

MeOH-gasoline blends. It has a lower oxygen content, less severe water separation problems, fewer front-end volatility effects, and also has a high octane quality. In addition, MTBE is useable in all proportions with gasoline. it is, however, more expensive than MeOH as a gasoline extender.

Methanol as a fuel in stationary combustion turbines for peak loads of electric utilities has often been mentioned. Large amounts of a reliable source of the alcohol would be needed to avoid the possibility of brownouts. Crude oil prices must eventually rise and, when they do, MeOH potential as a fuel may be realized.

Methanol is an excellent gas-turbine fuel, although it may be necessary to modify turbines somewhat. The sodium content of the fuel in a gas turbine should be kept below 1 ppm. MeOH readily picks up water and the water could be contaminated with alkali slats. On the other hand, MeOH as a gas-turbine fuel has low pollutant emissions, good performance and good handling and storage properties. In any case, supply and cost are the main factors which will influence the introduction of MeOH as a turbine fuel.

5.1-2J. Dissociated Methanol as a Fuel For Automobiles and Gas Turbines

It is well known that MeOH dissociates into CO and H_2 as the temperature is raised and the pressure is lowered according to the process

$$CH_3OH \underset{\text{high p, low T}}{\overset{\text{low p, high T}}{\rightleftharpoons}} 2H_2 + CO \ . \qquad (5.1\text{-}8)$$

At equilibrium, over 80% of the MeOH is dissociated at 1MPa and 473K. For this reason, the MeOH-combustion characteristics are similar to those of SG. The major difference in properties is caused by the heat of dissociation of MeOH, which is 90.56 kJ/mol at 298K and 1 atm for the gas (13.4% of the LHV) and 128.5 kJ/mol at 298K for liquid MeOH (20.1% of the LHV). It is possible, however, that a significant amount of exhaust heat used to evaporate and dissociate MeOH may be recovered and this is what is generally counted on in automotive use.

Dissociated MeOH may offer higher efficiencies than conventional liquid fuels for three reasons: (i) the just noted waste heat recovery, (ii) extended lean misfire limits, and (iii) higher allowable compression ratios. Also, exhaust emissions are lower. At 573K, a temperature which matches the available heat in an engine exhaust, equilibrium favors 99.9% conversion of MeOH to CO and H_2, although side reactions can occur. A

number of catalysts, including Pt, Pd, Cu, Zn, etc. are known to be active in the dissociation of MeOH.

The application of MeOH dissociation in combustion turbines has been discussed by Finegold et al.[29] Woodley et al.[30] have compared some advantages of burning liquid MeOH, dissociated MeOH, and steam-reformed MeOH.

5.1-2K. Ethanol as a Transportation Fuel

Methanol is toxic to humans. Ethanol (CH_3CH_2OH) is somewhat less polar than MeOH but the additional CH_2 group converts it into a beverage made and consumed in a great variety of forms all over the world. The CH_2 group also greatly influences the properties of ethanol as a transportation fuel. Ethanol is more HC-like than MeOH and is therefore more soluble in gasoline. Ethanol has a higher boiling point than MeOH (351.3 vs 337.7K), while their specific gravities are essentially the same. The oxygen atom in MeOH comprises half of its molecular weight, whereas, in ethanol, only 34.7% of the molecular weight of the molecule is due to oxygen; ethanol is thus less hygroscopic. The LHV of MeOH is 56,560 BTU/gallon (8,600 BTU/lb); that for ethanol is considerably higher, 75,670 BTU/gallon (11,500 BTU/lb). Both have excellent research octane ratings (106-108). The chemical and physical properties of ethanol make it a better gasoline extender.

The manufacture of ethanol has an interesting history, one that is presently changing rapidly. Ethanol for human consumption has been made by the fermentation of naturally occurring carbohydrates since prehistoric times. Such ethanol is still made by fermentation.

The first synthetic ethanol for industrial use was produced about 1930 in the US. It involved the hydration of ethylene with water in the presence of an acid catalyst. From almost complete dependence on fermentation processes until the late 1920s, over 95% of ethanol for industrial consumption was made synthetically from ethylene in the 1970s. But, with the growing use of ethanol in transportation fuels initiated as a result of the 1973 oil embargo, the production ration of fermentation ethanol to synthetic ethanol grew rapidly.

The use of alcohol fuels has been studied for many years in a number of countries. In 1907, for instance, the US Department of

Agriculture published a report on the use of alcohol-gasoline mixtures in farm engines.[31] Interest in grain alcohol was given impetus by the oil embargo in 1974. Since then, a great deal of work has been focused on the use of ethanol as a gasoline extender, octane enhancer or as an alternative fuel. There are many studies dealing with engine performance, emission characteristics and the advantages and problems associated with ethanol use in conventional spark-ignition engines.[32] US production of fermentation alcohol for fuel use was about 80 million gallons in 1979. A year later, production of ethanol by fermentation neared 300 million gallons, with production by fermentation continuing to grow. Gasohol and neat ethanol are now used in many countries, especially Brazil.

Ethanol from the fermentation of grain has been made competitive as a transportation fuel in the US largely because of federal and state subsidies aimed at reducing US dependence on imported oil. It is possible that US. production of fermentation alcohol may rise to about a billion gallons by 1990 and may then invade the industrial market of more than 200 million gallons.

Since this study deals with the use of SG, we shall not further explore the production of fermentation alcohol. We note, however, the important question as to the economic viability of using arable land for the production of fuel rather than food.

5.1-2L. Ethanol from SG

What are the possibilities of obtaining ethanol and higher alcohols directly from SG? This conversion would seem to be highly desirable because it would eliminate the need for subsidies and return some land for other uses. In the long run, ethanol from SG may be cheaper than fermentation alcohol and be independent of ethylene made from (imported) petroleum. Ethanol and higher alcohols are better energy-storage chemicals and are less toxic and corrosive than MeOH.

Ethanol and other C_2-oxygenated compounds have been synthesized directly from SG using modified FT catalysts. Ichikawa[33] studied rhodium catalysts on several moderately acidic oxides such as La_2O_3, TiO_2, CeO_2, and ZrO_2 as supports. He obtained large yields of ethanol and other C_2

oxygenated compounds such as acetaldehyde and some acetates. A heterogeneous catalyst prepared from $Rh_4(CO)_{12}$-La_2O_3 catalysts yielded, using 1 atm of SG at 473K, the following product distribution based on carbon efficiency (%): CH_3OH, 10; CH_3CH_2OH, 49; CH_3CHO + CH_3Coor, 2; CH_4, 14; C_2-C_4, 6; CO_2 + other products, 8.

This is a lucrative field for further investigation. A synthesis of ethanol directly for SG with over 90% selectivity would be a great step forward in the manufacture of transportation fuels and chemicals directly from SG.

5.1-2M. The Homologation of Methanol to Ethanol

The homologation or reductive carbonylation of MeOH to yield ethanol plus acetaldehyde and acetates has been extensively studied but has not yet been commercialized. Homogeneous transition metals have been used as catalysts[34,35] in the process

$$CH_3OH + 2H_2 + CO \xrightarrow[RuCl_3,I_2]{Co_2(CO)_8} CH_3CH_2OH + H_2O \; . \qquad (5.1\text{-}9)$$

While the methanation of MeOH is the most thermodynamically favored reaction at 298K and 0.1MPa, the formation of ethanol is almost as favorable. At higher temperatures, ethanol and CH_3CHO become less favored at the expense of dimenthyl ether and CO_2. The synthesis of ethanol is thermodynamically more strongly favored as the pressure is raised to 10MPa. The principal problem is kinetic control over the number of possible reaction products (CH_4, acetates, acetic acid, dimethyl ether, acetals, and CO_2).

Cobalt complexes were used first and are good catalysts in their activity and selectivity for the conversion of MeOH and SG to ethanol and CH_3CHO. Rhodium, usually more active than cobalt in homogeneously catalyzed reactions involving MeOH and SG, produces acids and esters, with ethanol a significant product at high H_2 partial pressures (H_2/CO = 40:1).

Operating temperatures in the 450-485K range are usually used with cobalt. As the temperature rises, selectivity to ethanol increases at the expense of acetaldehyde. A rise in pressure increases conversion of MeOH while product selectivity also remains constant. At high CO partial

pressures, the competing alcohol carbonylation dominates and over 70% selectivity to methyl acetate is observed. At high H_2 partial pressures, the catalyst tends to decompose to metal with an accompanying loss of MeOH to CH_4 and dimethyl ether. The highest ethanol selectivity is obtained at H_2/CO ratios of 1:1.

The most significant discovery in MeOH homologation has been the rate of enhancement associated with addition of iodine or iodide. This enhancement arises mostly from the <u>in situ</u> formation of CH_3I, which reacts with SG much faster than does MeOH. By the use of cocatalysts, a selectivity to acetaldehyde above 60% can be obtained at 68% conversion. For the production of ethanol, ruthenium has been found to be the best cocatalyst since all of the aldehyde is hydrogenated to ethanol. As an example, the use of cobalt acetate, I_2, $RuCl_3$, and PPh_3 at 450K and 27.2MPa converts 43% of MeOH to ethanol with a selectivity of 80%.[36,37] The addition of tertiary phosphine ligands to the catalyst has two desirable effects: greater catalyst stability and enhanced ethanol selectivity.

In conclusion, the cobalt-carbonyl-catalyzed reductive carbonylation of MeOH with SG to produce acetaldehyde, ethanol and acetates is a complicated system which allows a remarkable high degree of kinetic control over the thermodynamically favored product mixture; however, selectivities to ethanol of 80% are rare. While the chemical reactions and promoter effects are fairly well understood, it is difficult to see how the system can be perturbed to furnish higher activities or selectivities approaching the carbonylation of MeOH, for which over 99% selectivity to acetic acid is achieved. The diverse mixture of products coupled with low activity make MeOH reductive carbonylation an unlikely source of ethanol. A possible use of the product mixture is as a fuel blend.

Chen et al.[38] have shown that iron or ruthenium, promoted by a tertiary amine, catalyze the homologation of MeOH to ethanol at SG pressures near 30MPa and temperatures of about 475K. Carbon dioxide rather than water is the by-product and no alcohols higher than ethanol are formed, nor are acetates or acetals produced ($CH_3OH + H_2 + 2CO \longrightarrow 2CH_3CH_2OH + CO_2$). This reaction calls for further study, although reaction rates appear to be somewhat low.

5.1-2N. The Synthesis of Higher Alcohols

In 1923, Fischer and Tropsch[2,39] used alkalized iron catalysts to obtain mostly oxygenated products from SG; they called this the Synthol process. It was carried out at 460 to 500K and 2MPa and the product contained up to 70wt% of alcohols with carbon numbers up to C_{20}. The aim at the time, however, was to obtain HCs by the hydrogenation of CO. In 1953, Anderson[39] found that iron nitrides were durable, unique catalysts for the FT synthesis, yielding about 40wt% of alcohols.

It has long been known that MeOH-synthesis catalysts promoted with alkali and containing up to three metal oxides yielded higher alcohols [1-propanol and 2-methyl-1-propanol (isobutanol)] together with the expected MeOH. The catalysts for this synthesis generally operated at about 675 and 20MPa and lower space velocities than are employed for the usual MeOH synthesis. Cesium, rubidium and potassium were the most active promoters, with potassium obviously the most practical promoter.

Although the higher alcohols (C_1-C_6 especially) are desirable products for fuel use, there has been a paucity of studies dealing with the quantitative aspects of the kinetics and selectivity for these promoted MeOH catalysts which did not contain copper. The effect of promoting the more active, low-pressure, Cu/ZnO MeOH-synthesis catalysts has been reported mostly in the patent literature.

Work has lately begun to center on the use of MeOH-synthesis catalysts combined with FT catalysts, often in the presence of alkali. Courty et al.[40] at the Institut Francais du Petrole (IFP) have been studying the synthesis of higher alcohols. IFP and Japan's Idemitsu Kosan, both members of RAPAD (Research Association for Petroleum Alternative Development), have been working on syntheses of higher alcohols. Mixed alcohols of up to 30wt% of C_2 and higher alcohols have been produced using alkalinized zinc and chromium oxides. Using copper-cobalt catalysts, up to 70wt% of heavier alcohols were obtained at moderate conditions. Copper, cobalt, zinc, aluminum, and sodium oxides have been used, as well as copper, cobalt, chromium, and mixed alkali oxides.

The Idemitsu Kosan Company has built a 7000 BPD demonstration plant in Japan based on IFP's design.[41] First runs confirmed bench-scale

tests, with C_1-C_6 alcohols forming more than 99% of the product. The alcohol mixture appears to resemble tert-butyl alcohol as far as compatibility with gasoline is concerned.

The reduced cobalt probably acts as an FT catalyst, dissociating CO to furnish the alkyl part of the alcohols, while the action of the copper resembles its role in MeOH synthesis. Work is proceeding on understanding the mechanisms involved in these complex catalytic reactions. The procedures used in their preparation are critical, especially to avoid FT active catalysts which would yield HCs.

5.1-3. SG as a Source of Chemicals

Of the thirty top organic chemicals (in terms of weight) manufactured in the US in 1985, all but seven are or can be produced from SG.[42] Several of these are also used as fuels. SG is composed of various ratios of H_2 and CO.

The largest use of SG in the world is in the manufacture of molecular hydrogen, and most of the H_2 used worldwide is made from SG.

5.1-3A. H_2 Manufacture

Hydrogen can be separated cryoscopically or chemically from SG. The CO is SG is usually converted to an equivalent amount of H_2 via the water gas shift (WGS) reaction

$$CO + H_2O \longrightarrow H_2 + CO_2 \ . \qquad (5.1\text{-}10)$$

Hydrogen is used above all for the manufacture of ammonia:

$$N_2 + 3H_2 \xrightarrow[200 \quad 350 \text{ atm}]{Fe_2O_3} 2NH_3 \ . \qquad (5.1\text{-}11)$$
$$400 \quad 500^{\circ}C$$

As was stated earlier, about 5 trillion SCF of SG are used worldwide in NH_3 synthesis.

Hydrogen has many other uses and there is no doubt that the demand for this chemical will grow. It is employed in numerous hydrogenation reactions to saturate aromatics or other molecules containing double bonds. It is used in hydrocracking heavy oils, in hydrodealkylation reactions, hydrorefining, hydrodesulphurization reactions, etc. Hydrogen is used to upgrade petroleum residua, which constitute a growing part of the petroleum barrel. Synthetic fuels, when and if they are produced, will consume enormous amount of H_2, essentially all of which well be derived from SG.

5.1-3B CO Manufacture

CO is isolated from SG by cryogenic liquefaction or by selective absorption in cuprous ammonium salt solutions. Reactions involving the addition of CO to another molecule are called carbonylation reactions; those involving the reaction of both CO and H_2 (SG) with another chemical are called reductive carbonylations; those involving oxygen and CO are called oxidative carbonylations. These terms are helpful in describing the many reactions of SG, especially the conversion of MeOH to various chemicals.

5.1-3C. Methanol as a Chemical, Chemical Precursor and Fuel

In 1980, of the trillion SCF of SG used in the synthesis of MeOH, NG feedstock accounted for 75% of US and 70% of worldwide MeOH capacity. Methanol made from residual fuel oil accounted for about 15% of domestic and worldwide MeOH, naphtha was used to produce 5%, and coal was the raw material for under 2% of worldwide production. Methanol promises to continue to be not only one of many feedstock chemicals in the future but also an extensively used clean fuel. It is the precursor to a large and growing number of important organic chemicals that have significant uses. Historically, almost half of all MeOH produced has been converted to formaldehyde (HCHO), which is a precursor to a number of chemicals. In the future, formaldehyde will lose this position because of MeOH use in the production of faster growing chemicals (acetic acid, acetic anhydride, methyl-t-butyl ether, etc.). Methanol conversion to gasoline, olefins and

aromatics via Mobil's MTG process will account for increasing use of this compound.

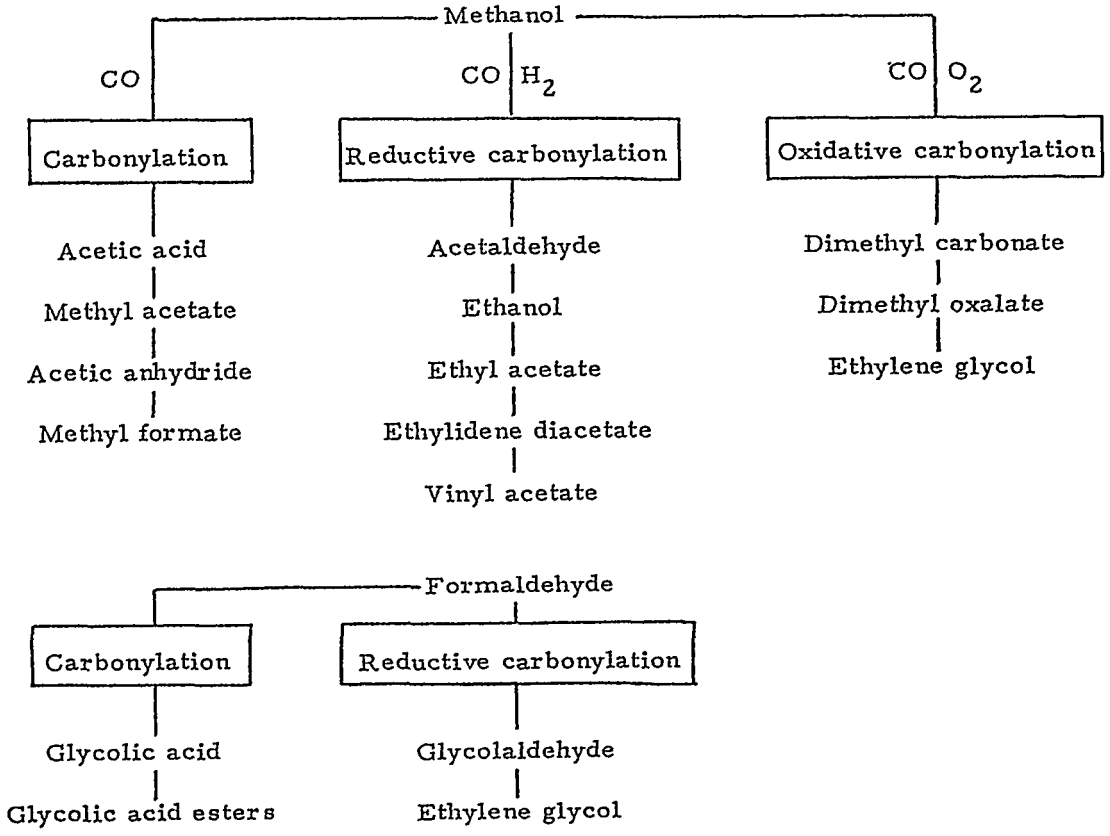

Fig. 5.1-4. Scope of methanol-syngas chemistry.

Chemicals made from MeOH can be divided into two classes: those now made commercially and those that are emerging commercial processes. The former include formaldehyde, methyl formate, formic acid, acetic acid, methyl acetate, chlorinated methanes, methylamines, dimethyl acetate, vinyl acetate, ethylene glycol, styrene, and dimethyl terephthalate. The scope of MeOH-SG chemistry is indicated in Fig. 5.1-4.

5.1-3D Formaldehyde (HCHO)

Formaldehyde is made from MeOH by dehydrogenation in the presence of Ag or Cu catalysts or by oxidation of MeOH in the presence of

iron-containing MoO_3 catalysts. Apart from direct applications of aqueous HCHO solutions (formalin), e.g., as a disinfectant and preservative and in the textile, leather, fur, and paper and wood industries, most HCHO is used for the manufacture of resins with phenols, urea and melamine. A number of other chemicals are made commercially from HCHO, including polyhydric alcohols, butynediol, isoprene, and β-propiolactone.

5.1-3.E. Acetic Acid (CH_3COOH)

About 3 billion pounds of this important chemical were produced in the US in 1985. As late as 1973, about 40% of the acetic acid capacity was made by oxidation of the acetaldehyde produced via the Wacker process, which was based on the oxidation of ethylene. All processes for the production of acetic acid have been or are being steadily replaced by processes based on the carbonylation of MeOH, so that SG rather than ethylene or other HCs is now the raw material of choice for acetic acid manufacture.

In 1960, BASF introduced the carbonylation of MeOH to acetic acid using a cobalt catalyst in 180°C and 3,000 to 10,000 psig: $CH_3OH + CO \longrightarrow CH_3COOH$. In 1976, two plants based on this technology were built in the FRG (35,000 TPY) and in the US (52,000 TPY), but then a new process took over. In the mid-sixties, the Monsanto Co. discovered that rhodium plus iodine was a considerably more active catalytic system for MeOH carbonylation than cobalt. In this process, MeOH and CO react in the liquid phase at 150-200°C at pressures below 500psi to form acetic acid with selectivities of over 99% (based on CH_3OH) and over 90% (based on CO). In 1970, the first industrial plant went on-stream in Texas City; its capacity was 150,000 TPY of acetic acid. The rhodium-catalyzed carbonylation of MeOH to acetic acid is the process of choice and all new plants will use this process with SG as the only raw material used.

Vinyl acetate is the principal outlet for acetic acid in the US (40wt%). Half as much goes into making cellulose acetate (22%). Another 10% is used in the production of butyl and isopropyl acetates, acetyl chloride and acetamide. There are many other growing uses for the cheap acetic acid produce by the carbonylation of MeOH.

In 1984, the Tennessee Eastman Co. started up the first integrated facility for the production of chemicals from coal at Kingsport, TN (Fig. 5.1-3). About 900 TPD of the high-sulfur bituminous coal are ground in

water to form a slurry of 55 to 65wt% by weight of the coal in water. The coal contains from 12 to 15 wt% of mineral matter. The slurry is fed to two Texaco gasifiers, each gasifying 200 gallons per minute of slurry. Each gasifier can provide all of the SG needed for the plant. The plant will produce about 500 million pounds per year of acetic anhydride.

The complex contains eleven separate units, four involved in the gasification of coal, four for SG preparation or by-product recover, and three of the synthesis of MeOH, methyl acetate and acetic anhydride. The reactions involved are:

$$2H_2 + CO \xrightarrow{Cu\text{-}ZnO} CH_3OH \quad , \qquad (5.1\text{-}12)$$

$$CH_3OH + CO \xrightarrow{Rh} CH_3COOH \text{ (acetic acid)} \qquad (5.1\text{-}13)$$

$$CH_3OH + CH_3COOH \xrightarrow{H^+} CH_3\overset{O}{\overset{\|}{C}}CH_3 + H_2O \quad , \qquad (5.1\text{-}14)$$

(methyl acetate)

$$CH_3\overset{O}{\overset{\|}{C}}CH_3 + CO \xrightarrow{Rh + I_2} (CH_3\overset{O}{\overset{\|}{C}})_2O \text{ (acetic anyhydride)} \quad , \qquad (5.1\text{-}15)$$

$$(CH_3\overset{O}{\overset{\|}{C}})_2O + \text{cellulose} \longrightarrow \text{cellulose acetate} + CH_3COOH \quad . \qquad (5.1\text{-}16)$$

(recycled)

All of these reactions, except for reaction (5.1-15), are known commercial reactions. A number of new catalytic systems for the conversion of methyl acetate to acetic anhydride have been developed by Tennessee Eastman and some were developed by Hancon International. Patents for this conversion have been obtained by Halcon, Hoechst, Ajinomoto, and Showa Denkon using rhodium as the catalyst. Halcon and Mitsubishi Gas Chemical Co. have also been granted patents for the use of a less expensive nickel catalyst for this conversion. It is probably that acetic anhydride is similar to MeOH carbonylation to acetic acid.

Eastman views this project as currently economically viable. Eastman's location near substantial reserves of high-grade coal is a

positive factor. It is possible that Eastman stands to be the first company to develop a whole series of important oxygenated chemicals from coal-derived SG.

5.1-3F. Methyl Formate, Formamide, and Formic Acid (HCOOH)

These chemicals are also made from MeOH and CO but in the presence of a base catalyst rather than a transition-metal catalyst. The reactions are

$$CH_3OH + CO \xrightarrow[343^{\circ}C,\ 2\text{-}20MPa]{NaOCH_3} HCOOCH_3 \text{ (methyl formate)} , \qquad (5.1\text{-}17)$$

$$HCOOCH_3 \xrightarrow{NH_3} HCONH_2 \text{ (formamide)} + CH_3OH , \qquad (5.1\text{-}18)$$

$$HCONH_2 \xrightarrow{H_2SO_4} (NH_4)_2SO_4 + HCOOH \text{ (formic acid)} \qquad (5.1\text{-}19)$$

World production of formic acid is about 100,000 TPY.

5.1-4. Fischer-Tropsch Synthesis

5.1-4A. Catalysts and Chemistry of FT Syntheses

The Fischer-Tropsch (FT) synthesis was first put into commercial operation by Viktor-Rauxel in 1935.[43] Numerous FT catalysts have been discovered since then. Of these, Fe, Co, Ru, and ThO_2 are of special interest. Both Fe and Co were used in commercial applications, but only Fe is employed at the SASOL plant in South Africa since it is inexpensive and allows versatile applications.

The catalysts Fe and Co are used at moderate pressure (up to about 450 psig) to produce paraffins and olefins. Iron catalysts generally produce large amounts of olefins and some oxygenates. Ruthenium and ThO_2 catalysts are used at high pressure (up to 14,000 psig). The Ru catalysts

are applied in paraffin wax production, while ThO_2 catalysts are used to make isoparaffins. During the early period of FT process development, Ni catalysts were also employed. They are predominantly utilized for methanation and are not suitable for liquid-fuel synthesis. The enhanced water gas shift (WGS) activity is also an important function of FT catalysts. Iron is well-known for its WGS activity, while neither Co nor Ru has WGS activity.[44]

The performance of FT catalysts depends strongly on other factors such as the promoters and supports, preparation and activation method, and reactor design. With few exceptions, all catalysts are sensitive to sulfur poisoning. A major exception is the sulfur-tolerant Mo-based catalyst developed by Dow,[45] which is mainly used to produce light paraffins. The following discussions are limited to Co and Fe catalysts.

Cobalt catalysts were first used for commercial FT operation but were later replaced by Fe because of the low cast and utility of the latter. A 100Co/18ThO_2/100kieselguhr catalyst was first used in an atmospheric-pressure direct heat-exchange reactor at Oberhausen-Holten, Germany, in 1936. A 100Co/5ThO_2/7.5MgO/200 kieselguhr was used later in a medium-pressure (100-150 psig), direct heat-exchange reactor.

The first commercial Fe catalyst was used in a medium-pressure, fixed, fluidized-bed reactor in the Hydrocol Process at Brownsville, TX, in 1950. Today, Fe is the only catalyst used in large-scale operation at SASOL. The catalysts can be made into various forms that match the different reactor types and different process conditions needed to make various product distributions. The following Fe catalysts are of special interest: (i) supported precipitated Fe promoted with Cu and K (direct heat-exchange reactor, Arge Process at SASOL I), (ii) fused Fe promoted with alkali and other proprietary promoters (entrained fluidized-bed reactor, Synthol process at SASOL I, II, and III), (iii) fused Fe promoted with 1wt% K_2CO_3 (fixed fluidized-bed reactor, Hydrocol process), (iv) unsupported, precipitated Fe promoted with Cu and K (slurry reactor), and (v) nitrided Fe catalyst developed by the US Bureau of Mines. Alkali components, usually K_2CO_3, are the most important promoters for the Fe compounds. Another common promoter is Cu, which supposedly promotes the reduction of Fe_2O_3 to active Fe and iron carbides.[46] Many other promoters have been proposed.

The products from FT reactions are HCs (mainly n-paraffins, terminal 2-methyl-branched-isoparaffins, and α-olefins) and oxygenates (mainly primary alcohols). The chemical reactions may be represented as follows:

$$(2n+1)H_2 + nCO \longrightarrow C_nH_{2n+2} + nH_2O \ , \qquad (5.1\text{-}20)$$

$$2nH_2 + nCO \longrightarrow C_nH_{2n} + nH_2O \ , \qquad (5.1\text{-}21)$$

$$2nH_2 + nCO \longrightarrow C_nH_{2n+1}OH + (n-1)H_2O \ . \qquad (5.1\text{-}22)$$

These reactions imply a minimum H_2/CO use ratio of 2 and an average use ratio slightly larger than 2, depending on the product distribution. For catalysts that promote the WGS reaction, the H_2O formed during FT reactions can react further with the CO to form H_2 according to reaction (5.1-10). At FT reaction temperatures (200-350°C), chemical equilibrium strongly favors H_2 formation. Consequently, as long as the catalyst has sufficient WGS activity, the apparent H_2/CO use ratio becomes much smaller, except for MeOH-synthesis. The minimum H_2/CO usage ratio is 0.5 for olefin formation and the maximum is 1.0 for CH_4 and ethanol formation.

The HCs and alcohols produced by FT reactions have a very wide carbon number distribution. This distribution is generally determined by the chain-growth probability mechanism, which is frequently used in describing polymerization.[47] The distribution is

$$\log(M_i/I) = \log(\ell n^2\alpha) + I(\log \alpha) \ , \qquad (5.1\text{-}23)$$

where M_i is the weight fraction of the I carbon number HC and α the probability of chain growth. A plot of $\log(M_i/I)$ vs carbon number yields $\log(\alpha)$ as the slope and $\log(\ell n^2\alpha)$ as the intersection. With a higher value of α, heavier components are produced. A Schulz-Flory distribution also implies that the heavier compounds are produced in reduced molar quantity.

A limited treatment on the thermodynamics of FT reactions has been given by Kuo,[1] while a thorough treatment may be found in Storch et al.[43] All FT reactions are highly exothermic. The heats of reaction range from 8

to 12 kJ/g-HC, excluding CH_4 and MeOH formation. Equilibrium H_2+CO conversion calculations show that high single-pass conversion may be achieved if the H_2/CO ratio in the feed gas matches the usage ratio. The equilibrium conversion at 250°C and 145 psig ranges from 94 to 99mol%, excluding CH_4, ethane and MeOH formation. The conversion decreases with increasing temperature and paraffin carbon number and also with decreasing olefin and oxygenate carbon numbers.

Low CH_4 and ethane formation are very often emphasized in FT syntheses when liquid fuels are made. Since CH_4 and ethane are thermodynamically more stable than other FT compounds, low CH_4 and ethane yields can only be achieved by careful selection of catalysts and process conditions. Iron catalysts yield less CH_4 and ethane than other FT catalysts. Proper use of alkali promoters will further reduce this yield. In terms of process conditions, low CH_4 and ethane yields may be achieved by low temperatures and H_2/CO ratios and by high pressures.

Carbon formation is an important factor that affects FT catalyst performance. It is described by the following two reactions:

$$2CO \longrightarrow C + CO_2 \ , \ \Delta H(250^{\circ}C) = -174kJ \ ; \qquad (5.1\text{-}24)$$

$$CO + H_2 \longrightarrow C + H_2O \ , \ \Delta H(250^{\circ}C) = -134kJ \ . \qquad (5.1\text{-}25)$$

The first process is the Boudouard reaction and may be more important than the second reaction in carbon formation. Generally speaking, carbon formation is expected to increase drastically with temperature and CO partial pressure. Dry[48] has given an excellent review of carbon deposition on Fe catalysts. Extensive experimental work at SASOL led to the conclusion that there was a strong relation between the carbon formation rate and the value of p_{CO}/p_{H_2} at the reactor entrance on a fused Fe catalyst.[49] In an earlier study,[50] the activation energy of the Boudouard reaction for a fused Fe catalyst was found to be 113kJ/mol, which is much greater than that for the FT reaction.

Mechanisms for FT reactions have attracted substantial scientific interest. Many mechanisms have been proposed including: (i) carbide by Fischer and Tropsch;[51] (ii) hydroxycarbene by Storch et al.;[43] (iii)

carbonium by Roginsky;[52] (iv) carbonyl by Pichler and Schulz.[53] The details of these mechanisms are not discussed here. However, they all contain the concept of chain growth and termination as in polymerization. Among these mechanisms, the carbide and hydroxycarbene mechanisms seem to give the best descriptions of experimental data. However, none of the other mechanism is firmly excluded.

FT kinetics is another area of great interest, although it is not well understood. Complications arise because of the many catalyst variables, such as composition, support, preparation activation, and aging. An excellent review of this work has been given by Storch et al,[43] while Kuo[1] provides a bried summary of the various forms of proposed kinetic expressions for catalysts, including Co, fused-Fe, and precipitated-Fe.

5.1-4B. Commercial Fischer-Tropsch Processes

For FT reactions, removal of the large exothermic heat is a major problem in commercial reactor designs. Heat removal is essential in order to maintain good temperature control and, hence, catalyst stability and product selectivity. Three types of reactors have been used in commercial application: fixed fluidized-beds, direct heat-exchange reactors and entrained fluidized-beds. The fixed fluidized-bed reactor was used in the Hydrocol process (Hydrocarbon Research Inc.).[54,55] The plant used NG feed and was erected at Brownsville, TX, in 1950. The reactor was 5m in diameter and had about a 100 m^3 volume holding 150-180 Mg of catalyst (with 80% in the size range 43-165μm). It also contained bundles of vertical water-cooling tubes to remove reaction heat. The reactor had the operating parameters listed in Table 5.1-1. The plant was shut down in 1957 because of the abundance of low-priced crude and never reached design capacity.

Three different designs of direct heat-exchange reactors have been used. All use the principle of keeping the catalyst close to a cooling surface in order to control catalyst temperature. Only one is still in operation today (at SASOL I). It is called the Arge Reactor and was developed by Lurgi and Ruhrchemie. The reactor is 2.9m in diameter and contains 2,052 tubes with 4.6cm id and a 12m catalyst-bed height. Reaction heat is removed by steam generation on the shell side. The average

performance of this reactor is summarized in Table 5.1-2. It has an HC capacity of about 18,000 Mg/year.

The other two designs of direct heat-exchange reactors are only of historical value. They were used in atmospheric and medium-pressure syntheses with Co catalysts during the 1930s.[54] The atmospheric pressure unit was 4.6m long, 2.4m high, and 1.8m wide and consisted of 555 laminated plates with cooling tubes penetrating the bundle perpendicular to the plates. The distance between the plates was about 7.4mm and the catalysts were loaded between the plates. The capacity of the reactor was small (nominally, 1 km^3/hr of synthesis gas). The medium-pressure unit consisted of 2,040 double tubes (2.5 and 4.8cm diameter), 4.6m in length. The catalysts were loaded in the annulus and the cooling water was circulated inside the inner tube and outside the outer tube for heat removal. Reactor capacity was comparable to that of the normal pressure unit.

Table 5.1-1. Operating parameters of the fixed fluidized-bed reactor used in the Hydrocol process.

Parameters	Numerical values
T, °C	300-350
p, psia	375-450
Molar H_2/CO ratio	1.8-2.1
Molar recycle ratio	2
C_3^+ yield, g/m^3 (H_2+CO)	165
H_2+CO conversion, %	90-95

The entrained fludized-bed reactor is the most important FT reactor used today (in SASOL I, II, and III) and is now identified as the SASOL Synthol Reactor. Figure 5.1-5 illustrates the major features of the reactor while Table 5.1-2 summarizes typical operating conditions and product selectivities for SASOL I and II. SASOL III is a duplicate of SASOL II. The difference in the product selectivities between the Synthol and Arge reactors is clearly shown. Then Synthol reactor generally produces more light HCs, gasoline, and oxygenates. The HCs are also more olefinic and contain fewer n-paraffins. The combined fresh feed and recycle gas is heated immediately to the reaction temperature (315°C) by the returning hot catalyst. The reaction heat is removed in the intercoolers located in the reactor section. There are two versions of the intercooler. The older version uses tube bundles with cooling oil on the shell-side. This method causes occasional catalyst plugging on the tube-side. The newer version uses serpentine coils placed vertically up and down in the reactor section as intercoolers. The entrained catalyst exits from the reactor section at about 340°C. SASOL II reactors use the new intercooler and have about two and a half times the capacity of the SASOL I reactor.

Table 5.1-2. The SASOL Fischer-Tropsch reactors.[56-59]

Operating conditions and product selectivity (wt%)	SASOL I		SASOL II
	Arge	Synthol	Synthol
Catalyst, alkali promoted Fe	Precipitated	Fused	Fused
Catalyst circulation rate, Mg/hr	0	8000	N.A.
T, °C	220-255	315	320
p, MPa	2.5-2.6	2.3-2.4	2.2
Fresh feed H_2/CO, molar	1.7-2.5	2.4-2.8	N.A.
Recycle ratio, molar	1.5-2.5	2.0-3.0	N.A.
H_2 + CO conversion, mol%	60-68	79-85	N.A.
Fresh feed, Nkm^3/hr	20-28	70-125	300-350
Diameter × height, m	3×17	2.2×36	3×75
C_1	5.0	10.0	11.0
$C_2^=$	0.2	4.0	
C_2	2.4	6.0	7.5
$C_3^=$	2.0	12.0	
C_3	2.8	2.0	13.0
$C_4^=$	3.0	8.0	
C_4	2.2	1.0	11.0
C_5-C_{12}	22.5	39.0	37.0 (C_5-191°C)
C_{13}-C_{18}	15.0	5.0	11.0 (191-399°C)
C_{19}-C_{21}	6.0	1.0	3.0
C_{22}-C_{30}	17.0	3.0	(399-521°C)
C_{30}	18.0	12.0	0.05 (>521°C)
Nonacid chemicals	3.5	6.0	6.0
Acids	0.4	1.0	N.A.

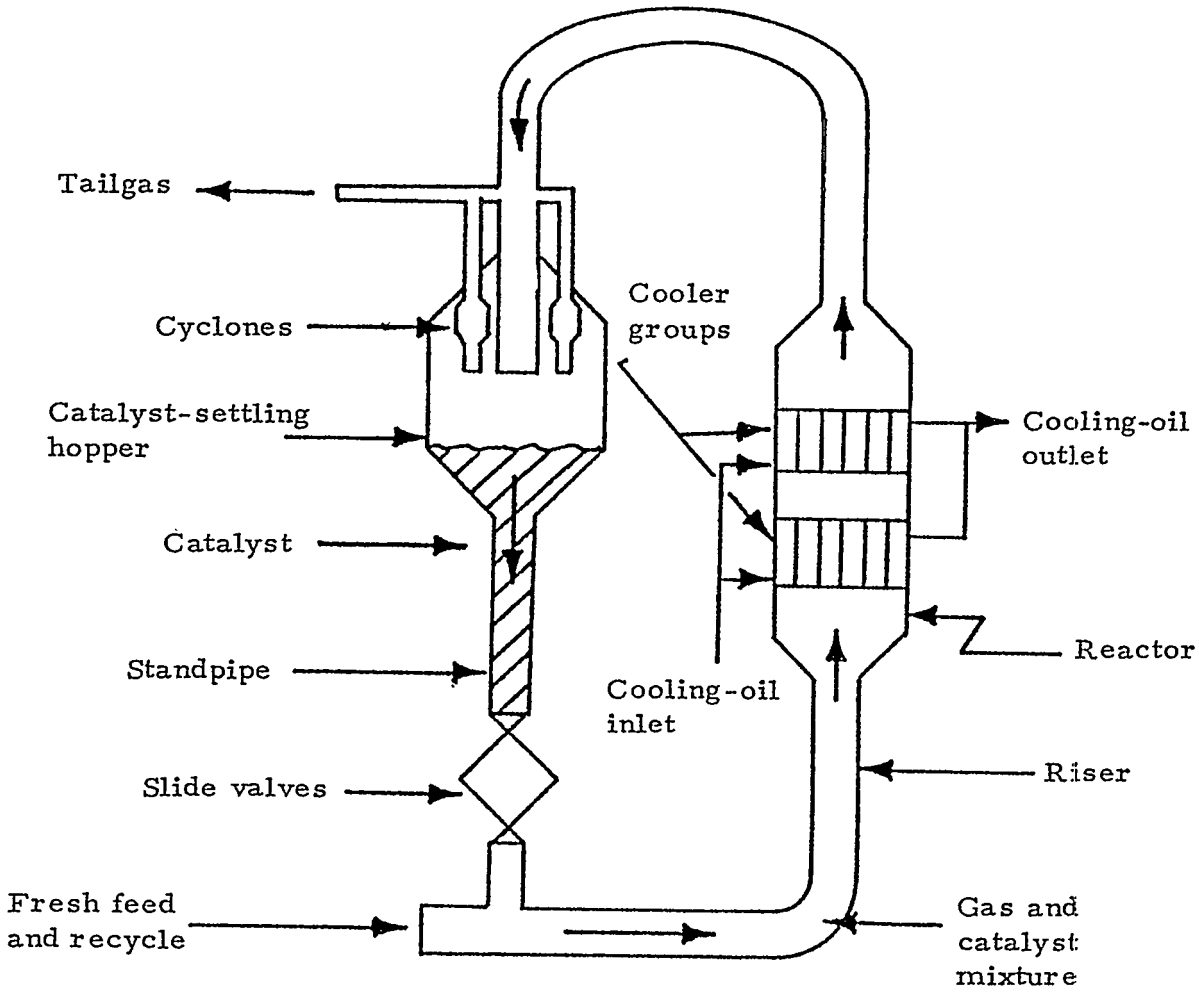

Fig. 5.1-5. Schematic diagram of an entrained fluidized-bed FT reactor.[60]

5.1-4C. Fischer-Tropsch Processes Not Yet in Commercial Operation

FT development work was and is being carried out in and outside of the US. The following discussions include the hot-gas recycle reactor, the oil-recycle reactor, the slurry reactor, SASOL development, the Shell SMDS process, and Dow's FT process.

The hot-gas recycle reactor recycles a large volume (about 100 times that of the fresh feed) of hot gas in a fixed-bed reactor for temperature control.[61] During the 1960s, work at what is now PETC was directed to use high-voidage catalysts in order to minimize the reactor pressure drop caused by high gas-flow rates.[62]

The oil-recycle reactor used recycle cooling oil over a fixed- or expanded-bed reactor to control the catalyst temperature. A fixed-bed reactor concept was investigated by Duftschmid and others in 1934.[63] Later, workers at PETC extended the concept to expanded-bed reactors.[62] Various FE catalysts were investigated. A 100-150 BPD demonstration plant was built at Louisiana, MO,[64] with a reactor diameter of 91cm and a height of 9.4m. Table 5.1-3 summarizes the operational data for the plant at half its design capacity. A low H_2/CO ratio synthesis gas was used because of good temperature control with an Fe catalyst.

A slurry FT reactor has been under development during the last few years. Using a precipitated Fe catalyst, the slurry reactor is the only FT reactor that was demonstrated to yield high single-pass H_2+CO conversion with low (0.6-0.7) H_2/CO ratio gases. It has the additional advantages of high C_3^+ product yields and a simple reactor design. By coupling it with a low-cost advanced gasifier and an improved FT product-upgrading scheme, this reactor could become the backbone for a potentially economical indirect coal-liquefaction process.

The slurry reactor was first used by Fischer and coworkers,[65] with a finely divided catalyst suspended in an oil reactor medium. Since then, substantial research and development work have been conducted by various workers, including Hall, [66] Schlesinger et al.,[67] Koelbel,[68] Mitra and Roy,[69] and Sakai and Kunugi.[70] An excellent review of the development of the slurry FT work up to the 1970s was given by Koelbel and Ralek.[46] A high point of the development was the construction and operation of the

Rheinpreussen-Koppers demonstration plant in 1953. The reactor had a diameter of 1.55m, was 8.6m in height, and had a capacity to produce 11.5Mg/day of HCs. Vertical cooling tubes with steam generation were placed inside the reactor for temperature control. Precipitated, unsupported FE catalysts (promoted with potassium and copper) were used. Table 5.1-4 summarized typical operational data from the plant; H_2/CO ratios as low as 0.67 were used.

Table 5.1-3. Operational data from the Louisiana oil-recycle FT demonstration plant.[64]

Parameter	Numerical Value
Fresh feed gas flow,	1,750 Nm^3/h
Feed-gas H_2/CO ratio	0.76 mole/mole
Recycle ratio	1.63 mole/mole
Maximum T	273°C
Rise in T	8°C
Maximum p	2.4 MPa
Pressure drop	0.2 MPa
Space velocity	531 vol/vol-hr
Oil-recycle rate	114 m^3/hr
H_2+CO conversion	85.9 mol%
C_1+C_2 yield	13.8 wt%

Table 5.1-4. Typical operational data from Rheinpreussen-Koppers slurry FT demonstration plant.[68]

Parameter	Numerical Value
Expanded slurry volume	10 m^3
Precipitated Fe catalyst	880 kg of Fe
Pressure	1.2 MPa
Temperature	268°C
H_2/CO molar ratio	0.67
Feed gas rate	2,700 Nm^3/hr
H_2+CO feed rate	2,300 Nm^3/hr
Superficial feed-gas velocity	9.5 cm/sec
CO conversion	91 mol%
H_2+CO conversion	89 mol%
Hydrocarbon products	
C_1+C_2	12 [$g/Nm^3(H_2+CO)$]
C_3^+	166 [$g/Nm^3(H_2+CO)$]
Water-soluble oxygenates	3 [$g/Nm^3(H_2+CO)$]

The major development on slurry FT processes since 1980 have been carried out at the Mobil Research and Development Corp., with partial funding from DoE.[71,72] The development was done in association with the concept of upgrading a total vaporous FT reactor effluent over a ZSM-5 catalyst. Two modes of operation were established: (i) a gasoline (G) or low-wax mode of operation and (ii) a gasoline and diesel (G+D) or high-wax mode of operation.

The major difference between these two modes is the HC distribution. In the G-mode of operation, the reactor wax yield is defined

as the liquid product for the FT reactor conditions and is 5-20wt% of the total HCs produced, while the CH_4 + ethane yields are 8-15%. Typical HC selectivities are given in Table 5.1-5. In the (G+D)-mode of operation, the reactor wax yield increases substantially to 40-60wt% with a decrease in CH_4 and ethane yield to 2-6wt%. As will be discussed later, the reactor wax can be further upgraded to make G+D. Table 5.1-6 shows typical HC selectivities for this mode. The intrinsic relation between the reactor wax yield and CH_4 yield found is one of the most interesting phenomena established (see Fig. 5.1-6). The high-wax mode of operation is excellent in maximizing the G+D yield. These different modes of operation were achieved by varying the catalyst preparation and process conditions. The ranges of normal operating conditions of the two-stage (slurry FT/ZSM-5) pilot plant are listed in Table 5.1-7. A method for using an on-line catalyst settling device was also successfully developed to withdraw continuously reactor wax containing less than 0.03wt% of solid catalyst. In both operations, single-pass H_2+CO

Table 5.1-5. Gasoline mode hydrocarbon selectivities obtained in the two-stage slurry FT/ZSM-5 pilot plant.[71]

Product Type	Yield, wt%		
	After FT synthesis	After the ZSM-5 catalyst	After Alkylation
C_1	7.5	7.7	7.7
$C_2^=/C_2$	1.6/3.0	1.1/3.1	1.1/3.1
$C_3^=/C_3$	8.0/2.0	4.0/5.1	0.0/5.1
$C_4^=$	6.6	4.4	0
i-C_4/n-C_4	0/2.0	7.8/4.3	(2.2)/4.3
C_5-C_{11}	33.5	52.8	71.2
C_{12}+ (liquid)	27.8	1.7	1.7
Reactor wax	8.0	8.0	8.0
Gasoline Properties			
RVP, psi		-	10
PONA, vol%		48/18/6/28	66/13/4/17
R+O		-	90
M+O		-	83

conversions of 80-85mol% were reached. In the G-mode of operation, an 86-day run was completed with a total HC production of 815g/gFe. In the high-wax mode of operation, a 34-day run with 350gHC/gFe was terminated when catalyst segregation occurred in the bubble-column reactor. This catalyst segregation is a new phenomenon and probably resulted from catalyst agglomeration or some unknown phenomenon, which requires further studies.

Table 5.1-6. High reactor-wax mode hydrocarbon selectivities for the two-stage slurry FT/ZSM-5 pilot plant.[72]

Product Type	Yield, wt%	
	After FT	After ZSM-5 (after alkylation)
C_1	3.3	3.4
$C_2^=/C_2$	1.8/0.7	1.1/0.7
$C_3^=/C_3$	2.8/0.8	0/3.2
$C_4^=$	2.5	0
i-C_4/n-C_4	0/0.9	(1.0)/0.7
C_5-C_{11}	22.4	39.6
C_{12}+ (liquid)	9.7	1.0
Reactor wax	50	51.3
Oxygenates	5.1	-
<u>Gasoline Properties</u>		
RVP, psi		10
PONA, vol%		60/14/7/19
R+O		92

Fig. 5.1-6. Reactor-wax vs methane yields for slurry FT operation.[72]

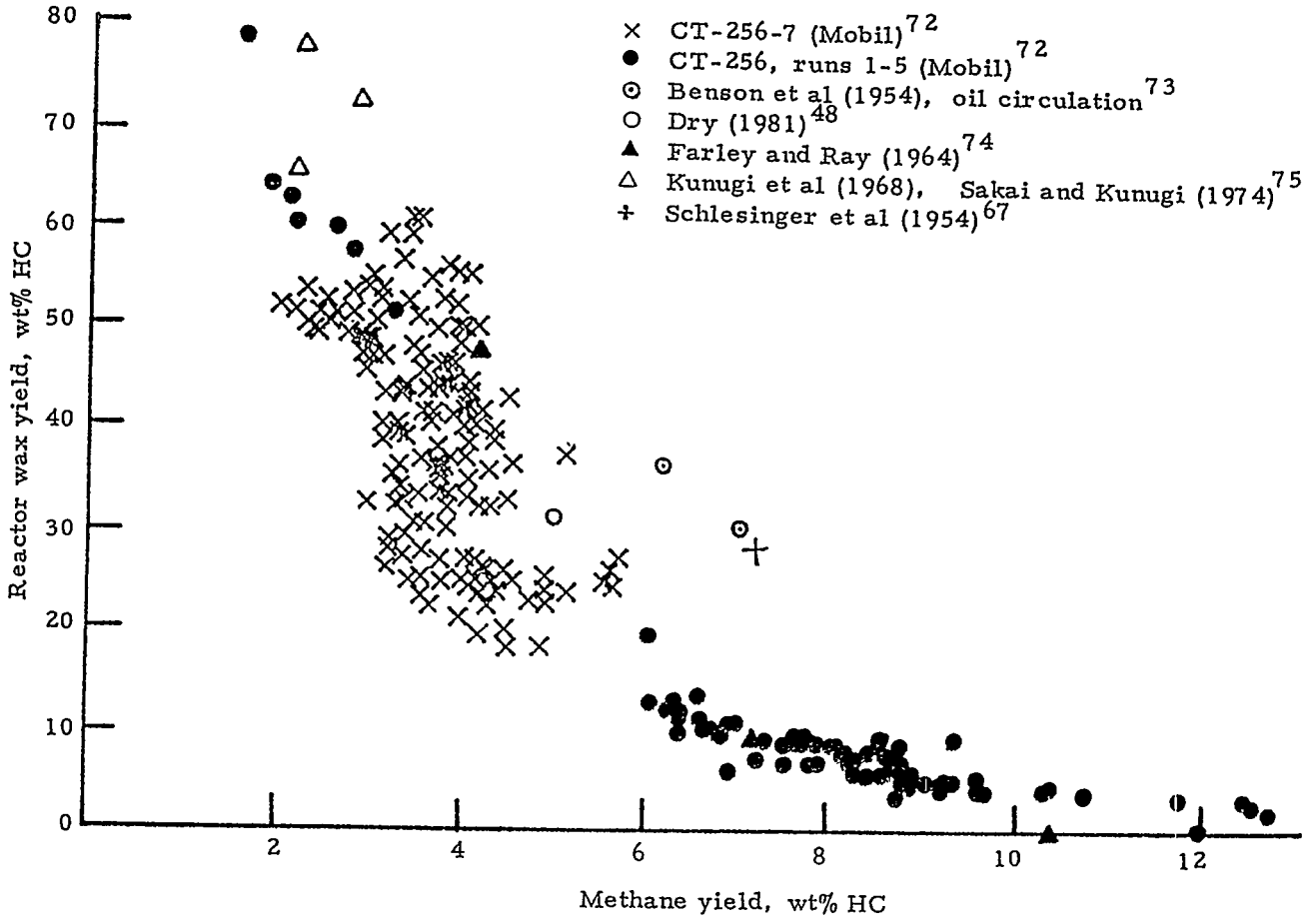

Table 5.1-7. Range of normal operating conditions for the two-stage slurry FT/ZSM-5 pilot plant.[71,72]

<u>First-Stage FT Reactor</u>	
T	240-280°C
p	150-350psig
Superficial gas velocity	2-6cm/sec
Molar ratio H_2/CO	0.6-0.7
Space velocity	1.5-5.0Nl/gFe-hr
Catalyst loading	10-20wt%
Slurry inventory	8-12kg
<u>Second-Stage ZSM-5 Reactor</u>	
Inlet T	288-454°C
p	150-350psig
Space velocity	0.5-1.5gHC/g-hr
Catalyst loading	200-300g
Severity index, molar ratio i-$C_4/(C_3^{=}+C_4^{=})$	0.2-0.2

Workers at SASOL have conducted a pilot plant study with a 5cm id and 3.8m long slurry bubble-column, utilizing a commercially precipitated FE catalyst.[48] This study differed form the other slurry FT work in two aspects: the use of synthesis gas with an H_2/CO ratio equal to 2 or higher and the use of a supported, precipitated Fe catalyst. Because of the use of gas with high H_2/CO ratio, the study is related to the dry-ash Lurgi gasifiers used at SASOL but not to advanced gasifiers which generate gases with low H_2/CO ratios.

Workers of SASOL have also investigated improvements to the existing Arge and Synthol reactors.[76] The potential improvements of the Arge unit involve either increasing the reactor diameter or else raising its operating pressure. The potential improvement of the Synthol unit is to replace it with fixed fluidized-bed reactor. Few details concerning these improvements have been reported.

In 1985, Shell announced its SMDS (Shell middle-distillate synthesis) process for producing middle distillates (kerosine and gas oil) from NG.[77] The synthesis gas is produced by a conventional partial-oxidation process and is then converted to highly paraffinic HCs over a proprietary FT catalyst in an Arge-type reactor. This paraffin synthesis reactor is highly selective in producing heavy paraffin wax; no light paraffin yield was reported. Since the synthesis gas is obtained from NG, it is expected to have little or no WGS activity because otherwise a large portion of CO will be converted to CO_2.

Gulf announced in 1983 the Gulf-Badger process for converting NG to HC liquid via CH_4 steam reforming followed by FT synthesis.[78] The proposed synthesis reactor is also an Arge-type reactor. The catalyst used is not disclosed but it has little or no WGS activity. Table 5.1-8 lists typical process conditions and HC product selectivities. The diesel fraction of the product has good properties. In order to maintain the H_2/CO feed ratio between 1.5 and 2, a CO_2 recycle to the steam reformer and H_2 removal from the synthesis gas are required. The integrated system appears to be complicated and expensive.

Workers at Dow have developed new Mo-based catalysts for the synthesis of C_2-C_4 paraffins and olefins.[45] The process was demonstrated in a single-tube, direct heat-exchange reactor containing 26-28 liters of catalyst. The catalyst is Mo on a carbon support (6-20wt% loading) promoted with 0.5-4 wt% K. The Mo is a known methanation catalyst. The addition of

K maximizes the C_2-C_5 yield. The C_2-C_5 is the main product and can be used as a feedstock in making ethylene in conventional thermal crackers. The major process disadvantage is the high CH_4 yield of 30-40wt%. The process used 0.8 H_2/CO feed gas, 350-400°C, 500psig and up, and yielded 57-80mol% H_2+CO conversion. The Mo catalysts have the advantage of S-tolerance up to 20ppm.

5.1-5. Syntheses of Chemicals Using SG, CO or Methanol Plus Other Chemicals

The hydroformulation (OXO) reaction is represented by the conversion

$$CH_3CH = CH_2 + CO + H_2 \rightarrow \underbrace{CH_3CH_2CH_2CHO + CH_3CH(CH_3)CHO}_{\text{H2 alcohols}} \quad (5.1\text{-}22)$$

Almost every olefin undergoes this reaction at 110-160°C and 20-250 atm of SG. The reaction was discovered by Roelen in 1937 while studying the mechanism of the cobalt-catalyzed FT reaction. World production of OXO alcohols is now about 10 billion pounds per year.

First-generation hydroformylation plants, most of which are still in operation, used cobalt salts or the simple transition-metal carbonyl, $Co_2(CO)_8$, as the catalyst. New plants use rhodium-tertiary phosphine complexes as catalysts; these operate at lower temperatures and pressures. Easily polymerized olefins such as styrene and methyl methacrylate react cleanly with rhodium catalysts to yield aldehydes having the one carbon atom more than the original olefin.

Products from the hydroformylation of olefins include solvent alcohols (n-propanol, n-butanol, C_5 alcohols), plasticizer alcohols (C_8, C_9, C_{10} alcohols) and detergent alcohols (C_{11} - C_{16} primary alcohols).

Table 5.1-8. Typical process conditions and HC selectivities of the Gulf-Badger process.[78]

Parameter	Values
Process Conditions	
T	210°C
p	250psig
H_2/CO feed ratio	1.5-2
Space velocity	500-1,000ℓ/hr
CO conversion	40-60mol%
C_5+ selectivity, % of carbon converted	>70%
Parameter	**Values**
HC Selectivities	
CH_4	13.7
C_2H_4 to C_4H_{10}	11.6
C_5-C_8 (naphtha)	25.4
C_9-C_{20} (distillate)	33.4
$C_{21}+$ (wax)	14.2
Oxygenates	1.7

The important plasticizer 2-ethylhexanol is made in large quantities from propylene. This olefin is hydorformylated to n-butyraldehyde, which then undergoes a base-catalyzed aldolization to 2-ethylhexenal that is hydrogenated to 2-ethylhexanol. The conditions used for preparation of this alcohol from propylene with commercial cobalt and rhodium catalysts are shown in Table 5.1-9.

Table 5.1-9. Preparation of 2-ethylhexanol.

Property	Catalyst	
	Cobalt	Rhodium
P, atm	250	20
T, °C	145	120
Selectivity to n-butyraldehyde, %	66	85

The hydroformylation of olefins with SG has been used with a great variety of compounds such as steroids, terpenes, and many other unsaturated compounds to synthsize various aldehydes and alcohols, solvents, and specialty chemicals.

5.1-5A. Methyl t-Butyl Ether (MTBE)

A steadily growing use for MeOH as a fuel is in the synthesis of MTBE, an effective octane booster, by the process reaction:

$$CH_3OH + CH_3\text{-}\underset{\displaystyle CH_3}{\overset{\displaystyle |}{C}} = CH_2 \xrightarrow[80°C]{\text{acid resin}} CH_3OC(CH_3)_3 \text{ (MTBE)} . \quad (5.1\text{-}27)$$

5.1-5B. Methyl Chloride from Methanol and HCl

Methanol can be esterified with HCl, either in the liquid phase at 100-150° in the presence of e.g., $ZnCl_2$ or, preferably, in the gas phase at 300-380°C and 3-6 atm with Al_2O_3 as the catalyst: $CH_3OH + HCl \rightarrow CH_3Cl + H_2O$. The selectivity to methyl chloride is almost 98% relative to MeOH. Stauffer Chemical developed a process of the latter type and produced 27,000 tons of CH_3Cl in 1973. Hoechst and Huls in the FRG, using a modified Stauffer process, produced about 40,000 tons of MeOH and 28,000 tons of CH_3Cl, respectively, in 1973. In 1976, Japanese production of this chemical exceeded 22,000 tons. Methyl chloride is also used instead of CH_4 for the synthesis of the higher chloromethanes ($CHCl_3$, CCl_4) by thermal chlorination.

5.1-5C. The Koch Reaction: Carbonylation of Olefins to Branched Acids

Several companies operate industrial processes based on the Koch reaction. This reaction involves the acid-catalyzed reaction of olefins with CO and water to give highly-branched acids which are thermally, oxidatively, and hydrolytically stable:

$$RCH_2CH = CH_2 + CO + H_2O \xrightarrow{H_2SO_4} R\text{-}\overset{\overset{CH_3}{|}}{\underset{\underset{CH_3}{|}}{C}}\text{-}COOH \quad . \qquad (5.1\text{-}28)$$

5.1-5D. Styrene From Methanol and Toluene

About 7 billion pounds of styrene are produced each year in the US. Traditionally, styrene is made by a two-step process: benzene is alkylated to ethylbenzene, which is then dehydrogenated to styrene. But toluene is cheaper than benzene and MeOH is or will be cheaper than ethylene. A one-step route to styrene via alkylation of toluene with MeOH would offer advantages of both lower raw material costs and smaller energy costs. This reaction can be accomplished, using a zeolite-containing boron, as follows:

$$C_6H_5CH_3 + CH_3OH \xrightarrow[\substack{4\text{Å pore} \\ 400°C}]{\text{CsBX zeolite}} \underset{\text{(styrene)}}{C_6H_5CH = CH_2} + H_2O + (H_2) \quad . \qquad (5.1\text{-}29)$$

The geometry and acidity of the cesium-boron type-X zeolite both activate the toluene molecule and protect it from attack at an undesirable location, i.e., at the para position of toluene. In a most unusual type of reaction, only the methyl group in toluene is exposed for alkylation. This process falls in the category of emerging processes.

5.1-5E. Terephthalic Acid From Toluene and Methanol and From Toluene and CO

Terephthalic acid is usually made by the oxidation of p-xylene obtained from petroleum reformate. But toluene can be used in two relatively new ways to synthesize the important chemical, terephthalic acid. The production of terephthalic acid is illustrated by the process

$$C_6H_5CH_3 + CH_3OH \xrightarrow[300 - 500C]{\text{P-modified H-ZMS-5}} \underset{(>80\%)}{\text{p-xylene}} \xrightarrow{\text{oxidation}} \text{terephthalic acid} \qquad (5.1\text{-}30)$$

The great concentration of p-xylene, because of the restricted pore size of the ZSM-5 shape-selective catalyst, could lower the costs of the separation process that is ordinarily used for its recovery from reformate.

An alternate route is to eliminate p-xylene completely by carbonylating toluene to p-tolualdehyde; the aldehyde is then oxidized to terephthalic acid.

A significant amount of MeOH is used to esterify terephthalic acid to dimethyl terephthalate. In 1985, 7.2 billion pounds of terephthalic acid were produced in the US.

5.1-5F. Some Miscellaneous Uses of Methanol

About 4% of MeOH is consumed in the manufacture of methyl methacrylate, a chemical used to produce acrylic sheet, surface coating resins, and molding and extrusion powders.

Methylamines are produced by catalytically reacting MeOH with NH_3.

Solvents account for about 8% of MeOH demand. It is also used as an antifreeze, gasoline de-icer, windshield washer fluid, and hydrate inhibitor in NG.

5.1-6. Other Chemicals from SG, Methanol and CO; Emerging Processes

As already indicated, SG, MeOH and CO are the raw materials for the syntheses of a number of fuels and chemicals of commercial and near-commercial use. It is well to summarize, at this point, the scope of MeOH-SG chemistry as it applies to the synthesis of important oxygenated chemicals. Some are already commercial, some are coming on stream, and some are of potential interest.

5.1-6A. Vinyl Acetate (VA)

The present commercial process for VA is based on SG for 70% of its weight and the process has high yields and moderate processing costs. It consists of the vapor-phase acetoxylation of ethylene:

$$CH_3\overset{O}{\overset{\|}{C}}OH + CH_2 = CH_2 + (1/2)O_2 \longrightarrow CH_3\overset{O}{\overset{\|}{C}}OCH = CH_2 + H_2O_2 \ . \qquad (5.1\text{-}31)$$

(VA)

Halcon has developed the reductive carbonylation of methyl acetate (made from SG) to ethylidene diacetate:

$$CH_3COOCH_3 + 3CO + 3H_2 \longrightarrow \underset{\text{ethylidene diacetate}}{CH_3CH(OCOCH_3)_2} + H_2O \ . \qquad (5.1\text{-}32)$$

The ethylidene diacetate may then be pyrolyzed to VA. The chemistry of the reductive carbonylation of methyl acetate strongly resembles that of its carbonylation to acetic anhydide, but the mechanism is not so well defined. Both palladium and rhodium have been claimed to be good catalysts for the reaction. This technology, while promising, is not competitive in the US at the present stage of development.

5.1-6B. Ethylene Glycol ($HOCH_2CH_2OH$)

About 4.7 billion pounds of ethylene glycol (EG) were produced in the US in 1985. The present commercial process for its synthesis proceeds from ethylene to ethylene oxide to EG.

$$H_2C = CH_2 + (1/2)O_2 \xrightarrow[\text{catalyst}]{Ag} H_2C\underset{\backslash\ O\ /}{-}CH_2 \xrightarrow{H_2O} HOCH_2CH_2OH \ . \qquad (5.1\text{-}33)$$

The synthesis is vulnerable to replacement by processes based on SG or raw materials derived from SG. The reaction for the direct production of EG from SG is $3H_2 + 2CO \longrightarrow HOCH_2CH_2OH$ and has been realized previously, although at pressures too high to be of commercial use. But the raw-material consumption in 1 lb of feed per lb of product is unity and the

H_2/CO ratio in the SG is 1.5, making this route to EG very attractive. The synthesis of EG from SG would present a case of high added value in the final product.

The driving force for the development of a route from SG to EG is high and there are a number of new processes under development to achieve this end. At the current stage of development, the route from MeOH and HCHO appears to have the edge. A large research and development program is underway to synthesize EG from SG or from CO.

EG from Methanol and Formaldehyde

Celanese and Redox Technologies [79] have developed an economically attractive process to EG from MeOH and HCHO. It has significant raw material advantages over the ethylene oxide process. Methanol and HCHO react in the liquid phase at 125-200°C and 300-600 psig using a free radical initiator. Both starting materials are made from SG and the selectivity to EG is high. The process is:

$$CH_3OH + HCHO \xrightarrow[125 - 250°C]{\text{peroxide}} HOCH_2CH_2OH \text{ (EG)} . \qquad (5.1\text{-}34)$$

EG by Carbonylation of HCHO

DuPont operated a commercial process catalyzed by H_2SO_4 until 1968 but it required high pressure and temperature and neutralization of the H_2SO_4 to recover the product. Chevron [79] has improved this route to EG by using HF as both catalyst and solvent, which results in much lower pressure (~100 psig) and ease of catalyst separation and recycle:

$$HCHO + CO + H_2O \xrightarrow[100 \text{ psi}]{HF} HOCH_2COOH \text{ (hydroxyacetic acid)} . \qquad (5.1\text{-}35)$$

The acid is esterified and then hydrogenated to EG.

EG from Oxalate Esters (Oxidative Carbonylation)

In this route to EG, oxidative coupling of MeOH and CO (Pd-based) is separated from a water-generation reaction (Cu-based) by using nitrous esters, which represents a preoxidation of the alcohol. The overall equation may be written as $2CH_3OH + (1/2)O_2 + 2CO \longrightarrow$ dimethyl oxalate + H_2O. The dimethyl oxalate is hydrogenated to EG and MeOH.

EG Directly from SG

Although the direct synthesis of EG from SG is the most attractive route from a raw material point of view, the following synthesis has thus far been an elusive goal: $3H_2 + 2CO \xrightarrow{\text{Rh or Ru}} HOCH_2CH_2OH$. The reaction rate is too low, pressures (up to 20,000 psig) too high, and the production of MeOH as a significant (20-40% carbon efficiency with rhodium) by-product have combined to make this route uneconomical at present. But the very significant potential rewards justify continuing efforts to improve this process.

EG by Reaction of HCHO with SG

A number of companies have obtained patents using the route [79]

$$HCHO + CO + 2H_2 \longrightarrow HOCH_2CH_2OH \ . \qquad (5.1\text{-}36)$$

This reaction proceeds under mild conditions but potentially serious problems may arise by side reaction of HCHO, i.e., reduction to MeOH and the formation of formose (sugar-like) products.

Newer Routes to EG Starting with Formaldehyde

One route, studied at Monsanto, is shown by the following equation:

$$HCHO \xrightarrow[\text{95\% conversion}]{\text{Rh complex}} HOCH_2CHO \xrightarrow{H_2} EG \ . \qquad (5.1\text{-}37)$$

Another approach is followed at Exxon:

$$HCHO \xrightarrow[150°C,\ H_2O]{\text{solid acid resin}} HOCH_2COOH\ (70\%) \xrightarrow[CH_3OH]{H_2} EG\ . \qquad (5.1\text{-}38)$$

5.1-6C. Big Acids From Little Ones: Homologation of Acids

Texaco has discovered a potentially useful reaction for increasing the chain length of a carboxylic acid by one carbon, i.e., converting acetic acid to propionic acid [80] in the presence of a RuO_2-HI catalyst at 100 atm and about 220°C. Since acetic acid is itself made entirely from SG, all of these acids can, if need be, be built exclusively from SG and no petroleum feedstock would be needed.

5.1-D. Single-Cell Protein From Methanol

A protein-rich animal feed ingredient has been made by the continuous fermentation of MeOH or ethanol. The product may eventually be processed into an ingredient suitable for human food. The Phillips Petroleum Company has a product called Provesteen which is 60% protein, 5% lipid and 18% carbohydrate with essential vitamins and minerals.

5.2. Catalytic Processing of Synthsis-Gas-Derived Products

5.2-1. Introduction

The discussions in this section deal mainly with further processing of two major synthesis gas derived products, namely, MeOH and FT products. In particular, they are targeted at making the following end products: light olefins (C_4-) and liquid fuels (gasoline and diesel).

Since MeOH is a chemically reactive compound, it is an excellent building block in making chemicals and liquid fuels. The MeOH-to-gasoline (MTG) process developed by the Mobil Research and Development Corp. is one

of the very few synthetic fuel technologies being put into commercial application since the 1973 oil embargo. Conversions of MeOH first to olefins and then to diesel are also being developed.

Established practices of upgrading FT products at SASOL will now be reviewed. The effort of producing more selective product slates directly from FT processes has been a failure after many years of intense studies. It is relatively easy to make light paraffins and high molecular-weight waxes. Further processing is necessary to produce desirable products such as gasoline, diesel, or olefins. The light paraffins are poor feedstocks for further processing because they are thermodynamically very stable. In contrast, the FT waxes have the unique characteristic that they are excellent feedstocks for catalytic cracking. Consequently, the high-wax mode of operation in FT synthesis is a prudent approach. Various approaches for upgrading the FT reactor wax will be summarized. The high-wax mode of operation also results in low CH_4 and ethane yield, which is highly desirable in making liquid fuels. Another prudent approach is the direct upgrading of the total vaporous FT reactor effluent. This procedure has the potential of saving a large number of upgrading units that are currently used in the SASOL plants.

The use of zeolites is essential in processing of the SG-derived products because of the unique shape-selective characteristics of these catalysts. A discussion of this aspect will also be given here.

5.2-2. Methanol to Gasoline (MTG)

5.2-2A. Catalysts and Chemistry of the MTG Process

The work on the MTG Process has been dominated by Mobil. The technology is based on the zeolites of the ZSM-5 class.[81] A review by Chang[82] on MeOH conversion to HCs included a detailed description of other zeolite and non-zeolitic catalysts for MeOH conversion. None of these catalysts give the following unique results that are obtained by using ZSM-5 catalysts: high gasoline yield, excellent gasoline quality, very low CH_4 + ethane yield, high activity, high stability, and very low coke yield.

Symbolically, MTG reactions may be represented by the following dehydration reaction.

$$nCH_3OH \longrightarrow (CH_2)_n + nH_2O \quad . \qquad (5.2\text{-}1)$$

The actual reaction path is quite complex [83] and will not be discussed here. The following steps describe the essence of the reaction path:

$$2CH_3OH \longrightarrow (CH_3)_2O + H_2O \ , \qquad (5.2\text{-}2)$$

$$CH_3OH\ (CH_3)_2O \longrightarrow \text{light olefins} + H_2O \ , \qquad (5.2\text{-}3)$$

$$\text{light olefins} \longrightarrow \text{heavy olefins} \ , \qquad (5.2\text{-}4)$$

$$\text{heavy olefins} \longrightarrow \text{aromatics, paraffins, naphthenes} \ . \qquad (5.2\text{-}5)$$

Because of the shape-selective pore structure of the ZSM-5 class catalysts, the HCs fall predominantly in the gasoline boiling range. A large yield of aromatics is obtained and the paraffins are dominated by isoparaffins. Consequently, the majority of the compounds in the C_5+ range are high-octane compounds. The aromatics are highly methyl-substituted as the result of the alkylation of the aromatics by methanol and dimethyl ether. C_9+ aromatics are dominated by symmetrically methylated isomers, reflecting the shape-selective structure of the catalysts.

The C_{10} aromatics are dominated by durene (1,2,4,5-tetramethylbenzene), which has an excellent octane number but a freezing point of 79°C. Too high a durene content in the gasoline may impair automobile driving characteristics because of the crystallization of durene at low temperatures. Workers at Mobil have conducted a fleet test and found no drivability loss at -18°C when using a gasoline containing 4wt% of durene.[84] Nevertheless, in order to remove process contraints on MTG operation and to retain a lower target of durene, Mobile has also developed a heavy gasoline treating (HGT) process to convert durene into other high-quality gasoline components by isomerization and dealkylation.[85]

The MTG reactions are highly exothermic. The heat of reaction ranges from 1.5 to 1.75kJ/g of MeOH and varies with product distributions. The product distribution varies with process conditions and reactor types.

MTG reactors are designed to remove the large amount of reaction heat in a manner that is similar to the procedure used in FT reactors.

5.2-2B. Various MTG Reactor Designs

Three types of reactors were developed for the MTG: (i) adiabetic fixed-bed, (ii) fixed fluidized-bed, and (iii) direct heat exchange. The first two types were developed by Mobil and the last by Lurgi.

The adiabetic fixed-bed process uses a two-stage concept. In the first-stage DME reactor, which contains a dehydration catalyst, the MeOH is dehydrated to an equilibrium mixture of MeOH, dimethyl ether, and water. The effluent is then mixed with the light recycle gas and fed into a fixed-bed ZSM-5 reactor. The temperature rise in this reactor is limited by the heat carrying capacity of the recycle gas. The ZSM-5 catalyst requires periodic oxidative regeneration to overcome gradual coke deposition. The typical cycle length is 20 to 40 days, depending on the space velocity and operating conditions. After extensive early development work using micro-reactors and bench-scale pilot plants, a 4-BPD demonstration plant was developed. It had a 5cm id and 4m long dehydration reactor. A 10cm id by 4m long MTG reactor was erected. Table 5.2-1 shows typical process conditions and product yields (averaged over one cycle) for this plant. The first commercial plant of 14,500 BPD gasoline capacity was constructed in New Zealand. The plant has been running successfully since 1985 start-up. The synthesis gas used is generated via steam reforming from the NG obtained from the off-shore Maui field. An HGT plant is also operating successfully in New Zealand and reduces the durene in the gasoline to 2wt%.

A fluidized-bed MTG reactor concept was developed concurrently with the fixed-bed reactor at Mobil. The heat of reaction can be removed either directly from the reactor using a cooling coil or indirectly by using an external catalyst cooler. The reactor can be made to maintain a constant catalytic activity by continous catalyst regeneration and makeup. This concept has gone through many stages of pilot-plant development, including bench-scale fixed fluidized-bed, 4BPD, and 100BPD cold-flow models, and finally a 100BPD semi-work plant. Typical process conditions and product yields from the 4BPD pilot plant are also given in Table 5.2-1. The product yields are

Table 5.2-1. Typical process conditions and product yields for MTG processes.[85]

Conditions	Fixed-bed reactor	Fluid-bed reactor
MeOH/water charge, w/w	83/17	83/17
Dehydration reactor inlet T,°C	316	--
Dehydration reactor outlet T,°C	404	--
Conversion reactor inlet T,°C	360	413
Conversion reactor outlet T,°C	415	413
p, kPa	2,170	275
Recycle ratio, mol/mol charge	9.0	--
Space velocity, WHSV	2.0	1.0
Yields (wt% of MeOH charged)		
MeOH + dimethyl ether	0.0	0.2
HCs	43.4	43.5
Water	56.0	56.0
CO, CO_2	0.4	0.1
Coke, other	0.2	0.2
	100.0	100.0
Hydrocarbon product (wt%)		
Light gas	1.4	5.6
Propane	5.5	5.9
Propylene	0.2	5.0
Isobutane	8.6	14.5
n-Butane	3.3	1.7
Butenes	1.1	7.3
C_5+ gasoline	79.9	60.0
	100.0	100.00
Gasoline (including alkylate), RVP-62kPa (9psi)	85.0	88.0
LPG	13.6	6.4
Fuel gas	1.4	5.6
	100.0	100.0
Gasoline octane (R+O)	93	97

quite different from those of the fixed-bed reactor, mainly because of non-recycle operation. Without recycle, large amounts of light olefins are preserved. By properly balancing the C_3 and C_4 olefin yields with those of isobutane, a maximum yield of high-quality alkylate can be produced when using conventional alkylation processes. This procedure results in a high gasoline yield. The fuel gas contains substantial amounts of ethylene, which may be recycled to make more gasoline.

The 100BPD semi-work program was jointly conducted by Union Rheinische Braunkohlen Kraftstoff AG (URBK), Uhde GmbH, and Mobile, with additional funding from the FRG Bundesministerium fur Forschung and Technologie (BMFT) and the US DoE. The program was successfully concluded in late 1984. The MTG reactor has a 60cm id and a maximum bed height of 15m.[86] The tests demonstrated better than 99.9% MeOH conversion, a gasoline yield of over 92wt% (including alkylate and recycle of the excess light olefins), and a low catalyst makeup rate.

A direct heat-exchange MTG reactor concept was developed by Lurgi.[87] Some light gas recycle, in addition to the primary heat removal accomplished by circulating a brine in the shell side, is also used to control the reactor temperature. The conversion, gasoline yield and quality are similar to those of the fixed-bed reactor. The cycle length is longer than that of the fixed-bed but the reactor is more costly.

5.2-3. Methanol Conversion to Olefins and Diesel

5.2-3A. Methanol Conversion to Olefins (MTO)

During the MTG development work at Mobil, it was discovered[88] that the HC-product distribution can be shifted to light olefins by increasing the space velocity, decreasing the MeOH partial pressure, and/or increasing the reaction temperature. Since then, major pilot-plant development work was conducted at Mobil, including the use of microreactors, a bench-scale fluidized-bed pilot plant, and a 4BPD fluidized-bed reactor. These tests finally led to demonstration runs in the 100BPD semi-work plant previously used for fluidized-bed MTG process development (see Sec. 5.2-2B). The runs were conducted under the sponsorship of the same partners as those of the

100BPD MTG program. The ranges of operating conditions are:[89] T, 470-515°C; p, 1.2-2.5 bar gauge; space velocity, 0.8-1.15ℓ/hr; reaction index ($C_3/C_3^=$), 0.5-0.1; superficial gas velocity, 0.35-0.55m/s. The catalyst makeup rate was less than 0.5% of the total catalyst inventory per day. The yield data agreed well with those from the 4BPD pilot plant. For the 4BPD pilot plant operation, the following typical yields were reported:[90] C_1-C_3 paraffins, 4wt%; C_4 paraffins, 4wt%; C_2-C_4 olefins, 56wt%; C_5+ gasolines, 36wt%.

Hoelderich et al [91] of BASF investigated the use of zeolites for the conversion of MeOH to olefins for MTO. The nominal conditions investigated were atmospheric pressure, 300-600°C, 2.7-7.8ℓ/hr WHSV and 25-80wt% MeOH. C_2-C_4 olefin selectivities as high as 80 wt% were reported.

Lurgi has also reported MTO pilot-plant results using commercial catalysts.[87] The following product yields were obtained based on an average over 1,000hr of operation: C_1-C_4 paraffins, 4wt%; C_2-C_4 olefins, 81wt%; C_5+ hydrocarbons, 13wt%. Catalyst and process conditions were not reported.

5.2-3B. Olefin Conversion to Diesel and Gasoline

Using olefins from the MTO and FT processes, diesel and gasoline may be made from MeOH via a process that converts olefins to D+G. Catalytic polymerization is a standard refinery process using acid catalysts and is currently being used at SASOL to convert C_3-C_4 olefins into G+D.[92] Detailed operational information is not available.

Recently, Mobil has developed an MOGD (Mobil olefins to gasoline and diesel) process using a Mobil commercial zeolite catalyst.[90,93,94] The G+D selectivity is better than 95wt% and is highly flexible with respect to G-to-D distribution (from 100% G to 90%D). Because of the catalyst shape-selectivity, the majority of the products are methyl-branched isoolefins. These compounds have good octane rating in the gasoline range. The diesel-range olefins may be hydrogenated to give isoparaffins, which

have excellent diesel properties. The qualities of the proper diesel and jet fuel fractions exceed the required product specification. A commercial-scale testing of the MOGD process was made in a Mobil refinery in late 1981. The feedstock was a mixture of C_3-C_4 olefins and paraffins from an FCC unit. The test was carried out successfully for 70 days.

5.2-4. Processing of Fischer-Tropsch Products

5.2-4A. Special Feature of Fischer-Tropsch Products

The FT products generally exhibit the following special features: (i) very wide carbon-number distribution for both HCs and oxygenates, nominally following the Schulz-Flory distribution [Eq. (5.1-23)]; (ii) no or minimal ring compounds; (iii) highly olefinic (mainly α-olefins) character; (iv) production of mostly n-paraffins; and (v) n-alcohols as oxygenates. These features are reflected in the following deficiencies of the FT raw products: (i) low gasoline and diesel yields; (ii) low octane number in the gasoline fraction; (iii) waxy diesel fraction; and (iv) large amount of oxygenates in the product water. Further processing of these products is necessary to overcome these deficiencies. Upgrading schemes will now be discussed briefly.

5.2-4B. SASOL Practices

Because the product selectivities from the Arge and Synthol reactors are very different, the upgrading schemes are also drastically different. Hoogendoorn and Salomon[59,95] have given an excellent review of SASOL I (containing both Arge and Synthol reactor) upgrading schemes. The SASOL II and III (containing only Synthol reactors) upgrading schemes were reported by Dry[96] and Brink.[92] Upgrading schemes for both cases are complex.

Following the Arge reactor, the C_3-C_4 fraction is sent to a catalytic polymerization unit to upgrade the C_3-C_4 olefins into G+D. The gasoline fraction is sent to a hot refining unit (a fixed-bed catalytic

reactor) to convert oxygenates into HCs and α-olefins into the higher octane-number internal olefins. A moderate pressure hydrogenation unit (a fixed-bed catalytic reactor) is used to upgrade the 370°C+ wax by converting olefins and oxygenates into paraffins. A de-oiling unit (solvent extraction) is used to remove oil from the hydrogenated 370-460°C wax. The 460°C+ wax is thermally cracked in a paraformer unit to make medium and soft wax. The same unit is also used to crack the 320-370°C wax into D+G. The oxygenates in the aqueous stream are first separated by distillation and then subjected to hydrogenation to convert aldehydes into alcohols.

The upgrading schemes for the Synthol products as SASOL II and III are different from those at SASOL I. Since the practices at SASOL I are probably out of date, we concentrate our discussions on SASOL II and III. At SASOL II and III, the C_2-fraction is cryogenically separated into CH_4, ethane, and ethylene. The CH_4 is converted into SG using a partial oxidation reformer and the ethane is converted to ethylene in conventional ethane crackers. A heavy catalytic polymerization unit is used to upgrade the olefins in the C_3-C_4 fraction to G+D. The C_5-C_6 fraction is subjected to catalytic isomerization in a fixed-bed catalytic reactor using a catalyst similar to cracking catalysts in order to convert α-olefins to higher octane-number isomers and to remove impurities. The C_7-190°C fraction is first hydrogenated to eliminate olefins and oxygenates and then sent to a UOP continuous regeneration platformer to make high-octane gasoline. An 82vol% gasoline yield is obtained at 88 RON. The 190° + fraction is first hydrogenated and the heavier fraction is sent to a selective cracking unit (a fixed-bed reactor using ZSM-5 zeolite) to lower its pour point. The water-soluble oxygenates are treated as in SASOL I to produce various alcohols and ketones.

5.2-4C. Direct Upgrading of Total Vaporous F-T Reactor Effluent

Use of this novel concept greatly simplifies the processing of FT products. The concept is to take the whole vaporous FT reactor effluent directly to a zeolite reactor without cooling and separation.[97] In a single step, a large portion of olefins is converted into aromatics and isoparaffins while cracking the heavy paraffins and olefins into

gasoline-range paraffins and olefins. Isomerization activity of the zeolites ensures that the product will contain larger quantities of high octane number isocompounds. Large amounts of isobutane can be alkylated with the remaining C_3 and C_4 olefins to make alkylate, a high quality gasoline blending stock. The process also converts all of the oxygenates into gasoline-range HCs.

This concept has the important potential of improving the process economics of the FT technologies. In connection with a slurry bubble-column FT reactor, operation of a pilot-plant of this concept has been conducted at Mobil since 1981.[71,72] A set of typical operational data from G-mode (low-wax mode) operation is given in Table 5.1-5. Comparison of the HC distribution of the FT effluents with those from the ZSM-5 reactor clearly demonstrates the function of the ZSM-5 catalyst. Similar conclusions may be drawn from the high-wax mode operational data given in Table 5.1-6.

5.2-4D. Processing of Fischer-Tropsch Reactor Wax

The FT reactor waxes are produced from slurry or Arge-type reactors that operate at relatively low temperature and moderate pressure. These waxes generally have the following special properties: (i) highly paraffinic; (ii) mainly straight-chain HCs and oxygenates with no or few ring compounds; (iii) some olefins and oxygenates; and (iv) no sulfur, nitrogen, or heavy metal compounds. These properties make FT reactor wax very different from conventional pertroleum waxes. High-carbon-number straight-chain compounds are easily cracked and are excellent feedstocks in making high-quality diesel. Considerable caution must be exercised to prevent production of undesirable products (such as light paraffins and coke) because of overcracking.

Commercial applications to upgrade FT reactor wax are practiced at SASOL I with operation of the Arge reactor. A description of the practice is given in Sec. 5.2-4B. It is used primarily to make high quality waxes.

Development work on the processing of FT reactor waxes was carried out at Mobil, SASOL and Shell. Mobil's work was partially supported by DoE[72] and included the following scoping experiments to convert FT reactor wax from the high-wax mode of operation of the slurry FT reactor: thermal

cracking, hydrodewaxing, hydrocracking, and fluidized-bed catalytic cracking (FCC). Thermal cracking does not produce the final products but provides instead a practical way to separate catalyst fines from the wax when coupled with vacuum distillation. The overhead solid-free wax can then be further upgraded. The other three studies use commercial catalysts. To compare these processes, the useful targets are high conversion and low C_3-paraffin yield. Using these targets, the hydrodewaxing route is inferior to the other two.

Scoping hydrocracking resulted in a single-pass conversion of 72wt% (343°C- as products) and 93wt% G+D selectivity was achieved using a Ketjen 742 catalyst (CoMo on alumina). The unconverted fraction may be recycled to extinction. The diesel obtained had excellent quality, while the small amount of gasoline produced is low in octane number and needs further processing.

Some very interesting results were reported in scoping FCC processing of the same reactor-wax. Better than 90wt% single-pass conversion was easily achieved using Engelhard HEZ-53 catalysts (fresh, commercial equilibrium, and coked). Very high olefin yield (70wt%) was obtained. Contrary to conventional petroleum-based FCC operation, the coke yield was very small. The small unconverted fraction may again be recycled to extinction. The highly olefinic product from the FCC is an ideal feedstock for MOGD processing (see Sec. 5.2-3B) in making G+D. It was estimated that, by combining an FCC with a MOGD and an alkylation unit, a total G+D yield as high as 95wt% can be achieved. Both G and D are expected to have excellent qualities after conventional hydrofinishing of the D. All of these results were derived from scoping experiments. Improved results may be expected if optimizations on both catalysts and process conditions are carried out.

Dry has reported SASOL development work on mild hydrocracking of FT wax from its Arge reactor.[98] A yield structure of 5wt% C_4-/15G/80D was given. No process conditions or conversions were reported.

The work at Shell of FT wax upgrading is associated with its SMDS process (see Sec. 5.1-4C). The FT wax is produced from a direct heat-exchange reactor using a proprietary catalyst. The heavy, waxy HCs (mainly paraffins) are separated after passing through a separator and are

fed to a heavy paraffin conversion (HPC) reactor.[77] The HPC reactor uses a commercial Shell catalyst performing hydroisomerization and hydrocracking. The process may be operated in a gas oil or kerosene mode. No light paraffin yield and conversion were reported. The unconverted fraction (heavier than gas oil) is recycled to the HPC reactor to extinction.

5.3. Interaction of Coal Gasifiers with Synthesis Gas Conversion Processes

5.3-1. Introduction

Matching a coal gasifier with a synthesis gas conversion process is an important factor in determining the technical and economic viability of coal conversion processes. In commercial applications, the ultimate factor that determines the viability of the process is economics. Unfortunately, good and consistent economic comparisons of various processes are essentially non-existent because economic process calculations use information and assumptions that are generated without consistent guidelines. Fortunately, large economic differences obtained under consistent guidelines are almost always caused by technical features and vice versa. Consequently, searching for sensible technical differences constitutes good reasoning when judging one process combination against another. The objective of this section is to define sensible, technical reasons for properly matching a coal gasifier with a downstream SG conversion process.

Coal-conversion processes are simply energy-conversion processes, and high thermal efficiency is an essential factor in maintaining good process economics. High thermal efficiency reflects not only high recovery of raw material but also means that less equipment is needed to transfer mass and reject additional waste energy. Consequently, thermal efficiency comparisons are useful technical tools for process-economics comparisons.

The issues associated with integration of coal gasifiers with SG conversion processes are many. The downstream conversion process dictates a minimum partial pressure of the active compounds (H_2 and CO) in the SG. This minimum partial pressure is affected by three factors in the gasifiers: gasifier pressure, oxygen purity used, and the amount of light paraffins

(mainly CH_4) generated in the gasifiers. In addition, the SG pressure is changed by using either a gas compressor or an expander.

The H_2/CO ratio of the SG is another important issue. It is costly to decrease the H_2/CO ratio because of thermodynamic constraints. However, the use of a WGS unit to increase the H_2/CO ratio is a proven technology that adds substantially to the process cost. Furthermore, the SG conversion processes use catalysts that usually require SG with less than a defined minimum threshold level of impurities (ususally of H_2S and COS). Expensive SG purification units are needed to remove excess impurities.

Another important integration issue is the co-production of energies in various forms. There are actually two sub-issues involved here. One is the co-production of fuel gas and SNG with liquid fuels to achieve high thermal efficiency. In a coal-based synfuel plan, it is almost always more costly to have a process set up to produce only liquid fuels. By recycling the light HCs to make additional SG, 30-40% of the energy in the light HCs is easily lost. The other sub-issue is the co-production of steam and electricity, as in cogeneration. With proper integration and optimization of a coal gasifier with an SG-conversion process, the resulting high thermal efficiency results in a large surplus of steam or electricity. The steam may be exported to nearby factories as process steam or to nearby communites as utility steam, while the electricity is exported to the local utility network. Cogeneration is more often practiced outside than inside the US and is a desirable practice.

5.3-2. H_2+CO Partial Pressure Requirements

The degree of importance attached to high H_2+CO partial pressures in the SG depends strongly on the SG-conversion process. Molar contraction almost always occurs with SG conversion; consequently, the conversion is thermodynamically more favorable at higher H_2+CO partial presssures. However, the importance of this requirement varies with the conversion process. Generally speaking, conversion reactions that are limited by chemical equilibrium, such as MeOH syntheses, will require higher partial pressures. The FT reactions are less strongly constrained by equilibrium

considerations and may tolerate low H_2+CO partial pressures. This contrast is clearly illustrated in Fig. 5.3-1, which shows thermodynamic equilibrium

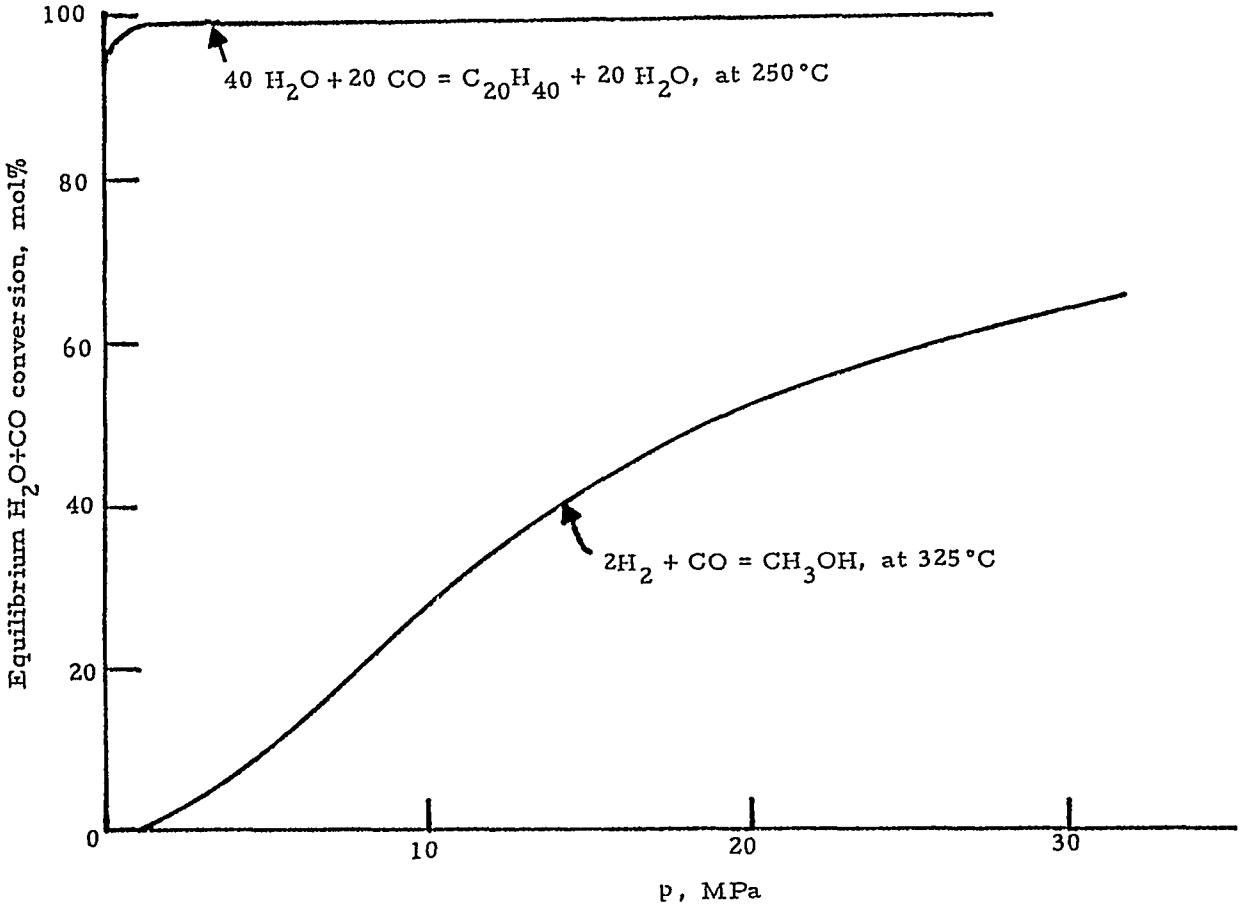

Fig. 5.3-1. H_2+CO conversion at thermodynamic equilibrium.

conversion for both reactions. For simplicity, a single reaction for C_{20} olefin formation is used to represent the FT reactions. In actual application, MeOH syntheses generally requires a minimum H_2+CO partial pressure of 600-700psia. Although the FT reactions may proceed to high H_2+CO conversion at low pressure, moderate to high partial pressures (200-1,000 psia) are usually used to improve process economics.

The easiest way to obtain the required H_2+CO partial pressure is to choose gasifiers operating at the proper pressure. If a low-pressure gasifier is used, the SG is simply compressed to the required value. The energy consumed for this compression may be very large if a coal-derived SG

at atmospheric pressure is compressed to 500-1,000psia; energy equivalent to 16-20% of the coal LHV will be needed to generate the compression work.[99] This reference also shows that the net thermal efficiencies of low-pressure gasifiers, such as the Kopper-Totzek and Winkler, are 15-20% lower than those of the moderate-pressure gasifiers used to produce clean, 400psia SG. This result implies that it is more efficient to compress the gasifier O_2 and use high-pressure steam for gasification than to compress the output SG and follows because the coal-gasification reactions are molar-expansion reactions and compression work increases linearly with the number of moles. However, the fuel penalty for gas compression is relatively smaller at high pressures (e.g., above 300psia) because the compression ratio is reduced. Thus, the best operating gasifier pressure ranges are 300-500 psia.

The other practical procedure for changing the H_2+CO partial pressure is to vary the purity of O_2 used for gasification. The thermodynamic constraint of the SG-conversion reactions again plays an important role in determining purity requirements for O_2. The requirement of high H_2+CO partial pressure in the conventional MeOH synthesis clearly demands SG from O_2 -blown gasifiers. The equilibrium H_2+CO conversion for MeOH synthesis at low temperature becomes so high that use of SG from air-blown gasifiers may become practical. FT synthesis may also tolerate SG from the air-blown gasifiers. This combination may, however, not be economical because it is costly to move large quantities of the inert gas (N_2) through the entire system. The procedure demands substantially larger facilities to handle all of the streams and results in larger energy degradation associated with heating and cooling N_2. The separation of HC products from the N_2 is also very costly. Furthermore, low H_2+CO partial pressure in the FT synthesis reactor may also induce undesirable effects such as high light HC yields and high catalyst-aging rates. It is preferable to use O_2-blown gasifiers. In theory, there is an optimal O_2 purity for any combination of gasifier and synthesis process. Unfortunately, these optimal oxygen purities are not generally known.

The last item that affects the H_2+CO partial pressure in the SG is the light paraffin content of the gas. The amount of CH_4 and ethane in the clean SG varies greatly with types of gasifiers and, to a lesser degree, with types of coals. Table 5.3-1 summarizes SG compositions of typical selected gasifiers. The H_2+CO compositions range from 82.6 to 99.3mol%.

Table 5.3-1. Properties of clean synthesis gas from typical coal gasifiers.

Operational parameters	Gasifier						
	Dry-ash Lurgi	Winkler	Koppers-Totzek	BGC-Lurgi slagger	Texaco	Shell-Koppers	KRW
Coal	Wyoming	German brown coal	TVA	Frances	Illinois No.6	Illinois No.6	Wyoming
Exit gasifier p, psia	430	30	20	365	600	435	415
Clean gas composition, mol%							
H_2	55.7	50.2	38.6	29.4	40.0	32.8	40.1
CO	26.9	46.1	60.1	58.4	58.8	66.5	52.4
CH_4	16.1	2.3	--	7.0	0.1	--	6.8
C_2	0.9	--	--	0.5	--	--	--
N_2	0.4	1.4	1.3	4.7	1.1	0.7	0.7
H_2/CO ratio	2.07	1.09	0.638	0.504	0.679	0.494	0.763
Clean gas LHV,%							
H_2+CO	59.7	93.0	100.0	79.5	99.6	100.0	81.8
C_1+C_2	40.3	7.0	--	20.5	0.4	--	18.2
Ref.	100	101	102	103	104	105	106

Generally, the gasifiers that allow long residence time for coal devolatiliztion (such as the dry-ash Lurgi) and the coals containing large amounts of volatiles (such as the Wyoming coals) produce the largest CH_4 and ethane yields. However, even the CH_4 and ethane content in the SG from the dry-ash Lurgi using Wyoming coal is tolerable for MeOH synthesis. The net effect is a somewhat higher total pressure requirement or as slightly lower H_2+CO conversion than is required for SG that contains little or no light paraffins.

The light paraffins in the SG affect the amount of chemical energy available for synthesis. For example, in the case of the dry-ash Lurgi with Wyoming coal, 40% of the chemical energy in the clean SG is in CH_4 and ethane (see Table 5.3-1). This yield is definitely inferior to the gases obtained from the Texaco and Shell-Koppers gasifiers. Of course, the CH_4 and ethane may be separated and then reformed to make H_2 and CO for use in the SG conversion process, but this recycle imposes a large (30-40%) thermal penalty.

5.3-3. H_2/CO Ratio Requirement

5.3-3A. Methanol Synthesis

Synthesis of MeOH from H_2 and CO requires a stoichiometric H_2/CO ratio of 2. In practice, the feed gas also contains some CO_2, which reacts with H_2 to make MeOH. The result is a stoichiometric $H_2/(2CO+3CO_2)$ ratio of 1. In commercial applications, this ratio in the fresh feed gas is slightly larger than 1 to provide a kinetic driving force; consequently, this synthesis requires an H_2-rich gas.

5.3-3B. Fischer-Tropsch Synthesis

Depending on the H_2/CO use ratio, FT processes may be classified into two groups according to catalyst types. One uses catalysts of little or no WGS activity while the other has significant WGS activity. A typical catalyst used in the first group is Co and in the second Fe.

For catalysts without WGS activity, the oxygen in the CO is rejected as water, which results in an H_2/CO use ratio of 2 in making olefins and alcohols and an H_2/CO use ratio slighly larger than 2 in making paraffins (see reactions (5.1-20 to 5.1-22). These catalysts thus always require high H_2/CO ratio gases.

For catalysts that promote the WGS reaction, the oxygen in CO will be mainly rejected as CO_2, i.e., the H_2O formed in the FT reaction reacts with the CO to form additional H_2 resulting in an apparent H_2/CO use ratio of 0.5 for olefin formation. However, because of formation of paraffins and oxygenates and the incompleteness of the WGS reaction, the actual mimimum H_2/CO use ratio is about 0.6. Consequently, low H_2/CO ratio gases can be used with these catalysts.

There are potential process limitations that result from the use of low H_2/CO-ratio gases in FT reactor, including excessive carbon formation, carbide formation, reaction heat generation, and reactor-wax formation. Based on the thermodynamics of the Boudouard reaction, the potential for carbon formation is proportional to the square of the CO partial pressure. The trend of carbide formation also depends strongly on CO

partial pressure. Excessive reaction-heat generation results directly from the possibility of high single-pass conversion when SG with an H_2/CO ratio close to the use ratio is employed. The FT HC product distribution is expected to shift to heavier compounds when the H_2/CO ratio of the feed is reduced. Consequently, low H_2/CO ratio gases promote reactor-wax formation.

In a fluidized-bed reactor such as the Synthol reactor, the carbon, carbide, and reactor-wax formation may strongly affect catalyst fluidization. In a direct heat-exchange reactor such as the Arge reactor, the carbon and carbide formation may cause reactor plugging. The excessive reaction heat generation may cause catalyst overheating. Consequently, higher H_2/CO ratio gases may be required, even with catalysts that have WGS activities for these two types of reactors.

Applications of SASOL technology are further complicated by use of the dry-ash Lurgi gasifier, which gives H_2/CO ratios ranging from 1.7-2.4.[59] The discussions in the proceding paragraphs are then irrelevant. However, the indicated constraints are important when low H_2/CO ratio gasifiers are employed.

Recycle operations are used in both the Synthol and Arge reactors at SASOL to achieve two goals: increase overall H_2+CO conversion and decrease overall WGS conversion. The second goal is achieved by the accumulation of CO_2 in the recycle gas to retard the WGS reaction. The recycle operation causes large increased in the H_2/CO use ratio to match the high H_2/CO ratios in the fresh feed. H_2/CO ratios for both Arge and Synthol reactors at SASOL I are summarized in Table 5.3-2

Slurry reactors using unsupported, precipitated Fe catalysts were demonstrated to give high single-pass H_2+CO conversion over a long period of time when using SG with 0.6-0.7 H_2/CO ratios.[68,71,72] This result is attributed to the following system properties: (i) micron-size, very active precipitated Fe catalyst with high WGS activity; (ii) a feed H_2/CO ratio close to the single-pass usage ratio; (iii) excellent temperature control in the slurry reactor; (iv) a slurry reactor that sustains catalyst disintegration; and (v) a slurry reactor that sustains reactor-wax formation. Consequently, low H_2/CO ratio SG may be used directly. The H_2/CO ratios for slurry FT reactors are also included in Table 5.3-2.

5.3-3C. Synthesis Gas H_2/CO ratios from Coal Gasifiers

Table 5.3-1 summarizes the H_2/CO ratios of the synthesis gases from typical gasifiers. The ratios range from 0.5 to 2.1. Shinnar and Kuo[99] evaluated the thermal efficiencies of various gasifiers and concluded that advanced, high-efficiency gasifiers use little steam (or water), thus producing low H_2/CO-ratio gases. Of course, it is easy to convert some CO in the gas to H_2 by adding steam in a separate WGS unit to obtain a higher H_2/CO ratio. However, a part of the efficiency gained by using the advanced gasifiers will then be negated because a WGS unit will require large amounts of steam and the construction of an a new unit and will also suffer thermal degradation because of additional cooling and heating. Furthermore, any SG conversion processes using high H_2/CO ratio gases must reject the oxygen in CO as H_2O and, therefore, has the inherent deficiency of pushing large amounts of additional water (or steam) through the downstream synthesis system. Since water has a very high latent heat, moving large amounts of water also implies a large movement of energy. This large movement of mass and energy strongly affects process economics, as was pointed out by El Sawy[107] and Jones.[108] It is therefore always prudent to adopt an SG-conversion using directly a low H_2/CO-ratio gas from an advanced gasifier.

5.3-3D. Use of Water-Gas Shift Units

A separate WGS unit may be employed to increase the H_2/CO ratio of any SG stream. WGS technologies are well-developed and commercially proven. Kuo[1] has given a concise review of WGS catalysts and chemistry. Chemical equilibrium in the WGS reaction leads to increasing H_2 formation with decreasing temperature. The equilibrium constant K_p is defined as $P_{H_2}P_{CO_2}/P_{CO}P_{H_2O}$ and is greater than 20 when T is less than 350°C. Although the WGS reaction attains equilibrium rapidly, the required exothermic reaction heat implies considerable effort in reactor design, especially for low H_2/CO ratio SG.

There are basically three types of WGS catalysts: high-temperature shift catalysts (HTS) operating at 440-700°C (Cr-Fe oxide

or Zn-Cr oxide); low-temperature shift catalysts (LTS), 230-350°C (Cu-Cr oxide); raw-gas shift catalysts (RGS), 180-550°C (Co-Mo sulfide). The

Table 5.3-2. H_2/CO ratios of FT reactors.

Parameter	SASOL I (from Ref.54) Slurry reactor[71,72]			
	Arge reactor	Synthol reactor	Low-wax mode	High-wax mode
Fresh feed	1.70	2.77	0.67	0.67
Tail gas	1.71	15.6	--	--
Combined feed	1.72	4.65	--	--
Usage	1.69	2.45	0.585	0.560

LTS catalysts are used mainly to achieve high CO conversion, which is important for H_2 and NH_3 syntheses but not for MeOH and FT syntheses. The HTS catalysts are relatively more stable and yield partial CO conversion which is sufficiently high to prepare the SG for MeOH and FT syntheses. Both LTS and HTS catalysts require a low sulfur level in the synthesis gas. On the other hand, the RGS catalysts require some sulfur in the gas to maintain activity. This feature adds the advantages of directly processing the raw gasifier gas without extensive cooling and cleaning. Part of the waste sensible heat in the raw gas may also be used to generate steam for the WGS reaction. Furthermore, a single SG purification unit may now be used to remove both the sulfur compounds and CO_2.

Further optimization of WGS operation may be possible by minimizing the amount of the excess steam in the feed gas and utilizing a low-temperature heat source to raise steam required for the WGS unit.

5.3-4. Purity Requirements for Synthesis Gas

Most of the impurities in the gasifier SG can easily be removed, except for sulfur compounds. Coal dust, ash, tar, and oil are removed by water washing or by mechanical means. Ammonia and phenol are removed by water washing.

Removal of sulfur compounds is essential since these may poison many catalysts in the downstream processes. There are many commercially established purification processes for removal of sulfur compounds. A concise review has been given by Kuo.[1] The maximum allowable sulfur levels depend on the catalyst used downstream; rough guidelines are provided in Table 5.3-3.

5.4. Zeolites as Shape-Selective Catalysts

5.4-1. Introduction

Zeolites may be viewed as solid analogs of such classical acids as sulfuric acid or aluminum chloride and have with them in commmon the ability to promote a large number of acid-catalyzed reactions, including polymerization, cracking, isomerization of olefins, paraffins and aromatics, alkylation of aromatics and of paraffins, transalkylation, and many others. Some, such as gas oil cracking, belong to the largest catalytic processes.

The first solid acid catalysts were activated natural clays and synthetic binary oxides, such as silica-alumina. Their acidic properties have been well described.[109] They have remained a very important class of catalysts, both as acidic catalysts and as acidic components in dual functional catalysts, by the addition of a second function of hydrogenation and oxidation, etc. The evolution and optimization of these catalysts has remained a highly empirical art, partly because these amorphous catalysts are difficult to characterize. By contrast, zeolites are crystalline porous solids that have a well defined pore system and large intracrystalline surface area.[110,111] It was discovered in the late fifties at the Mobil laboratories that catalytic reactions can take place inside these structures. This discovery marked the real beginning of zeolite catalysis.

Two aspects make zeolites unique. The intracrystalline surface is an inherent part of the crystal structure and hence topologically well defined, in sharp distinction to amorphous and even most crystalline solids for which the outer surface may be considered to be a crystal defect with atoms whose coordination number differs from atoms in the crystal. The second distinctive feature of zeolites is that the diameter of their pores

is uniform and of similar magnitude as that of many organic molecules of interest. Molecular sieving and shape selectivity, previously unknown with man-made catalysts, became possible.

Each zeolite has a unique pore system and crystal structure. Nature has provided us with 34 different zeolites.[111-114] However, among those of interest to catalysis, only a few are found in abundance. The ability to synthesize zeolites of known and new structures in the laboratory made new discoveries in zeolite catalysis possible. To date, nearly 100 synthetic zeolites have been identified covering a large variety of different framework structures, with pore openings ranging from less than 5 Å to larger than 10 Å.

In heterogeneous catalytic processes, one usually considers three major performance characteristics: activity, selectivity towards one or several products, and stability of operation, i.e., low catalyst aging. These performance features are complex, interacting functions of

Table 5.3-3. Approximate minimum allowable sulfur levels for selected catalysts.

Catalysts	Minimum sulfur level (ppmv)
Low-p methanol	1
High-p methanol	Higher than 1
FT, except Mo-based	1-2
Mo-based FT	20
LTS and HTS WGS	1
RGS WGS	Very high

several basic catalyst properties: sorption energies for feeds and products; rates of transport of molecules to and from the active sites (mostly by diffusion); and intrinsic activities for various reactions. With zeolites, it has now become possible to vary these properties in a systematic way and one at a time.

5.4-2. Classification of Zeolites

Zeolites are porous tectosilicates,[110] i.e., three-dimensional

networks built up of TO_4-tetrahedra (T = Si or heteroatom) such that each of the four oxygen atoms is shared with another tetrahedron. The most common forms are alumino-silicates, although structures containing boron, gallium or iron in place of aluminum and germanium in place of silicon have been reported.[110] The tetrahedron can link up to form a variety of secondary building units from which zeolites of various framework topologies are derived. Meier and Olson[113] have summarized the structures of 38 zeolites; in addition, the framework topologies of ZSM-12,[115] ZSM-22,[116,117] ZSM-23,[118] and of ZSM-48[119] and others have been described. Altogether, the crystal structure of about 50 zeolites is now known.[120]

The structure characteristics of greatest interest for catalysis is the channel system, which is described for some of the more important zeolites in Table 5.4-1. Depending on the largest channel, zeolites are characterized as small, medium or large pore zeolites if they contain apertures made by rings of 8, 10 or 12 linked tetrahedra. Framework structures and pore openings of representative zeolites of each group are depicted in Fig. 5.4-1. Within each group, there is considerable variation in the aperture, both in size and ellipticity. For example, the opening in Linde A is circular (4.1 Å), but in erionite it is elliptical (3.6 x 5.2 Å).

The projections of a series of similar zeolites (Fig. 5.4-2) show the subtle variations of channel dimensions and shapes available. The channel system may be one-dimensional, e.g., ZSM-22, ZSM-48, two-dimensional as in ferrierite, or three-dimensional as in ZSM-5 (Fig. 5.4-3). Multi-dimensional channels often intersect each other, but this is not always the case. The interconnecting channels can be of the same size (e.g., faujasite) or smaller (ferrierite); they may be straight (ZSM-11) or tortuous (ZSM-5). The connectivity of the channel system has major consequences for diffusion and aging characteristics. For example, zeolites with one-dimensional channels are more subject to deactivation than those with a three-dimensional pore system because of their susceptibility to pore mouth plugging.

The pores in some zeolites are relatively uniform tubes, e.g., in ZSM-48 (Fig. 5.1-3); in other zeolites, they contain larger cavities (e.g., erionite, Linde A) or supercages (e.g., zeolite Y, Fig. 5.4-1) which are connected by windows. Zeolites containing large cavities are more prone

to deactivation since molecules such as condensed aromatics can form but cannot escape through the smaller port holes and are trapped.[121,122] Most medium pore zeolites have pores of uniform dimensions. This particular feature is believed to account for their unusually low coke-forming propensity in acid-catalyzed reactions. Their non-aging character is one of the major contributing factors to the successful industrial applications of these zeolites.

Table 5.4-1. Channel system of representative zeolites.

Structure Type	Ring Size of Channels[a]	Largest Channel, A[b]
Linde Type A	8-8-8	4.1
Chabazite	8-8-8	3.6 x 3.7
Erionite	8-8	3.6 x 5.2
ZSM-22	10	4.5 x 5.5
ZSM-23	10	4.5 x 5.6
ZSM-48	10	5.3 x 5.6
Ferrierite	10-8	4.3 x 5.5
ZSM-5	10-10	5.4 x 5.6
ZSM-11	10-10	5.1 x 5.5
ZSM-12	12	5.7 x 6.1
Linde Type L	12	7.1
Mazzite	12	7.4
Mordenite	12-8	6.7 x 7.0
Offretite	12-8-8	6.4
Faujasite	12-12-12	7.4

(a) Number of either T- or O-atoms forming the smallest rings of the channels.

(b) Crystallographic free diameter, based on an oxygen radius of 1.35Å, of the smallest ring or window in the channel.

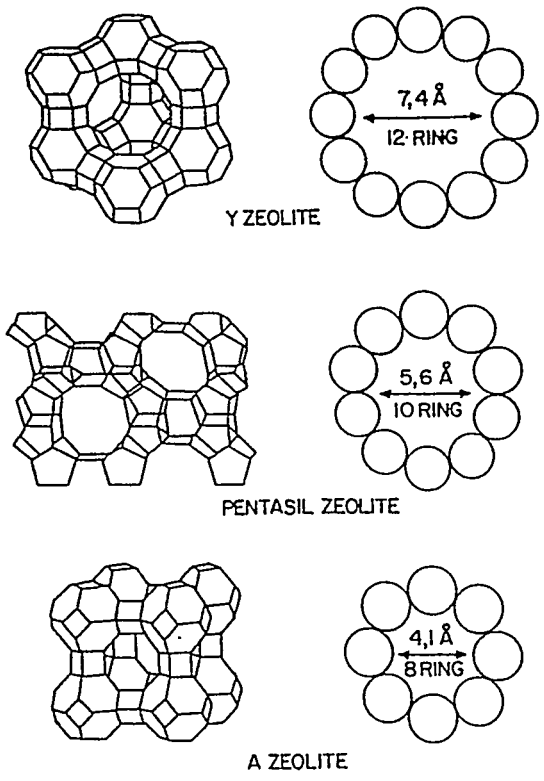

Fig. 5.4-1. Framework structures and projections of representative large, medium, and small pore zeolites.

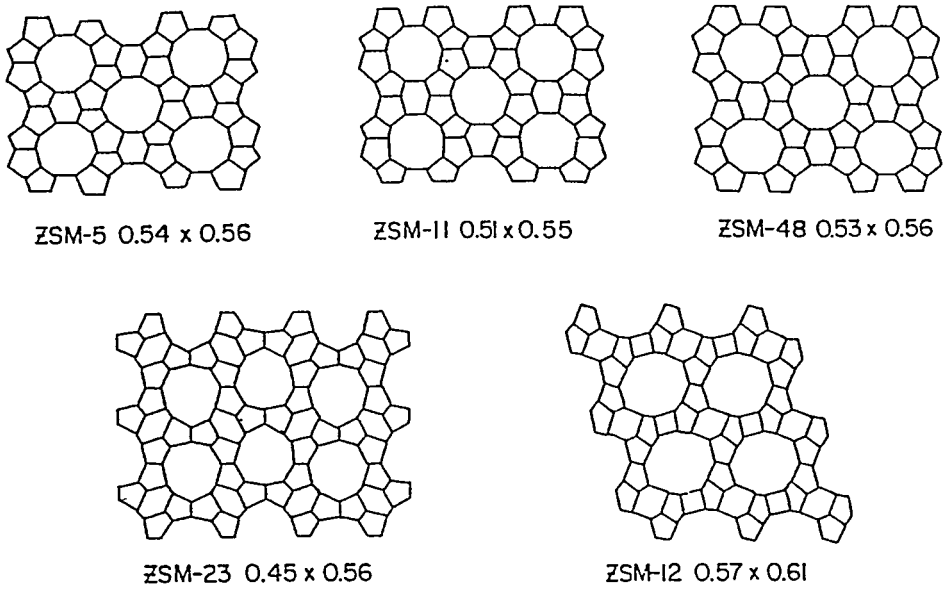

Fig. 5.4-2. Projections of ZSM-5, -11, -12, -23, and -48 structures. The axes of the channels (in nm) are indicated.

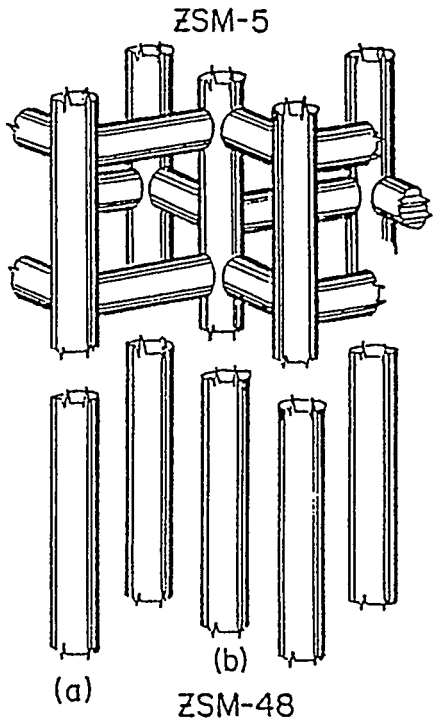

Fig. 5.4-3. Schematic channel system of ZSM-5 (three-dimensional) and ZSM-48 (one-dimensional).

Zeolites with 8-membered rings sorb only straight chain molecules such as n-paraffins, n-olefins and primary alcohols. Some larger pore zeolites also behave like small pore zeolites, when their structure contains many stacking faults which reduce the effective pore diameter. Examples are gmelinite, stilbite, dachiardite, Linde T, ZSM-34, epistilbite, heulandite/clinoptilolite, ferrierite, etc.

Medium pore zeolites with 10 membered ring systems are of most interest as shape selective catalysts. Not only do they sorb straight, chain molecules, they also can discriminate, either by size exclusion or by rate of diffusion, among a variety of branched and cyclic molecules. Included in this group are ZSM-5, ZSM-11, ZSM-22 (Theta-1), ZSM-23, ZSM-48, and ferrierite.

The 12-membered ring zeolites include all the large pore zeolites. The synthetic faujasites, zeolite X and Y, and mordenite are the best known and most studied zeolites in this group.

The silica to alumina ratios of different zeolites structures are

another distinguishing feature. Within each group, the ratio can be varied, especially with medium pore silica-rich zeolites. Figure 5.4-4 shows the compositional ranges for selected zeolites structures.

5.4-3. Intrinsic Catalytic Properties of Zeolites

The acid activity of zeolites depends on the presence of three-valent ions such as Al^{3+} in the zeolite framework of share SiO_4-tetrahedra. Without their presence, crystalline or amorphous silicas have no acid activity. These Al-ions give rise to Bronsted acid sites whose structure is depicted in Fig. 5.4-5.

The catalytic activity in HZSM-5 preparation with an Si/Al from about 17 to 180,000 has been found to be strictly proportional to their aluminum concentration and hence to their contents of active sites, which range from 5.6×10^{16} to 5.6×10^{20} sites per gram. The correlation line goes through the origin (Fig. 5.4-6). The proportionality between activity and number of Al atoms indicates that every acid site contributes equally to the observed activity, independently of the total site concentration.

5.4-4. Shape Selectivity

Molecular shape-selective catalysis in zeolites can be obtained when the dimensions of reactant or product molecules approach those of the intercrystalline pores. Several reviews describe the phenomenological aspects of shape selectivity.[123, 124]

Two different mechanisms operate to cause shape selectivity. In one, selectivity results from a large difference in the diffusivity of the participating molecules in the zeolite channels (mass transport selectivity). In the other, selectivity is caused by steric constraints in the transition state of the catalytic transformation step (transition state selectivity).

The unique properties of zeolites as acid catalysts has led to their rapid commercial utilization. A summary of processes in which zeolite catalysts have been used is shown in Table 5.4-2.

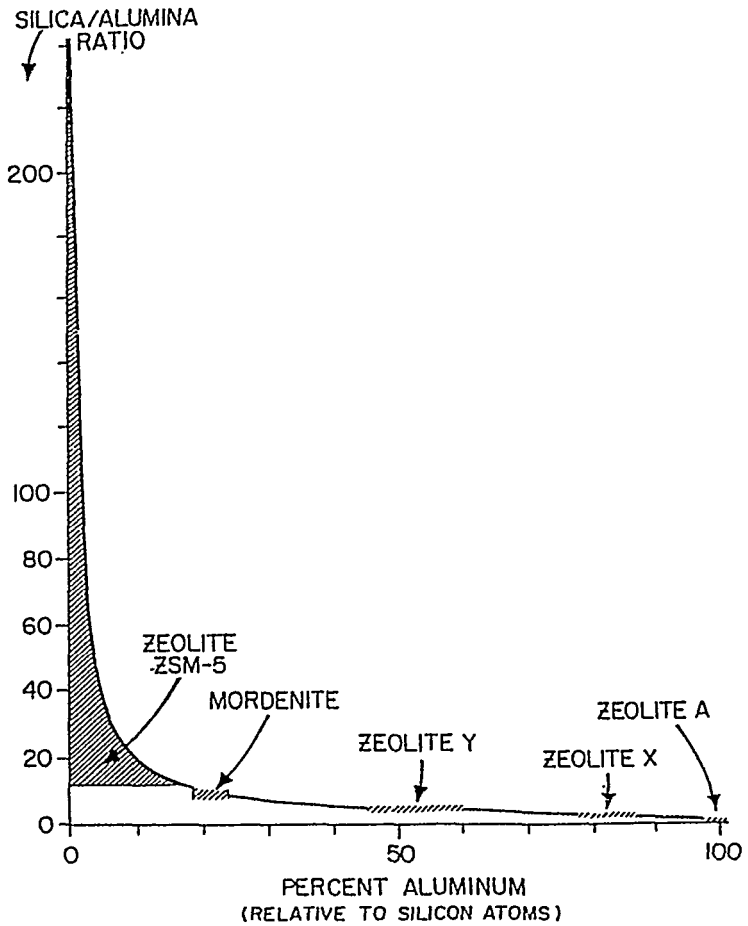

Fig. 5.4-4. Aluminum concentration and silica/alumina ratio for various zeolites.

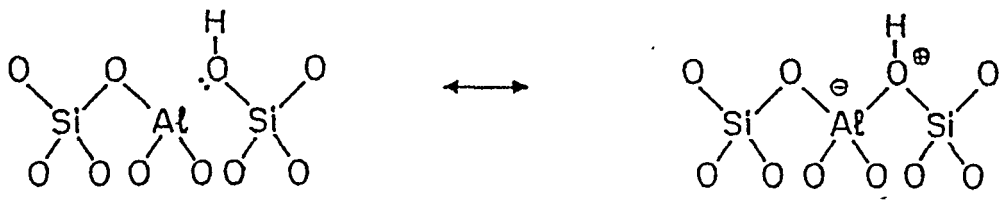

Fig. 5.4-5. The structure of the Bronsted acid site in zeolites.

Table 5.4-2. Processes utilizing zeolite catalysts.

Process	Application	Catalyst
Cracking	Gas oil to gasoline and Distillates	REY, US-Y ZSM-5
Hydrocracking	Heavy fractions to naphtha and distillates	ME + REX, REY, US-Y
Hysomer	Isomerization of pentane and hexane	Pt/mordenite
Selectoforming	Post reforming process	Erionite
M-Forming	Upgrading of reformate	ZSM-5
MDDW, MLDW	Dewaxing of distillates and lube oil	"
MLPI, MVPI, MHTI	Xylene isomerization	"
MTDP	Toluene disproportionation	"
MEB	Ethylbenzene synthesis	"
MOGD	Conversion of olefins to gasoline and distillate	"
MTG	Methanol conversion to gasoline	"
MTO	Methanol conversion to olefins	"
M2-Forming	Formation of aromatics from paraffins and olefins	"
Para Selective	Synthesis of p-ethyltoluene, synthesis of p-xylene from toulene	"

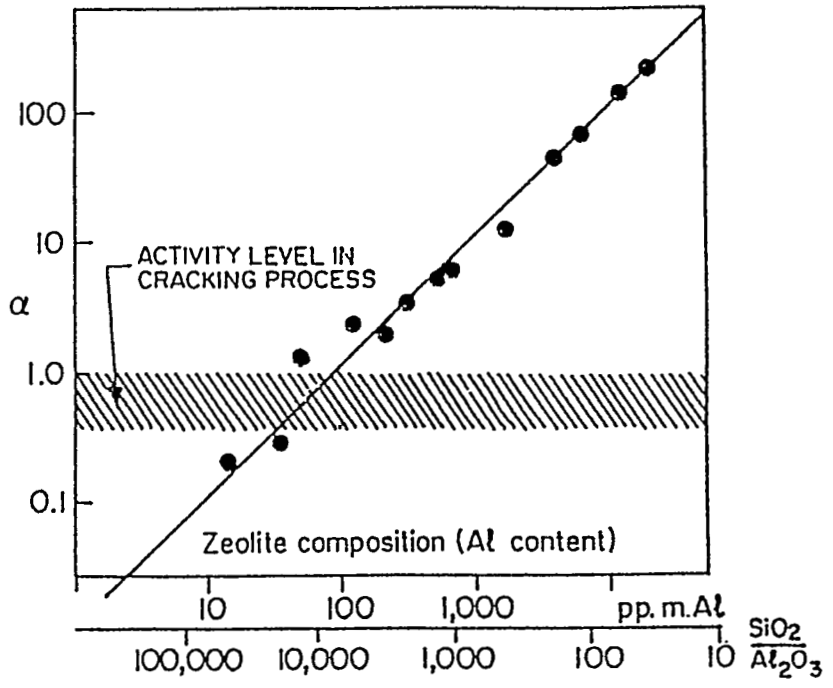

Fig. 5.4-6. The hexane cracking activity[83] α plotted agains the aluminum content in HZSM-5. The shaded band indicates activities near $\alpha \simeq 1$.

References

1. J. C. W. Kuo, "Gasification and Indirect Liquefaction" in The Science and Technology of Coal and Coal Utilization, B. R. Cooper and W.A. Ellingson, eds., Plenum Publ. Corp. NY (1984).
2. F. Fischer and H. Tropsch, Brennst. Chem. 4, 276 (1923).
3. P. Sabatier and J. B. Senderens, Ann. Chim. Phys. 4, 418 (1905).
4. G. Natta, "Methanol," in Catalysis, Vol. 3, P. H. Emmett ed., Reinhold Publ. Corp. NY (1955).
5. S. Strelzoff, "Methanol: Its Technology and Economics," pp. 54-68 in Methanol Technology and Economics, G. A. Donner ed., AIChE Symposium Series 66, No. 98 (1970).

6. A. Stratton, D. F. Hemning and M. Teper, "Methanol Production from Natural Gas or Coal," IEA Coal Research, EAS Report No. E4/82, London, England (Dec. 1982).
7. G. C. Chinchen, P. J. Denny, D. G. Parker, G.D. Short, M.S. Spencer, K.C. Waugh, and D.A. Whan, ACS Preprints (Div. of Fuel Chem.) 29, 178 (1984).
8. H. H. Kung, Catal. Rev. -Sci. Eng. 22, 235 (1980).
9. K. Klier, Adv. Catal. 31, 243 (1982).
10. A. Ya Rozovski, G. Lim, L. B. Liberov, E. V. Slivinskii, S. M. Loktev, Yu. B. Kagan, and A.N. Bashkirov, Kinetics and Catalysts (English translation) 18, 691 (1977).
11. M. L. Poutsma, L.F. Clek, P.A. Ibarabia, A. P. Risch, and A. J. Rabo, J. Catal. 52, 157 (1978).
12. R. G. Herman, K. Klier, G. W. Simmons, B. P. Finn, J. B. Bulko, and T. P. Kobylinsky, J. Catal. 56, 407 (1979).
13. F. Marschner F. W. Moller and R. Schulze-Bentrop, "Methanol from Synthesis Gas," Chap. 9 in Chemical Feedstocks from Coal, J. Falbe ed., John Wiley & Sons, NY (1982).
14. C. N. Satterfield, Heterogeneous Catalysts in Practice, pp. 295-301, McGraw-Hill, NY (1980).
15. J. Klosek and R. J. Mednik, "Progress in Liquid-Phase Methanol Snythesis," in Ninth Annual EPRI Contractor's Conference on Coal Liquefaction, Palo Alto, CA (May 8-10, 1984).
16. J. W. Evans, P. W. Casey, M. S. Wainwright, D. L. Trimm, and N. W. Cant, Appl. Catal. 7, 31 (1983).
17. H. Brendlein, German Patent No. 809, 803 (Aug. 2, 1951).
18. H. F. Woodward, Jr., "Methanol," pp. 370-398 in Kirk-Othmer Encycl Chem. Technol., 2nd ed., Vol. 13, John Wiley & Sons, NY (1967).
19. P. A. Buckingham, D. D. Cobb, A. A. Leavitt, and W. G. Synder, "Coal-to-Methanol. An Engineering Evaluation of Texaco Gasification and ICI Methonal Synthesis Route," EPRI Report No. AP-1962, Project No. 832-4, Palo Alto, CA (1981).
20. J. P. Leonard and M. E. Frank, Chem. Eng. Progr. 75, 68 (1979).
21. D. R. Simbeck, R. L. Dickensen and E. D. Oliver, EPRI Report No. AP-3109, Project No. 2207, Palo Alto, CA (June 1983).

22. F. H. Kant, R. P. Cahn, A. R. Cunningham, M. H. Farmer and W. Herbst, "Feasbility Study of Alternative Fuels for Automotic Transportation," EPA-4603-74-009A, Band C, Exxon Res. and Engrg. Co., Linden NJ (June 1974).
23. J. Pangorn and J. Gillis, "Alternative Fuels for Automotive Transportation - A Feasibility Study," EPA-460/3-74-012-a,b,f, Institute of Gas Technology, Chicago, IL (July 1974).
24. G. J. Anderson, B. Berger, J. Carlson, W. Crothers, D. Gregg, and A. Pasternack, "LLL Contribution to the AEC Methanol Report: Fuel Utilization and Environmental Impact," UCB/LBL, CA, UCID-1642 Lawrence Livermore Labs., Livermore, CA (January 18, 1974).
25. P. E. Cassady, "The Use of Methanol as a Motor Vehicle Fuel," paper presented at the 169th ACS National Meeting, Philadelphia, PA (April 6-11, 1975).
26. D. L. Hagen, Ph.D. Thesis, University of Minnesota, Minneapolis, MI (December 1976).
27. Royal Swedish Academy of Sciences and the Swedish Methonal Development Co., "Methanol as a Fuel," Proc. Symp., Stockholm, Sweden (March 23, 1976).
28. Chem. Eng. News. pp. 9-15 and pp. 31-35 (July 16, 1984).
29. J. H. Finegold, J. T. McKinnon and M. E. Karpuk, "Dissociated Methanol as a Combustion Hydride for Automobile and Gas Turbines," paper presented at the World Hydrogen Energy Conference IV, Pasadena, CA (June 1984).
30. N. M. Woodley, D. A. Nordman, J. R. Legro, and D. G. Davies, "Reformed Alcohol Fuels for Combustion Turbines: Technical and Economic Feasbility Assessment," Report No. AST-82-1683, Westinghouse Electric Corp., Pittsburgh, PA (1982).
31. C. E. Lucke and S. M. Woodward, "Use of Alcohol and Gasoline in Farm Engines," USDA Farmers Bulletin, Washington, D.C. (1907).
32. T. Tarr and J. R. Jones, "Ethanol in Motor Gasoline," pp. 55-70 in Monohydric Alcohols, Manufacture, Applications and Chemistry) E. J. Wickson ed., ACS Symposium Series 159 (1981).
33. M. Ichikawa, ChemTech. 12, 674 (1982).
34. I. Wender, R. Levine and M. Orchin, J. Am. Chem. Soc. 71, 4160 (1949).
35. M. E. Fakley and R. A. Head, Appl. Catal. 5, 3 (1983).

36. R. A. Fiato, US Patent No. 4,233,460 (1980).
37. R. A. Fiato, US Patent No. 4,253,987 (1981).
38. M. J. Chen, H. M. Feder and J. W. Ruthke, J. Am. Chem. Soc. 104, 7346 (1982).
39. R. B. Anderson, The Fischer-Tropsch Synthesis, Academic Press, NY (1984).
40. P. Courty, D. Durand, E. Freund, and A. Sugier, J. Mol. Catal. 17, 241 (1982).
41. J. Haggin, Chem. Eng. News. pp. 7-13 (May 19, 1986).
42. Chem. Eng. News, p. 35 (June 9, 1986).
43. H. H. Storch, N. Golumbic and R. B. Anderson, The Fischer-Tropsch and Related Syntheses, John Wiley & Sons, NY (1951).
44. T. J. Huang and W. O. Haag, "Aromatic Gasoline from Hydrogen/Carbon Monoxide Over Ruthenium/Zeolite Catalysts," in Catalyst Activation of Carbon Monoxide, P. C. Ford ed., ACS Symposium Series 152 (1981).
45. C. B. Murchison, "Synthesis Gas to Hydrocarbon Feedstocks," paper presented at the 182nd ACS National Meeting (Div. of Ind. & Eng. Chem.), NY (August 23-28, 1981).
46. H. Koelbel and M. Ralek, Catal. Rev.-Sci. Eng. 21, 225 (1980).
47. P. L. Flory, Principles of Polymer Chemistry, Cornell University Press, Ithaca, NY (1967).
48. M. E. Dry, "The Fischer-Tropsch Synthesis," Chap. 4 in Catalysis Science and Technology, J. R. Anderson and M. Boudart ed., Springer Verlag, NY (1981).
49. M. E. Dry, Hydrocarbon Processing 59, 92 (February 1980).
50. M. E. Dry. T. Shingles, L. J. Boshoff, C. S. van H. Botha, J. Catal. 17, 347 (1970).
51. F. Fischer and H. Tropsch, Brennst, Chem. 7, 97 (1926).
52. S. Z. Roginsky, "Molecular Mechanism of Some Catalytical Reactions as Revealed by Means of Isotopic Kinetic Effects and Experiments with Tracer Molecules," pp. 939-956 in Proceedings of the Third International Congress on Catalysis, W. M. H. Sachtler, G. C. A. Schuit and P. Zwietering eds., Amsterdam, Netherlands (July 20-25, 1964).
53. H. von Pichler and H. Schulz, Chem. -Ing. -Tech. 42, 162 (1970).
54. "Carbon Monoxide-Hydrogren Reactions," pp. 446-489 in Kirk-Othmer Encycl. of Chem. Technol. Vol. 4, John Wiley & Sons, NY (1964).

55. H. von Pichler, Brennst. Chem. 30, 105 (1949).
56. J. C. Hoogendoorn, "Experience with Fischer-Trpsch Synthesis at SASOL," in Clean Fuels from Coal Symposium Papers, IGT, Chicago, IL (September 10-14, 1973).
57. J. C. Hoogendoorn, "New Applications of the Fishcer-Tropsch Process", in Clean Fuels from Coal Symposium Papers, IGT, Chicago, IL (June 23-27, 1975).
58. T. D. Pay, "Foreign Coal Liquefaction Technology Survey and Assessment, SASOL-The Commercial Experience," Gilbert Associates, Inc., ORNL/Sub-79/13827/4 (1980).
59. J. C. Hoogendoorn and J. H. Salomon, Brit. Chem. Eng. 2, 308 (1957).
60. D. Gray, M. Lytton, M. B. Neuworth, and G. Tomlinson, "THe Impact of Developing Technologies on Indirect Liquefaction," Final Report (MTR-80W326), DoE Contract No. EF-77-C-01-2783, Mitre Corp., McLean VA (November 1980).
61. W. Faragher and J. Foucher, "The CO+H_2 Synthesis at I. G. Farben," p. 123 in F.I.A.T. Final Report 1267, PB 97368, Vol. 1, Part C, (1947).
62. M. J. Baird, R. R. Schehl, W. P. Haynes, and J. T. Cobb, Jr., IE&C Prod. Res. Dev. 19, 175 (1980).
63. F. Duftschmid, E. Linckh and F. Winkler, US Patent No. 2,159,077 (May 23, 1939).
64. M. L. Kastens, L. L. Hirst and R. G. Dressler, Ind. Eng. Chem. 44, 450 (1952).
65. F. Fishcher, O. Roelen and W. Feist, Brennst. Chem. 13, 461 (1932).
66. C. C. Hall, D. Gall and S. L. Smith, J. Inst. Petr. Technolog. 38, 845 (1952).
67. M. D. Schlesinger, H. Benson, E. Murphy, and H. H. Storch, Ind. Eng. Chem. 46, 322 (1954).
68. H. Koelbel, P. Ackerman and F. Engelhardt, p. 227 in Proceedings of Fourth World Petroleum Congress, Section IV/C, Carlo Colombo Publishers, Rome (1955).
69. A. K. Mitra and A. N. Roy, Indian Chem. Eng. 5, 127 (1963).
70. T. Sakai and T. Kunugi, Sekiyu Gakkai Shi 17, 863 (1974).
71. J. C. W. Kuo, "Slurry Fischer-Tropsch/Mobil Two-Stage Process of Converting SG to High Octane Gasoline," Final Report (DoE/PC/30022-10) DoE Contract No. DE-AC22-80PC30022, Mobil Res. and Dev. Copr., Paulsboro, NJ (June 1983).

72. J. C. W. Kuo, "Two-Stage Process for Conversion of Synthesis Gas to High Quality Transportation Fuels," Final Reports (DoE/PC/60019-9 and -9A) DoE Contract No. DE-AC22-83PC60019, Mobil Fes. and Dev. Corp., Paulsboro, NJ (October 1985).
73. H. E. Benson, J. H. Field, D. Bienstock, and H. H. Storch, Ind. Eng. Chem. 46, 278 (1954).
74. R. Farley and D. J. Ray, J. Inst. Pet. Technology 50, 27 (1964).
75. T. Kunugi, T. Sakai and N. Negishi, Sekiya Gakkai Shi 11, 636 (1968).
76. M. E. Dry, "Recent Developments in SASOL Fischer-Tropsch Technology," paper presented at 191st ACS National Meeting (Div. of Fuel Chemistry), NY (April 13-18, 1986).
77. M. J. van der Burgt, J. van Kliken and S. T. Sie, "The Shell Middle Distillate Synthesis Process," paper presented at the 5th Synfuels Worldwide Symposium, Washington, D.C. (November 11-13, 1985).
78. A. H. Singleton and S. Regier, Hydrocarbon Proc. 62, 71 (1983).
79. A. Aquilo, J. S. Alder, D. N. Freeman, and R. J. H. Voorhoeve, Hydrocarbon Processing, pp. 57-65 (March 1983).
80. J. F. Knifton, ChemTech 609 (1981).
81. S. L. Meisel, J. P. McCullough, C. H. Lechthaler, and P. B. Weisz, Chem Tech 6, 86 (1976).
82. C. D. Chang, Catal. Rev. -Sci. Eng. 25, 1 (1983).
83. C. D. Chang and A. J. Silvertri, J. Catal. 47, 249 (1977).
84. J. E. Penick, W. Lee, and J. Maziuk, ACS Symposium Series 226, 19 (1983).
85. C. D. Chang and A. J. Silvertri, "The MTG Process: Origin and Evolution," paper presented at the 21st State-of-the-Art ACS Symposium on Methanol as a Raw Material for Fuels and Chemicals, Marco Island, FL (June 15-18, 1986).
86. A. A. Avidan, M. Edwards, W. Loeffler, H. -H. Gierlich, N. Thiagarajan, and E. Nitschke, "The Fluid-Bed MTG PRocess," in Ref. 85.
87. E. Supp, Energy Progr. 5, 127 (1985).
88. R. F. Socha, C. T. W. Chu and A. A. Avidan, "An Overview of Methanol-to-Olefins Research at Mobil: From Inception to Demonstration Plant," in Ref. 85.

89. J. L. Soto and A. A. Avidan, "Status of the 100 BPD Fluid-Bed Methanol-to-Olefins Demonstration Plant," in Proceedings of the 5th DoE Contractors Conference on Indirect Liquefaction, Houston, TX (December 2-5, 1985).
90. S. A. Tabak, A. A. Avidan and F. J. Krambeck, "MTO-MOGD Process," in Ref. 85.
91. W. Hoelderich, H. Eichhorn, R. Lehnert, L. Marosi, W. Mross, R. Reinke, W. Rappel, and H Schlimper, pp. 545-555 in Proceedings of the 6th Int. Zeolite Conference (1983).
92. A. Brink, "New Developments in the Field of Fischer-Tropsch Synthesis," paper presented at the 50th API Refining Department Mid-Year Meeting, Kansas City, MO (May 13-16, 1985).
93. S. A. Tabak and F. J. Krambeck, Hydrocarbon Proc. 64, 72 (September 1985).
94. S. A. Tabak, A. A. Avidan and F. J. Krambeck, "Production of Synthetic Gasoline and Diesel Fuel from Non-Petroleum Resources," presented at the 191st ACS National Meeting (Div. of Fuel Chemistry), NY (April 13-18, 1986).
95. J. C. Hoogendoorn and J. H. Salomon, Brit. Chem. Eng. 2, 368 (1957).
96. M. E. Dry, ChemTech 12, 744 (1982).
97. J. C. W. Kuo, U.S. Patent No. 4,046,830 (September 6, 1977).
98. M. E. Dry, Proceedings of the 10th Annual COGLAC International Conference, Pittsburgh, PA (August 1983).
99. R. Shinnar and J. C. W. Kuo, "Gasifier Study for Mobil Coal to Gasoline Processes," Final Report No. FE-2766-13, DoE Contract No. EF-77-C-01-2766, Mobil Res. and Dev. Corp., Paulsboro, NJ (October 1978).
100. M. Schreiner, "Research Guidance Studies to Assess Gasoline from Coal by Methanol-to-Gasoline and SASOL-Type Fischer-Tropsch Technologies," FE-2447-13, Mobil Res. and Dev. Corp., Paulsboro, NJ (August 1978).
101. C. E. Jahnig, "Evaluation of Pollution Control in Fossil Fuel Conversion Processes, Gasification, Section 8: Winkler Process," Exxon Res. and Eng. Corp., PB-249-846 September 1975).
102. D. A. Waitzman H. L. Faucett, D. E. Nichols, S. V. Tomlinson, and W. J. Broadfoot, "Evaluation of Intermediate-Btu Coal Gasification Systems for Retrofitting Power Plants," TVA, EPRI AF-531, Palo Alto, CA (August 1977).

103. British Gas Corporation, "Reports on Runs TSP 001-001-002-003 (Westfield Slagger)," Westfield, Scotland (October-November 1977).
104. K. Chandra, B. McElmurry, E. W. Neben, and G. E. Pauk, "Economic Studies of Coal Gasification for Combined Cycle System for Electric Power Generation," Fluor Engineers and Constructors, Inc., EPRI AF-642, Palo Alto, CA (January 1978).
105. E. V. Vogt and M. H. van der Burgt, CEP 76, 65 (1980).
106. D. Gray, M. B. Neuworth and G. Tomlinson, "Further Studies on Developing Technology for Indirect Liquifaction," DoE Report DE-AC01-77ET10280, MITRE Corp., McLean VA (March 1982).
107. A. El Sawy, D. Gray, M. B. Neuworth, and G. Tomlinson, "A Techno-Economic Assessment of the Mobil Two-Stage Slurry Fischer-Tropsch/ZSM-5 Process," Final Report No. MTR-84W173, DoE Contract No. 58-0336, MITRE Corp., McLean, VA (November 1984).
108. W. S. Jones J. Shen and E. Schmetz, "Liquid Fuels from Coal Derived Synthesis Gas," in Reg. 94.
109. K. Tanabe, Solid Acids and Bases, Academic Press, NY (1970).
110. R. M. Barrer, Hydrothermal Chemistry of Zeolites, Academic Press, London (1982).
111. D. W. Breck, Zeolite Molecular Sieves , Wiley-Interscience, NY (1974).
112. R. M. Barrer, Chem. Ind. (London) 1203 (1968).
113. W. M. Meier and D. H. Olson, "Atlas of Zeolite Structure Types", Intern. Zeolite Assocn., Polycrystal Book Service, Pittsburgh, PA (1978).
114. W. M. Meier, Z. Kristallogr 115, 439 (1979).
115. R. B. La Pierre, A. C. Rohrman, Jr., J. L. Schlenker, J. D. Wood, M. K. Rubin, and W. J. Rohrbaugh, Zeolites 5, 346 (1985).
116. G. K. Kokotailo, J. L. Schlenker, F. G. Dwyer, and E. W. Valyocsik, Zeolites 5, 349 (1985).
117. S. A. I. Barri, G.W. Smith, D. White, and D. Young, Nature 312, 533 (1984).
118. A. C. Rohrman, Jr., R. B. La Pierre, J. L. Schlenker, J. D. Wood, E. W. Valyocsik, M. K. Rubin, J. B. Higgins and W. J. Rohrbaugh, Zeolites 5, 382 (1985).
119. J. L. Schlenker, W. J. Rohrbaugh, P. Chu, E. W. Valyocsik and G. T. Kokotailo, Zeolites 5, 355 (1985).

120. R. von Ballmoos, Collection of Simulated XRD Powder Patterns for Zeolites, Butterworth Scientific Publ., Guildford, UK (1984).
121. P. B. Venuto, L.A. Hamilton and P.S. Laudis, J. Catal, 5, 484 (1966).
122. P. B. Venuto and P. S. Laudis, Avd. Catal. 18, 259 (1968).
123. S. M. Csicsery, Zeolites 4, 202 (1984).
124. S. M. Csicsery, "Shape Selective Catalysis" in Zeolite Chemistry and Catalysis, J. A. Rabo ed., Am. Chem. Soc. Monograph 171, 680 (1976).

CHAPTER 6:
COAL GASIFICATION IN FUEL-CELL APPLICATIONS

A potentially important application of coal gasifiers (CGs) involves gas processing for use in fuel cells (FCs). In this chapter, we present first an overview of FC development status and then discuss design features of CGs for these uses.

6.1. Overview of FCs*

In order to appreciate gasifier requirements properly, it is desirable to begin with a description of salient features of fuel-cell operation.

6.1-1. Introduction

Hydrogen-containing fuels have two heating values (molar heats of combustion), corresponding to the formation of water in the gaseous state (low-heating value, LHV) or in the liquid state (high-heating value, HHV). The free energy of reaction of the fuel, i.e., the maximum energy theoretically available as work, also has two values. While the heat of reaction shows only a small change with temperature, the free energy of reaction varies nearly linearly according to the relation

$$\Delta G = \Delta H - T \Delta S, \qquad (6.1\text{-}1)$$

---

* This section has been written by A. J. Appleby, Electric Power Research Institute (EPRI), 3412 Hillview Ave., Palo Alto, CA 94303. Figures, illustrations and design diagrams have been deleted but may be found in the publication of the DoE Advanced Fuel Cell Working Group. Energy 11, 1-229 (1986).

where ΔH is the heat (enthalpy) of reaction, ΔG the free energy or chemical potential, ΔS the entropy of reaction, and T the absolute temperature. When the combustion reaction has been completed, the free energy of reaction is close to zero, no remaining chemical potential exists which can be converted directly into work, and the heat of reaction is transformed into ambient heat equal to $T\Delta S$ at temperature T. If this heat is to be converted into useful work, a heat engine is required with a thermodynamic cycle between a heat source at T_1 and a heat sink at T_2. The heat engine usually uses the expansion and contraction of a fluid to provide work; however, thermoelectric devices and thermochemical cycles to split water into H_2 and O_2 are also in practice heat engines.[1] Carnot[2] in 1824 showed that the maximum efficiency, E, of an ideal (reversible or quasi-stationary) thermodynamic cycle is given by

$$\varepsilon = (T_1 - T_2)/T_1. \qquad (6.1\text{-}2)$$

Real cycles involve motion, and their efficiencies will always be less than the theoretical value. In a typical cycle using steam as the working fluid, a practical efficiency equal to 2/3 of the limiting Carnot value may be obtained. In such a cycle, T_1 is limited by materials considerations to about 900 K, and T_2, by the minimum turbine water condensation temperature (about 310 K). The non-ideality of the cycle therefore limits the best large coal-fired utility power plants to a practical heat-to-work efficiency (high-heating-value of coal to AC electricity) of 40%. Recent implementation of effluent controls has lowered efficiencies to about 35% or 9860 Btu/kWh. Small coal plants (~ 200 MW) are less efficient. Coals are unlike liquid and gaseous fuels in that they contain more H_2 as moisture. In general, the HHV for coals is 1.5-2% higher than the LHV for anthracites, 5-7% higher for bituminous and subbituminous coals, and about 9-10% higher for lignites. Since fuels are always burned to give gaseous products in which the heat of evaporation of the product water is not recovered, LHVs should be used when efficiencies with different fuels or systems are compared. For high-quality coals, the difference is not important. For fuel oil, the HHV is about 6% higher than the LHV, whereas for natural gas, the corresponding value is 10% because of its high H/C ratio. For H_2, it is

15% and, therefore, efficiencies based on HHV and LHV differ considerably. As we will see, this difference is important in considering fuel-cell efficiencies. Steam plants using natural gas or other clean fuels have 40% LHV efficiencies, but high fuel costs. The use of more than one thermodynamic cycle in the same plant (e.g., a gas-turbine Brayton cycle with exhaust-heat recovery via a Rankine steam cycle) may yield up to 45-47% LHV efficiency in smaller units (≈200 MW_e), at a relatively low capital cost ($500/$kW_e$, compared with $1100/$kW_e$ for a modern coal plant). In contrast the cheapest generating units, combustion turbines without steam cycle ($270/$kW_e$), have poor LHV efficiencies (10,000-13,800 Btu/kWh or 25-34% efficiency, depending on size and characteristics).

6.1-2. The FC as a Direct Energy-Conversion Device

FCs are not limited by the Carnot efficiency for heat-to-work conversion. They are used to convert the thermodynamically available free energy in fuels at a relatively low temperature directly into useful work in the form of direct-current electricity: ΔG is numerically equal to $-nFE$, where n is the number of equivalents per mole (number of electrons per mole transferred in complete oxidation), and E is the theoretical potential that would be developed between two thermodynamically reversible electrodes in contact with the fuel and O_2.

The FC is essentially a primary battery. In a Zn-MnO_2 cell with saline ($ZnCl_2$-NH_4Cl) electrolyte, Zn is oxidized at the negative electrode by anodic dissolution, whereas the MnO_2 is reduced in a stoichiometric process. Electrons flow in the outer circuit because of the potential difference (E for reversible conditions) between about 1.0 to 1.5 V, depending on the total current and state of discharge of the cell. The electronic current, under the potential difference, is capable of doing work as in an electric motor. The circuit is completed by ions moving in the electrolyte.

In the battery, the fuel (Zn) and oxidant (MnO_2) are solids and are themselves the electrode structure through which electrons are conducted. On the other hand, the electrode structures in an FC are not consumed and are continuously supplied with a fuel (normally gaseous H_2) at

the anode and with an oxidant (normally atmospheric O_2) at the cathode. Anodic oxidation of the H_2 and cathodic reduction of O_2 produce electrons in the outer circuit and ions in the electrolyte. For an FC with an acid electrolyte, electrons and H^+ ions are produced at the anode, and both combine with O_2 at the cathode to form water, thus completing the reaction and the electrical circuit.

For H_2 and O_2 at 25°C, ΔG to form $H_2O(\ell)$ is a substantial fraction of the HHV. The quantities ΔG and ΔH are 56.69 and 68.39 kcal/mole for $H_2O(\ell)$, respectively. Since the formation of one mole of water involves two electrons (n=2) via the process

$$H_2 \rightarrow 2H^+ + 2e^-, \quad (1/2)O_2 + 2H^+ + 2e^- \rightarrow H_2O, \qquad (6.1\text{-}3)$$

we can convert these quantities into electron-volts (1 eV = 23.06 kcal), obtaining 1.23 and 1.48 V, respectively, for ΔG and ΔH for the formation of $H_2O(\ell)$. If we could make a theoretically perfect, thermodynamically reversible FC operating under these conditions in an aqueous electrolyte, it would develop 1.23 V across the electrodes and would produce work in the form of electricity at an efficiency of $\Delta G/\Delta H$ or 83% of the HHV of H_2. For comparison with thermal machinery, this represents 96% LHV efficiency for H_2, which is more than twice the efficiency obtained for the best heat engine and the primary motivation for FC development.

However, in practice, FCs do not operate under ideal conditions, just as heat engines never show the theoretical Carnot efficiency. The most obvious loss in an FC results from its internal ohmic resistance, although this loss can be minimized by careful design. Of greater importance in most FCs are losses due to the irreversibility or time increments required for the electrode reactions and to concentrate gradients of the reactants and products of reaction (ions, water) in a cell operating at a useful net rate. These losses are also minimized by careful electrode design.

At temperatures between ambient and ~200°C in acid electrolyte, the H_2 electrode is sufficiently rapid for practical use if well-designed electrodes allowing effective gas supply and suitable catalysts are used. Unfortunately, the O_2 electrode is much less ideal, even with the most active catalysts; the low rate of molecular O_2 reduction, as compared for

example with that of the halogens, makes biochemical evolution possible. The rate of O_2 reduction is typically about 10^{-6} times slower than that of H_2 under similar conditions. Electrochemical reactions proceeding at a net forward rate normally obey Tafel's law,[3] which may be regarded as a generalization of the thermodynamics of irreversible processes or processes occurring sufficiently far from equilibrium to neglect the back reaction.[4] Tafel's law may be expressed in the form

$$\log i = A + B\eta, \qquad (6.1\text{-}4)$$

where A and B are constants for a given process, and η is the overpotential (i.e., the displacement in electrical potential of the electrode from the equilibrium value E at a net current density i, in A/cm^2). A is the logarithm of the rate of the process at equilibrium (the exchange current), which varies in a rather complex manner with concentration of reactants raised to a normally fractional power, the electrochemical reaction order. At a constant potential on some independent or reference scale, electrochemical reactions obey the usual laws of chemical kinetics. For example, the rate of the O_2-reduction reaction is proportional to the first power of the O_2 partial pressure (i.e., the reaction is first order), which is useful in assessing the effect of pressurization on FC performance. The electrochemical reaction order arises from the fact that the equilibrium potential varies with reactant partial pressure (P), corresponding to concentration, according to the expression $(RT/nF)\ln P$, where R is the molar gas constant and F the Faraday unit. A similar (negative) expression applies to reaction products. When the change in equilibrium potential with pressure or concentration is combined with the change in equilibrium rate from the Tafel equation, the resulting electrochemical reaction order becomes a fraction of the normal chemical reaction order. According to this simplified theory, the value of B in the Tafel equation is given by the expression $\alpha F/RT$, where α normally lies between 0.5 and 1.5, depending on the reaction mechanism followed. The theory is given in greater detail in Refs. 5 and 6.

According to this theory, α should be temperature-independent but, for O_2 in acid electrolyte, it seems to be proportional to the absolute

temperature.[7] As a result, the Tafel slope (B) appears to be temperature-independent and is typically equal to about 100 mV/decade on Pt-catalyzed acid FC electrodes. For O_2 reduction in basic media, α lies between 1.0 and 1.5, depending on the catalyst used. In alkaline solution, the cathodic Tafel slope is therefore lower, and thus η is also generally reduced, since A in the Tafel equation is about the same for both media.[8] A more detailed overview of electrochemical kinetics is given in Ref. 5. For the purposes of this overview, it suffices to say that, with the exception of alkaline fuel cells (AFCs) operating at high temperature (~200-250°C), the slow kinetics of the O_2 electrode in aqueous solution means that an H_2 FC never operates close to its theoretical standard potential of about 1.23V [~1.14 V at 200°C, cf. Eq. (6.1-1)], even under open-circuit (zero current) conditions. The O_2 electrode rest potential for these aqueous electrolyte cells is typically 0.9-1.0 V, which is a potential at which O_2 reduction and a parasitic anode process (corrosion of the electrode) have equal rates.[9] According to the Arrhenius equation, an increase in cell-operating temperature increases the net rate and hence the value of A. Thus, η will decrease with temperature. At the same time, however, ΔG and E decrease somewhat with temperature [compare Eq. (6.1-1)], although this thermodynamic effect is small compared with the kinetic effect on η. As a consequence of the reduced cathodic η value, the usual operating voltage of acid cells is 0.65-0.75 V at practical current densities, whereas AFCs may operate at about 0.8 V. In both cases, correctly designed cathodes are not affected by diffusion (O_2 concentration gradients), and Tafel's law is obeyed.

As already discussed, H_2 electrodes operate close to their reversible potential with properly chosen catalysts. Catalytic poisons reduce actually achieved potentials. The maximum efficiency of AFCs operating on pure H_2 will be about 0.8/1.28 or 62.5% based on the LHV of H_2 consumed in the cell. For acid cells, the efficiency will be less because of their lower voltage. The operating potential given for acid cells corresponds to operation on an H_2/CO_2 mixture produced by steam-reforming a practical fuel such as natural gas (NG), followed by water-gas shifting to reduce CO to low levels. While the acid cell will run advantageously on pure H_2 (with a performance gain of about 20 mV), in practical terms use of

the unseparated H_2/CO_2 mixture is more effective, since the system is simplified.

Since the AFC is not CO_2-rejecting and carbonate formation in its electrolyte reduces performance, it must be fed with pure H_2 separated from the H_2/CO_2 fuel gas. This separation requires work and reduces overall electrical efficiency with methane. This loss is compensated, to some extent, by the fact that all of the pure H_2 supplied can be consumed in the AFC, whereas the H_2/CO_2 fuel for acid cells becomes progressively more dilute as H_2 is consumed. This fact limits practical utilization to about 85% of total H_2, but the tail gas can be used (instead of NG) to provide heat for endothermic reforming. Finally, practical AFCs are limited to operation at 80°C by materials constraints, whereas acid cells with phosphoric acid electrolyte (PAFCs) can operate at 200°C. The waste heat of PAFCs can then be used to provide steam for reforming, which leads to an overall system efficiency advantage with practical fuels such as NG. High temperature cells are even more advantageous, since their waste heat can also be used to provide enthalpy for reforming.

DC power from the FC is converted to grid-quality AC at an efficiency of about 98.5% using a solid-state inverter. The overall NG-AC LHV efficiency for the PAFC system is 46.5% and thus equal to the best large combined cycles. In the future, molten carbonate fuel cells (MCFCs) may yield LHV efficiencies of 60% or more on NG.

A useful way to classify FCs is by electrolyte type. Historically, the first gaseous voltaic battery demonstrating the principle of the FC was described by Sir William Grove in 1839-42.[10] It used sulfuric acid electrolyte. The first cell of practical importance was an AFC. Acid electrolyte cells, molten salt electrolyte cells, and solid oxide cells will be briefly reviewed, with emphasis on current developments. For historical developments of FC types, readers are referred to Ref. 11.

6.1-3. Alkaline Fuel Cells (AFCs)

It was soon realized that it might be easier to make an effective aqueous FC using a caustic electrolyte rather than acid. The reason for this is the much broader choice of materials available for the less

aggressive alkaline solutions, even at the high positive potential of the O_2 electrode. This advantage is shown by Pourbaix's compilation of thermodynamic data for elements in the presence of water as a function of potential and pH.[12] The Pourbaix diagrams represent the thermodynamic stability of materials but do not show what is theoretically unstable or quasi-stable in practice because of very slow corrosion kinetics. In acid, only the noble metals and the oxides of Ta and Nb are stable at the O_2 cathode. In alkaline solution, many metal oxides are stable, and many metals can be used as construction materials, since they form protective passive oxide films. According to thermodynamics, carbon or graphite should be oxidized in both acid and alkaline solutions at the O_2 cathode. This process is, however, extremely slow, and graphite was used as the basis of the first effective AFC electrodes in a small non-optimized cell by Tobler in 1933.[13] His electrodes operated at low temperature and at low current density (7.5 mA/cm^2) and used graphite impregnated with catalysts and the concept of controlled wetting to make the catalytic electrolyte-gas interface as large as possible, so that the highest current density at a given over potential could be achieved. He did this by impregnating the electrode with water-repellent paraffin, so that it consisted of a partially-wetted electrolyte side and a dry gas side, with a very large area containing microscopic wetted and unwetted pores inside. Maximization of the gas-electrolyte-catalyst interface in the three-phase boundary electrode has since proved to be the key to effective FC performance.

Bacon's contribution to AFC technology started at about the same time as Tobler's 1933 work. His approach was that of an engineer: first, use commonly available construction materials and avoid costly catalysts; second, increase reaction rates at constant cell potential by employing high pressures and temperatures. Bacon, whose work[14] extended into the early 1960s, used nickel components, 40 wt% KOH electrolyte at 200°C, and pure H_2 and O_2 at pressures up to 40-45 atm. Since no wet-proofing agent was available for use at 200°C, Bacon depended on sintered nickel powder electrodes for capillarity to maintain the correct three-phase boundary. His electrodes consisted of two layers, one of sintered fine-pore nickel (4-5 μ particle size, 16 μ pore diameter) in contact with the electrolyte and totally wetted by it, with a layer of similar particle diameter but 32 μ

average pore diameter facing the gaseous reactants. The coarse-pore layer was kept open by control of the gas and electrolyte pressures to give maximum active area. The electrolyte was circulated for temperature control. The results obtained were very good, about 800 mA/cm^2 at 0.8 V, and may be attributed to the use of high temperature and pressures.

The Bacon cell was modified at the Pratt & Whitney Division of United Technologies Corporation (UTC) for use aboard the Apollo service module to provide electric power and potable water (PC3A-2 units). To reduce weight, they lowered the cell pressure but maintained a high performance by increasing the system temperature to 260°C, which required the use of 75 wt% KOH to avoid boiling of the electrolyte. The three-phase boundary was maintained by the use of a gas pressure of 0.7 kg/cm^2 above the electrolyte pressure (3.5 kg/cm^2). Heat removal and water-vapor control were maintained using a closed-loop H_2 recirculation system.[15] The Apollo system used three 110 kg modules, designated PC3A-2, each 57 cm in diameter and 112 cm high. Each delivered 1.42 kW at 27-31 V, with an average mission power requirement of 0.6 kW. Module life was limited by corrosion of the sintered cathode structure, which consisted of chemically lithiated NiO under the conditions of cell operation, and design life was only about 500 hr. No further PC3A-2 units were made after termination of the Apollo program.

A lighter and much higher performance AFC system (the PC-17C) was developed by UTC for the Space-Shuttle. Each of the three Space-Shuttle units is 35 cm high, 38 cm wide and 101 cm long. Original units had a peak power of 12 kW at a weight of 91 kg, so that the power density is ten times that of the Apollo unit. The system operates at lower temperature (82-89°C) than the PC3A-2 unit, which allows a service life of 2000 hr. The high performance is obtained by use of electrodes of the same general type as those developed for various acid applications. They are descendents of Tobler's using a wet-proofing agent to maintain the three-phase boundary. However, like all modern wet-proofed electrodes, the most stable and hydrophobic of organic waxes, polytetrafluorethylene (Teflon®), are employed. For high performance, the catalysts are pure noble metals. The anode consists of 10 mg/cm^2 of metal black (80% Pt, 20% Pd); the cathode has 20 mg/cm^2 (90% Au, 10% Pt). The cell yields 0.5 A/cm^2 at 0.9 V for a

reactant gas pressure of only 4-4.4 atm. The pure H_2 and O_2 reactants are supplied from the cryogenic fuel supply of the Space-Shuttle. The system uses electrolyte immobilized in a asbestos matrix and is of bipolar (filter-press) construction to give very low intercell IR drop and uniform current density. Gold-plated magnesium bipolar conduction plates are used between cells. Cooling is by a dielectric liquid, and water removal is by evaporation, with condensation in the H_2 feedback loop. The system operates like other FCs on the free energy of conversion of H_2 to water vapor, and its efficiency should therefore be expressed in LHV terms. The system is described in Ref. 16.

During the 1960s and 1970s, a number of small AFC units were developed, often using exotic fuels such as hydrazine for specialized applications.[11,15] At that time, research was conducted on AFCs in Europe and elsewhere because of the ability to utilize inexpensive materials.[11] Another practical attraction is the cathode reaction, which often occurs via a rapid two-electron O_2 reduction process to peroxide ion, followed by chemical disproportional of peroxide to H_2O and O_2, which is further reduced to peroxide in a cyclic process as follows:

$$O_2 + H_2O + 2e^- \longrightarrow O_2H^- + OH^-, \qquad (6.1\text{-}4)$$

$$O_2H^- \longrightarrow (1/2)O_2 + OH^-. \qquad (6.1\text{-}5)$$

This cycle sequence allows the use of a wide range of inexpensive catalysts, including active carbons, at relatively low temperatures. It was often felt that only AFCs would find wide application, since acid cells appeared to require costly construction materials and noble-metal catalysts. As already noted, however, AFCs have the great disadvantage that the electrolytes do not reject CO_2, and hence all common fuels must be converted to pure H_2 before introduction into the cell anode. Furthermore, air would normally have to be scrubbed to remove CO_2 before use at the cell cathode. Removal of CO_2 from steam-reformed hydrocarbons requires significant amounts of energy, and fuel is required to raise steam for reforming and for the endothermic reforming process itself if no waste heat is available. Since AFCs using inexpensive materials will not operate satisfactorily at

temperatures higher than 80°C, fuel must be burnt to provide the 50% excess of steam required for efficient reforming. This energy represents about 15% of the LHV of methane or light distillate fuel. PAFCs now operate at temperatures up to 200°C using cheap materials (graphite), their waste heat may be used to raise steam, and they do not require CO_2 removal from the fuel stream. In consequence, interest in the AFC using reformed hydrocarbon fuels has waned in recent years. They are now used in specialized applications using pure H_2 (aerospace, deep-sea, emergency power requiring instant start-up) and may in the future find large-scale use when H_2 will be available in quantity (e.g., in chlorine plants today and in the future H_2 economy). In the H_2 economy, H_2 will be produced by water electrolysis using hydroelectric or off-peak nuclear power and eventually solar energy.[18] Very simple, cheap AFCs with about $50/kW of active area not including catalysts should have about the same cost and are being examined for industrial chlorine-plant application;[19] they may find future use for transportation using fossil or non-fossil H_2 or cracked ammonia[20] as fuel. Their wide application is not limited by the availability of noble-metal catalysts, as is the PAFC.

6.1-4. Acid Fuel Cells

There are presently two types of acid fuel cells: those with liquid electrolytes and those with an acid solid polymer ion-exchange membrane as the electrolyte (solid polymer electrolyte or SPE cells). By far the most important are the liquid electrolyte cells using phosphoric acid (PAFCs), since they are likely to find wide application for the dispersed generation of electricity. SPE cells are described in Refs. 15 and 16. The first SPE system was developed by the General Electric Co. for the Gemini capsule. It used high Pt loadings, operated at ambient temperature, and used polystyrene sulfonic acid as electrolyte.[11] Typical current densities were about 37 mA/cm^2. A new polymer, Nafion® (a sulfonated polyfluoroolefin) then became available, allowing operation at temperatures up to about 90°C and giving a system which could be used at very high current density (up to 1 A/cm^2) under pressure conditions, even at high differential pressures. The SPE has the advantage of a totally

immobilized semi-solid electrolyte, thereby reducing system materials problems. Its main disadvantages are the need for high Pt loadings, since the catalyst-membrane interface is linear rather than three-deminsional as in a conventional three-phase-boundry electrode, and the high cost of the membrane ($400/m^2). In addition, the membrane dries out and becomes non-conductive at temperatures above 100°C (this is apparently true of all fluorinated sulfonic acids). Thus, like the AFC, it cannot be used to raise steam for reforming.

Since acid cells are CO_2-rejecting, they can theoretically be employed to oxidize carbonaceous compounds directly. The liquid electrolyte cell grew out of attempts to make a direct hydrocarbon fuel cell in the late 1950s. Most of this work took place at the General Electric Research and Development Center.[11] Since the hydrocarbon oxidation reaction is very slow, even compared to O_2 reduction, very high catalyst loadings (20-40 mg/cm^2 of Pt or its alloys) were required to obtain rates of a few mA/cm^2 in 5N sulfuric acid at the maximum operating temperature of about 80°C; the acid is reduced by H_2 at higher temperatures. The only common inorganic acid stable at high temperatures is phosphoric acid and was therefore tried as an electrolyte. Even at 150°C, rates of reaction were poor, and the concept was abandoned as not cost-effective. The Pt catalyst cost alone was $(1984)15,000/kW.

In 1967, the American Gas Association started the TARGET program to develop small 12.5-kW FC generators intended to supply both electricity and domestic heat-from NG in a co-generation mode to individual households. It occurred to workers at UTC (the prime contractor) that a PAFC operating at temperatures of 150°C or above would be capable of using the dirty (i.e., CO-containing) H_2/CO_2 mixture produced by steam-reforming of NG, since poisoning of the H_2 electrode by CO is minimal above this temperature. In addition, the high PAFC operating temperature would allow steam to be raised for reforming, thus yielding and integrated high efficiency system. The principal problems were economic: catalyst requirements, stack-construction materials, and whether the chemical engineering system in a 12.5-kW unit would prove to be practical.

The major breakthrough occurred in 1968-69, when graphite was shown to be a satisfactory cell-construction material, with an exceptionally

low corrosion rate even at the O_2 cathode at 200°C.[21] Work conducted since about 1970 showed how it was possible to increase the effective surface area of pure Pt (compared with that of the pure Pt black previously used) by more than a factor of 5 by depositing it on a conductive support (high-surface-area carbon black). Improvements in teflon-bonded electrode structures allowed higher catalyst utilization: $0.5 mg/cm^2$ of Pt at 10 wt% on a high-surface-area carbon carrier was shown to be as active as the $20 mg/cm^2$ pure Pt of older electrodes. Cell performance in the early 1970s was less than 0.6 V at $150 mA/cm^2$ in atmospheric-pressure cells. The scope of the program was later changed to include larger units for which operation under pressure would prove to be economical. In the late 1970s, the resulting PAFC system existed in two versions: a 40-kW, atmospheric-pressure design fueled by reformed NG and intended for gas-utility on-site use (the PC-18, an up-dated version of the original TARGET PC-11) and a 4.5-MW (AC), 3.4-atm unit intended as an electric utility prototype. Experimental 4.5-MW units were constructed in New York and at Goi on Tokyo Bay. The latter ran successfully for the first time in April 1983. About fifty 40-kW on-site co-generation units were ordered by various gas utilities for testing and are presently (1985) operating successfully.

All UTC PAFC stacks now use the ribbed-substrate stack technology,[22] in which a fibrous, graphite-ribbed electrode substrate allows for the distribution of gaseous reactants and can also serve as an electrolyte reservoir. In this way, sufficient phosphoric acid can be stored in the cell to allow for gradual evaporation over a 40,000-hr lifetime. Each of the ribbed substrates is about 2 mm thick. They are arranged in a crossflow configuration in contact with a solid graphite bipolar plate 1.2mm thick. The teflon-bonded catalyst layers are applied to the inner flat faces of each ribbed substrate, and these in turn contact the silicon carbide matrix (about 0.5 mm thick) containing the electrolyte. The matrix is bonded with about 10 wt% teflon and is still satisfactorily wetted by electrolyte. On the other hand, the hydrophobic electrodes contain about 40 wt% of teflon. The stacks are cooled by pressurized water in cooler plates for every five cells, and the produced steam is fed to the reformer. The on-site unit was designed to develop 0.65 V/cell at end-of-life at

140mA/cm^2 (for the later 200 kW-units, this will be about 200 mA/cm^2). The 4.8-MW (3.4-atm) unit ran at the same voltage but at 270 mA/cm^2. The LHV heat-rate of the latter was about 8,650 Btu/kWh LHB on naphtha or NG (39.5% LHV efficiency). Cells in the former system were 0.20 m^2 in area; those of the latter, 0.34 m^2.

In 1985, UTC began to develop a 200 kW version of the on-site unit, using 0.34 m^2 components, for GRI. International Fuel Cells (IFC), a UTC-Toshiba joint venture, will produce an electric utility unit rated at 11 MW[23] and using 0.98 m^2 stack components. This unit will operate at 8.2 atm, allowing 0.73 V/cell at 216 mA/cm^2. This large PAFC uses 0.25 mg/cm^2 of Pt at the anode and a proprietary Pt alloy with about 0.5 mg/cm^2 loading at the cathode on a corrosion-resistant, treated carbon black support. The fuel-processing system will be a simplified version of that used in the 4.8-MW demonstrator; the higher pressure and higher cell voltage increase power to 11 MW. LHV system efficiency will be 46% or better. This unit will be offered to utilities starting in 1986.

Other U.S. corporations involved in acid FC development are Engelhard Industries and Energy Research Corporation (ERC). Both are concentrating on small acid units for special applications. ERC uses an air-cooled stack technology, which has been licensed to Westinghouse in the U.S. and to Sanyo in Japan. Westinghouse plans to offer a 7.5-MW, air-cooled PAFC to electric utilities, which will use small rectangular cells, each about 0.14 m^2 in area, in a cruci-form arrangement cooled by air passing through cooling plates in the stacks to a central plenum. Steam will be raised for reforming using a heat exchanger. The system will operate at 190°C and 4.8 atm, giving 0.68 V/cell at 250 mA/cm^2. The cell voltage is 50 mV lower than that of the IFC unit, but the system heat-rate will be the same as the result of an improved heat-recovery cycle in the turbocompressor. The Westinghouse system uses stacks of ribbed bipolar plate construction, which do not have an electrolyte reservoir and require an acid-replenishment system. Further details of the design are given in Ref. 24. Finally, a series of electric utility PAFCs, inspired by UTC's pressurized stack technology, are under development at Toshiba, Hitachi, Fuji Electric, and Mitsubishi Electric in Japan, with partial funding from

the Japanese government. Their present aim is to construct two 1-MW demonstrators for operation in 1986.

While PAFC-system LHV efficiency is currently 46-47%, it may be slightly improved by future modifications to turbocompressors and other system components, but any major increase can only be brought about by increasing cell potential. Presently-used catalysts are close to the theoretical limit of small particle size, and it is unlikely that a further increase in performance will be obtained unless more active stable catalysts can be developed. Another possible approach is to improve electrode structure, so that higher catalyst loadings can be used effectively. The use of higher temperatures and pressures will also yield higher cathode potentials, but this combination of physical factors will result in increased cathode-support corrosion and shorter cell life, which may be improved by the use of new support materials. The upper limits of temperature and pressure will finally be dictated by the rate of surface-area loss of the catalyst by disolution/recrystallization. An upper limit for cathode potential of 0.8 V may possibly be achieved and will result in a maximum PAFC (LHV) system efficiency of about 52% (6,600 Btu/kWh). Finally, the PAFC can also be used with a low-sulfur medium- or low- Btu gas from a coal gasifier.

6.1-5. Molten Carbonate Fuel Cells (MCFCs).

Molten carbonate fuel cells in their present form have been examined since the 1950s.[11] The electrolyte (usually between 70 wt% Li_2CO_3, 30 wt% K_2CO_3 and 50 wt% Li_2CO_3, 50 wt% K_2CO_3) is intrinsically CO_2-rejecting. At the high operating temperature of the cell (600-650°C), the O_2 electrode process is much more nearly reversible than in acid electrolytes at 200°C. Even at atmospheric pressure, the cell will function well at reactant concentrations which would cause large losses as the result of diffusional gradients at 200°C, despite the relatively low active area of MCFC electrodes, which results from sintering and other materials constraints at the high cell operating temperatures. While the kinetic and parasitic losses in the cell are low, this advantage is partially offsite by the thermodynamic change of open-circuit potential with temperature [see Eq.

(6.1-1)], which amounts to about 215 mV between 25 and 650°C. However, the gain in overall system efficiency justifies the high operating temperature. While HC fuels have measurable oxidation rates in the cell, their direct use leads to cracking, which can be prevented by steam injection. This fact suggests the possibility of reforming fuels such as NG internally by using cell waste heat.

The MCFC anode consists of an Ni sinter containing sintering inhibitors. The structure is often ribbed to provide gas passages. The anode generally incorporates a fine pore layer or bubble barrier to prevent gas crossover under differential pressure conditions. The inner side of the anode contacts a relatively fine pore matrix consisting of lithium aluminate containing the molten electrolyte. The cell has a porous cathode (currently Li-doped NiO) and a metal bipolar plate; a current collector is located between cells. The bipolar plate consists of 316 stainless steel on the cathode side and clad with Ni on the anode side. No wet-proofing agents are used: the electrolyte three-phase-boundaries are maintained by surface tension resulting from matched pore-size distributions.

MCFCs are being developed at UTC, ERC and IGT, under DoE and EPRI sponsorship. The system is expected to have two utility applications: as modular dispersed internal-reforming NG units (IR MCFCs) with 5,800 Btu/kWh or better LHV heat-rate (59% or more LHV efficiency) using clean fossil fuels[25] and as units integrated with coal gasifiers with bottoming cycles for central stations with 6,500 Btu/kWh coal-AC heat rate.[26] In both cases, emissions will be very low, even less than for the PAFC, with about 1 ppmv NO_x and 0 ppmv S (PAFC emmissions are 0 ppmv S, 3-17 ppmv NO_x). NSPS standards for combustion turbines are currently 75 ppmv.

The MCFC has a sufficiently high operating temperature to supply not only the steam for NG reforming but also the reaction heat. Thus, a separate reformer is not needed, and all fuel-processing operations (except desulfurization) can be carried out in the anode compartment if a suitable steam-reforming catalyst is present. From the systems viewpoint, the cell behaves as if it used NG directly as fuel, and it is therefore much more efficient and simpler than a PAFC unit fueled by NG. Since NG has an LHV of 1.04 V, 100% utilization at a cell voltage of 0.73 V would yield an overall LHV efficiency of 0.73/1.04 or 70%. In a practical system, the major energy

loss is that for transferring CO_2 from the depleted anode stream to the cathode as required by the stoichiometry of the reactions in the MCFC:

$$H_2 + CO_3^{=} \longrightarrow H_2O + CO_2 + 2e^{-} \quad \text{(anode)} , \qquad (6.1\text{-}6)$$

$$(1/2)O_2 + CO_2 + 2e^{-} \longrightarrow CO_3^{=} \quad \text{(cathode)} . \qquad (6.1\text{-}7)$$

These chemical mechanisms require a CO_2-transfer device.

An energy-efficient process to deplete CO_2 from one gas stream and enrich it in another in a sufficiently energy-efficient manner does not exist at present, and the transfer is therefore accomplished by burning the depleted cell anode stream and condensing the water to obtain a mixture of N_2 and CO_2. This mixture is then added to air in the correct amount to provide the cathode reactant. The presence of excess N_2 inevitably leads to a dilute reactant gas mixture (typically about 7.5% O_2, 15% CO_2), and recycle will be used on both the anode and cathode sides to keep reactant concentrations at as high effective values as possible to minimize polarization losses. The anode-gas utilization in the cell can probably be kept at 85% or better, with a minimum total LHV efficiency of 60% on NG fuel. Parasitic losses for energy used in pumping and in the DC-AC inverter will reduce this value by about 3%. The overall IR MCFC efficiency is much higher than that of a PAFC unit, which is limited to 47% LHV efficiency at the same cell potential (0.73 V) because it requires external fuel processing. The IR MCFC is also much simpler from a systems viewpoint than a PAFC and it should therefore be less costly.

Efficiency, cost and systems aspects of an IR MCFC in the 2-MW class have been studied.[25] The baseline system used hot recycle of the fuel and oxidant gas streams, operated at atmospheric pressure, and required only one heat exchanger with a total area of 3.5 m^2. Other systems were more complex variants of the baseline unit; some incorporated pressurization. To the extent possible, off-the-shelf components were used in the evaluation; the only exception was the high-temperature blower for the baseline system.

An inverter efficiency of 97% was assumed, and parasitic power losses were estimated to be 5% of rated output; more reasonable values are 98.5% and 4%, respectively. The cell potentials were estimated by using a

simple model for the dependence of polarization on reactant pressures. When HHV efficiencies were calculated, the more complex systems showed little improvement over the baseline system, which had an estimated 0.705 V/cell at 200 mA/cm^2 with 80% fuel utilization at 659°C average temperature, giving 46% HHV efficiency (51% LHV). At 90% fuel utilization and 160 mA/cm^2 average current density, the same system should give 0.73 V/cell, corresponding to 52% HHV efficiency (58% LHV). This figure has been confirmed using an extensive computer analysis of internal-reforming cells, provided that thin, low-resistance electrolyte layers and high-performance off-eutectic electrolytes are used.[27]

This study shows that improved, simple, dispersed MCFCs with 60% (LHV) system efficiencies are possible if development problems can be solved. The units should have simpler, smaller and more efficient chemical engineering systems than PAFCs. Assuming stack costs of $200/kW of active area ($20/kg, compared with average material costs of $7/kg), plant costs of $800/kW uninstalled, with non-automated assembly, were estimated for breadboard units based on 40-kW stacks. The use of larger, better optimized stacks should reduce the cost of mature units by more than a factor of 2.[25]

Higher efficiencies (to 65% LHV) may be obtained if higher capital costs can be justified (more complex systems with bottoming cycles and CO_2-transfer devices when developed). Dispersed NG-fueled units will prove the value of the MCFC to electric utilities. Eventually, MCFCs can be anticipated in pressurized coal-fired central stations, using O_2-blown gasifiers and bottoming cycles. Such stations will have a coal-AC heat-rate of about 6,800 Btu/kWh[26] or 50% efficiency. As remarked earlier, they will have essentially zero emissions.[26]

Though IRMC single cells have been run successfully, they do not show the effect of the electrolyte-management problems on performance that are characteristic of stacks. Recent (1984-85), non-internal-reforming, pressurized 20-cell, 9.3-cm^2 stacks developed at UTC have shown excellent performance with very little dispersion between cells over 1000-2000 hr, when end cells started to flood at the negative end of the stack, and electrolyte loss occurred at the positive end. This transfer is caused by osmotic pumping up the manifold gaskets, particularly at the cathode. The electrolyte migration results from transfer of carbonate from the anode of

each cell to the outside of the wet-seal by reduction of depleted cathode gas (surrounding the stack) on the outside of the anode hardware. Parasitic reduction of anode gas takes place in the cell to complete the ionic circuit. This electrolyte transfer can be reduced by careful design of cell-edge and manifold seals and stack design but cannot be totally eliminated. Only the electrolyte content of the final five cells at each end of the stack appears to be affected. Hence, transfer will be less important in large stacks that have greater electrolyte inventories per unit of edge-seal length. Practical stacks may have to be designed with suitable reservoirs at each end, so that controlled osmotic pumping can be used to maintain correct inventory and electrolyte composition throughout.

Materials problems presently include slow cathode dissolution, anode creep, corrosion of the cathode-current collector and contamination of the reforming catalyst. With the possible exception of cathode dissolution, they can all be handled with materials that are now available. Dispersion-hardened Ni anodes largely eliminate creep. Formation of lithium ferrite on the 316 stainless steel cathode current collector will lead to films of about 4 mils (0.1 mm) thickness after 40,000 hr and will not be life-limiting. The metal edge-seal areas in contact with anode and cathode gases are effectively protected from corrosion by aluminizing. Finally, any electrolyte loss (e.g., by evaporation) can be made up using electroosmotic transfer up the cell stack.

The slow dissolution and reprecipitation of the Li-doped NiO cathode material was first discovered by UTC in cells with then new, thin tape-cast electrolyte layers under high pressure (high partial pressures of CO_2, P_{CO_2}). Investigations have shown that the Ni^{2+} solubility depends inversely on melt oxide-ion concentration, which accounts for the P_{CO_2} dependence. The Ni diffuses down its concentration gradient to the anode, where it precipitates and can eventually short-circuit the cell. The effects of dissolution are seen earlier in life with thin, low-resistance electrolytes, especially under high-pressure operation, and resulting lifetimes may not be acceptable unless improvements become possible. These include slowing NiO dissolution by chemical modification of the electrode and/or electrolyte or by the use of cells at low P_{CO_2} and reduced operating temperature (average 625°C).

Other conducting oxides are being examined as substitutes for NiO. Many materials, for example, p-type perovskites, have been shown to be unstable. Ideally, any substitute should not have a component which can precipitate as metal under anode conditions. The best candidates would be cell-corrosion products, e.g., lithium ferrite. Workers at ANL have examined this compound using Mn^{2+} as dopant, together with Mg^{2+} -doped lithium manganite. Results have not been reproducible.

Many practical problems are involved in the design of a cost-effective IRMC fuel cell stack. This must take into account materials and electrolyte-management problems, plus pressure requirements for electrical contact, cell-edge resiliance, sealing, creep, and the location of the anode-reforming catalyst. The latter is on a carbonate-resistant support but must be protected from excessive wetting by carbonate. For this purpose, a non-wetting anode of the cermet type developed at GE may be a possible direction, since pure Ni is not wetted by molten carbonate. Another approach is the use of a fine-pore Ni protective layer to retain carbonate by surface tension, which could also serve as the bubble-barrier to prevent gas cross-over if micro-cracking of the electrolyte layer occurs after a thermal cycle. Destructive cracking of the cell is now prevented by the use of coarse-particle crack-arresters in the electrolyte.

The rapid development of cell stack technology is indicative of the progress made over the last 5 years. The component design and assembly requirements for a cost-effective IRMC stack are being actively pursued by ERC and IGT. A prototype stack is planned for about 1988 and an internal reforming FC may be available by 1995.

6.1-6. Solid Oxide Fuel Cells (SOFCs)

Some doped inorganic oxides show oxide ($O^{=}$) ion conductivity at high temperature (~ 1000°C). Yttria-stabilized zirconia is one of the best of these materials. Their use for FCs and other applications goes back to the Nernst glower[28] of 1900 and is reviewed in Ref. 11. This class of materials as FC electrolytes is attractive because of their thermal stability and the absence of problems of electrolyte management, with no composition-buffering requirement by transfer of a neutralizing agent from

one electrode to another. The latter procedure is needed in the MCFC, where CO_2 must be transferred by an external circuit from anode to cathode to preserve neutrality, as in the automatic internal H^+ transfer from and to the cathode via the electrolyte in the PAFC. Materials similar to those used in carbonates may be employed for the electrodes, but the all-solid-state system reduces the possibility of chemical interaction and consequent lack of stability.

The low conductivity of the solid oxide materials (at 1000°C, about 10% of that of carbonate at 650°C) requires very high operating temperatures and very thin, gas-tight electrolyte layers (~ 50 μm or less) to give good performance. Thermal expansions require that electrodes, electrolyte layers and other components are accurately matched to prevent cracking or delamination, thereby reducing the overall choice of suitable materials. Finally, means must be found to construct individual cells by building up layers of components and to transfer current from cell to cell with connections that are electrically in series. A satisfactory filter-press system with geometrically parallel bipolar cells proved difficult to fabricate. Early cells were therefore constructed on a porous support tube in the form of short cylindrical units, arranged linearly in series along the tube. Current was collected along the length of each cell. A typical cylindrical length was a few mm to avoid excessive IR drop. The anode of each cell was in contact with the porous tube, which was supplied with fuel gas on the inside. The cathode was outside, over the concentric electrolyte layer, and a masked ceramic was used to connect the anode of one cell to the cathode of the next to provide a series arrangement. A ceramic interconnect material was required which had chemical stability and electronic conductivity in both the cathode and the anode environments. Lifetests on these cell arrangements have shown stability for more than 34,000 hr with suitable materials.[29] At that time, problems which require solution in practical systems were not addressed. These include sealing of the tube ends and thermal cycling.

In 1980, workers at the Westinghouse R & D Center developed a new arrangement of the basic components, which simplified construction, allowed the use of larger cells, could be cycled thermally, and avoided the end-seal problem. The cell is turned inside out by putting the cathode directly onto

the porous support tube (non-conducting calcia-stabilized zirconia) and is closed at one end. A narrow arc of the tube, along its length on top of the cathode layer, is now occupied by a strip of interconnect material, with the remainder of the cathode covered by electrolyte. Finally, the anode layer is placed on top of the electrolyte, thus avoiding contact with the interconnect by masking during manufacture. The interconnect is then attached to the next cell by a linear Ni felt in the fuel-gas atmosphere along the length of each tubular cell. The cell is provided with air via a narrow central alumina tube reaching the closed end; fuel is supplied to the outside in a co-flow arrangement. Reformate fuel, coal gas or possibly NG with steam, can be used; depleted fuel (after 85-90% utilization in the cell) is burned with depleted air after passing through a leaky ceramic header into a plenum chamber. The heat produced preheats the reactants and can be used in a bottoming cycle. The whole ingenious arrangement has been tested in thermally-cycled three-cell and larger stacks.

The only suitable materials, in view of thermal expansion and physicochemical requirements, are lanthanum chromite for the interconnect, Sr (or another alkaline or rare earth) doped with lanthanum manganite for the air electrode, and an Ni-stablized zirconia cermet for the anode. The layers are applied successively to the cathode by filtration onto the support tube. This step is followed by cathode sintering, which requires a lower temperature than the sintering of stabilized zirconia. After masking, the interconnect is applied, and then the electrolyte is deposited by EVD. The cathode is applied in the form of a slurry, followed by EVD zironcia-cermet formation. The EVD involves reaction of a mixture of vapor-phase chlorides on one side of the tube, with water vapor on the other. A film of yttria-stabilized zirconia is formed and conducts $O^{=}$ ions; thus, H_2 is formed by reduction of water vapor on one side and chlorine on the other. Because of ionic conduction in the film, the latter forms and continues to grow at 100% density, even at 25-μm thickness. However, many steps are involved in tube preparation, and costs are presently undetermined. Materials costs are about $150/kW.

At 1000°C, activation polarization is not apparent in the cell, but the change in ΔG with temperature [Eq. (6.1-1)] results in low open-circuit potentials. In addition, the IR drop around the circumference

of the air electrode is high. Typical tubes of 1.7-cm diameter yield 0.65V under the same conditions (160 mA/cm^2) as an MCFC at 0.73 V. Unless air-electrode resistance and/or tube diameter can be reduced, individual cell efficiencies will always be about 10% less than those of the MCFC system. On the other hand, the higher-quality waste heat can be used in an efficient bottoming cycle in a sufficiently large system. The costs for the numerous small tubes, headers and manifolds are as yet unknown.

Recently, workers at ANL have focused on a tape-cast filter-press variant (the monolithic cell) with shorter current pathways and therefore lower IR drop.[30] Manifolding, thermal cycling and cost problems for this concept are not presently known.

6.1-7. Conclusions

FCs have very high efficiencies, even at part load and in small units (200 kW to several MW), are silent, and have virtually zero emissions. They can therefore be placed anywhere (e.g., in inner cities or on-site for cogeneration). In addition to these advantages over combustion turbines, their main attraction to U.S. electric utilities is rapid availability in small, very efficient units which allow rapid capital pay-back. FCs can therefore be introduced as new capacity is required, as an alternative to installing coal or nuclear central stations several years earlier, in anticipation of future demands. A 46% efficient (LHV) unit can be expected to achieve a 6.6% penetration of total installed capacity in the early years of the 21st century, provided that reasonable cost goals (about $800/kW) are met.[31] For a 51% efficient (LHV) unit, the corresponding figure is 18.2%. We believe that the PAFC, which will be commercialized first, will gain the initial market share, with the higher-performance MCFC system later taking a further share. Both types of cell have a bright future for utilities. The SOFC may also have some place in the utility generation mix if it is used with a bottoming cycle and if its final cost is acceptable. Finally low-cost alkaline systems using inexpensive catalysts may find wide application in mobile systems for transportation when storable H_2 is available as a fuel.

6.2. Coal Gasifiers for FCs *

The development of coal gasifiers for FCs has tended to concentrate initially on gasifiers for the earliest commercial system, namely, phosphoric acid fuel cells (PAFCs). Design criteria and gasifier requirements are summarized in Table 6.2-1 for two gasification plants, namely, a 20-30 MW_e plant for United Power Association (UPA) and a 150-MW_e unit for Southern California Edison (SCE).

A schematic of the coal-gasification-FC system is shown in Fig. 6.2-1. The initially chosen gasifier is an air-blown, fixed-bed design, which involves commercially-tested technology and statisfies the requirements of modular construction with high conversion efficiency. These gasifiers are, however, small units that produce coal fines, heavy oils, and tars. A schematic of the single-stage, fixed-bed gasifier is shown in Fig. 6.2-2. A more detailed flow diagram of system functions is reproduced in Fig. 6.2-3.

6.2-1. The Site-Specific UPA Design

The procedure followed in designing the UPA unit is described in Table 6.2-2, where both plant requirements and study objectives are listed. Table 6.2-3 shows performance comparisons of the gasifier-FC system with a coal-fired boiler, a fluidized-bed unit, and a gasifier-combined-cycle system. Reference to Table 6.2-3 indicates that the gasifier-FC system has by far the highest expected overall plant-conversion efficiency. Furthermore, costing studies summarized in Table 6.2-4 show that the anticipated bus-bar cost of electricity is relatively low for the gasifier-FC system, roughly comparable with that of a direct coal-fired boiler. However, compared with this system, it has significantly less emission of NO_x and SO_x (compare Table 6.2-5).

---

* This section has been abstaced (by S. S. Penner and D. Wiesenhahn) from viewgraphs presented by D.Rastler of EPRI at the Second Technical Meeting of COGARN (Lawrence Berkeley Laboratory, February 25, 1986).

Table 6.2-1. Design criteria for coal gasifiers for PAFCs.

Design Criteria	SCE†	UPA‡
Plant size	150 MW_e	20-30 MW_e
Coal type	Western low-S	North Dakota lignite
Operational requirements	4-1 turn down	base load
Emission requirements that must be met	California	Minnesota
Atmospheric, air-blown, fixed-bed gasification	X	X
UTC 11.6-MW_e FC power section and inverter	X	X
Commercially-proven equipment	X	X
Truck-transportable, factory-fabricated equipment	X	X

†SCE = Southern California Edison; ‡UPA = United Power Association

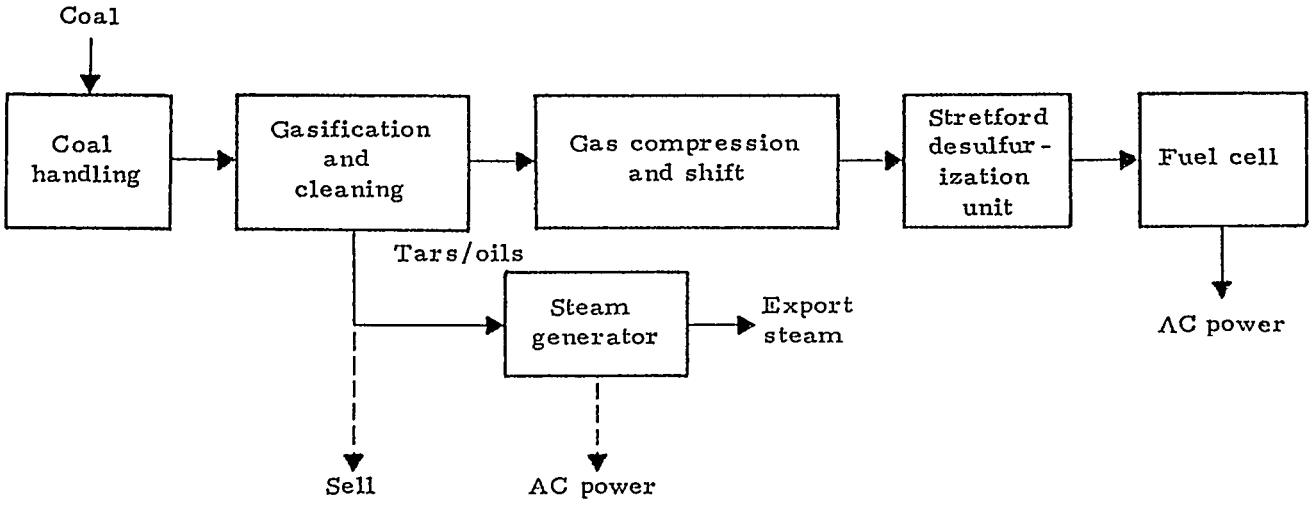

Fig. 6.2-1. Schematic of the coal-gasification-PAFC process.

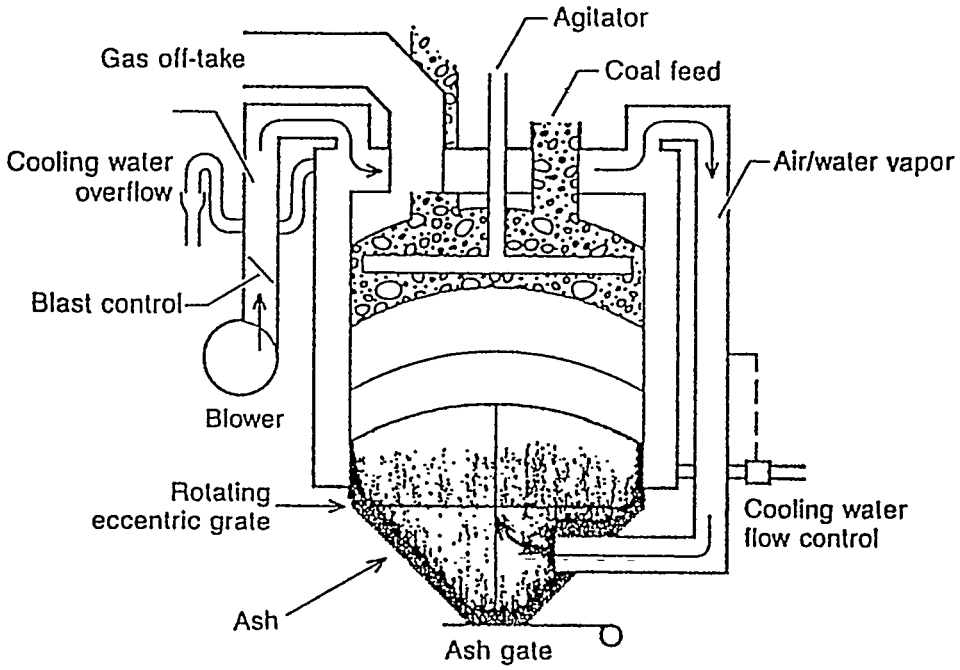

Fig. 6.2-2. Schematic of a single-stage, atmospheric pressure, fixed-bed coal gasifier.

Table 6.2-2. Background on site-specific studies for the UPA unit.

Host utility: United Power Association (UPA).
Contractor: Ralph M. Parsons.
Sponsors: EPRI/NRECA.
Study site: Willmar, Minn.
Plant requirements: N. D. lignite, 20-50 MW_e cogeneration, UTC fuel-cell modules.
Study objectives: cost/economics of small coal plant, optimal configuration, verification of cost estimates, assessments of alternative technologies, detailed environmental assessments.

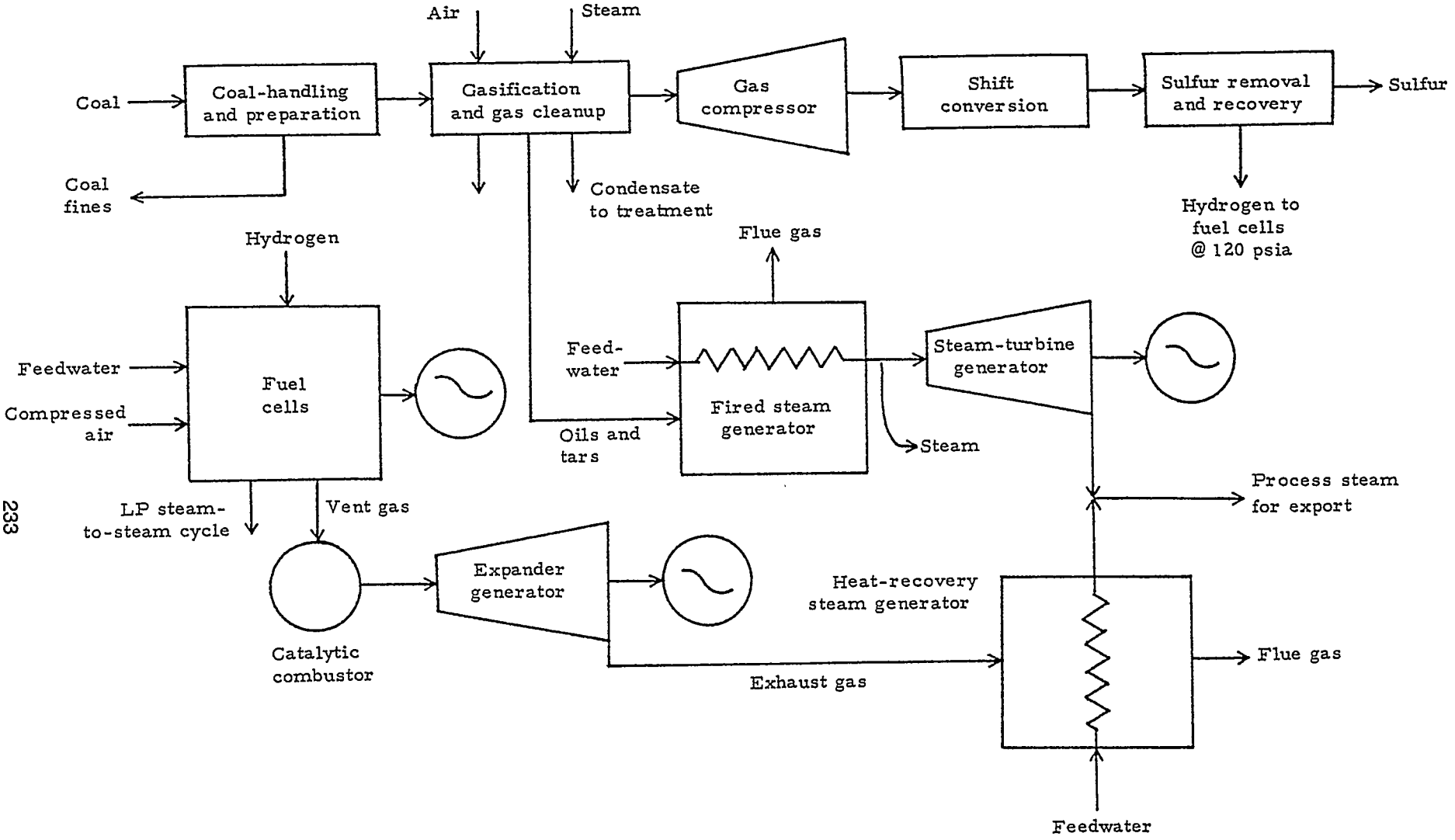

Fig. 6.2-3. Gasification-FC flow diagrams.

Table 6.2-3. Performance comparison of four design options studied for the UPA site.

Plant Feed and Output	Gasifier-PAFC	Gasifier-Combined-Cycle System	Fluidized-Bed Unit	Direct Coal-Fired Boiler
Net lignite feed rate, TPD	740	740	740	740
Plant output, MW_e export	32.5	20.1	20.6	21.5
Steam (150 psig), lb/hr	107,000	100,400	100,000	100,000
Overall plant efficiency	56.1	44.1	43.1	43.6

Table 6.2-4. Economic comparison of options for the UPA site-specific study.

Capital and Other Costs†	Gasifier-PAFC	Gasifier-Combined-Cycle System	Fluidized-Bed Unit	Direct Coal-Fired Boiler
Capitalization charges, mills/kWh	35	45	36	32
Fuel cost	24	40	36	35
O&M	29	30	29	25
Steam and by-products credits	(20)	(34)	(27)	(26)
Busbar costs, mills / kWh	68	81	74	66

†Costs are in 1983 constant dollars, levelized over 30 years at 80% capacity factor.

Table 6.2-5. Environmental comparison of options for the UPA site-specific study.

Emissions (lb/10^6 BTU)	Gasifier-PAFC	Gasifier-Combined-Cycle System	Fluidized-Bed Unit	Direct Coal-Fired Boiler
NO_x	0.004	0.05	0.11	0.35
SO_x	0.06	0.06	0.06	0.11
Particulate matter	0.02	0.02	0.02	0.02

6.2-2. The Site-Specific SCE Design

The procedure followed in designing the SCE unit is described in Table 6.2-6. Figure 6.2-4 shows a cost breakdown for the SCE facility. The estimated total cost of electricity is 69 mills/kWh and is divided in the manner illustrated in Fig. 6.2-5.

Table 6.2-6. Site-specific studies for the SCE unit.

Host utility: Southern California Edison Company
Contractor: Kinetics Technology International Corporation
Sponsors: EPRI/SCE
Study site: Barstow, CA
Plant requirements: Colorado subbituminous coal, 150 MW_e all electric plant, UTC fuel-cell modules
Study objectives: Assess scale-up issues, determine environmental impacts, provide a detailed cost and economic analysis

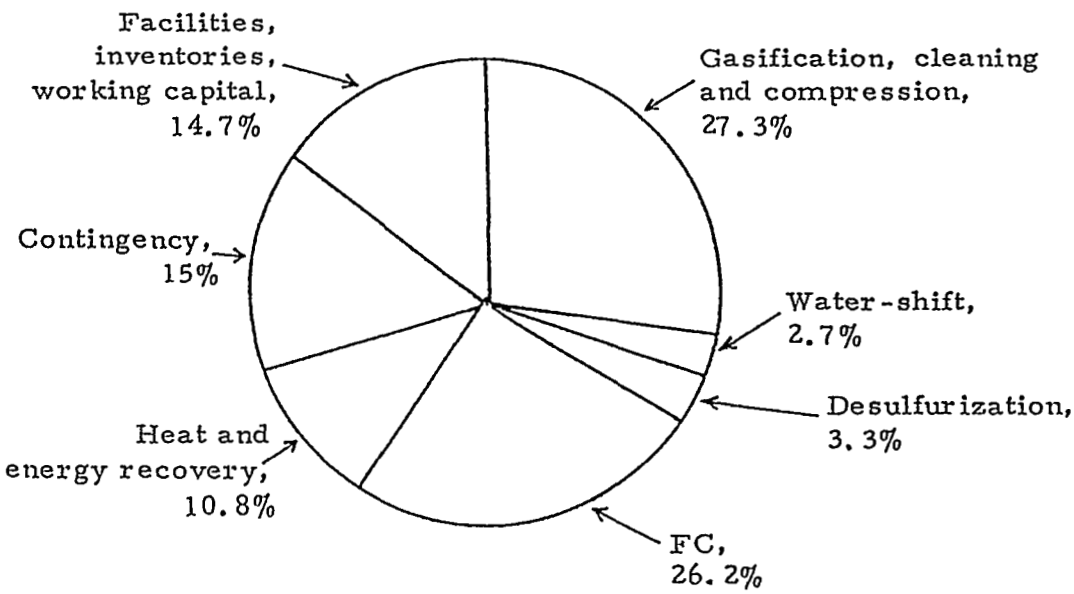

Fig. 6.2-4. 150-MW plant cost summary ($1630/kW).

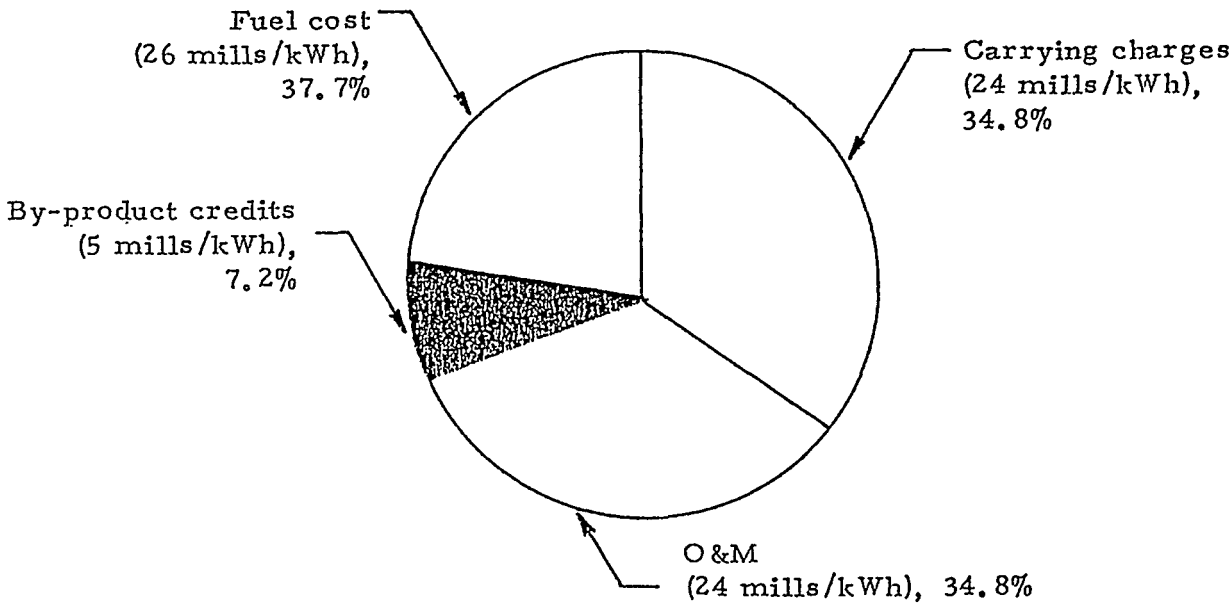

Fig. 6.2-5. The total cost of electricity is 69 mills/kWh and is broken down as shown in this diagram. A 25-yr book life, 65% cumulative load factor, and a constant January 1983 dollar were used.

6.2-3. Conclusions

The following are the principal conclusions reached from these evaluations: (i) No technical barriers appear to exist to successful operation of the conceptual design. (ii) Except for the FC-inverter, all process equipment and systems are commercially available. (iii) Site-specific emission requirements can be easily met. The use and disposition of plant by-product must be evaluated on a case-by-case basis. (iv) The plant configuration is modular and can be erected and on-stream within a 3-4 year period. (v) The coal gasifier FC plant is expected to compete well with other coal-based power generation options in the plant range of 100-150 MW_e.

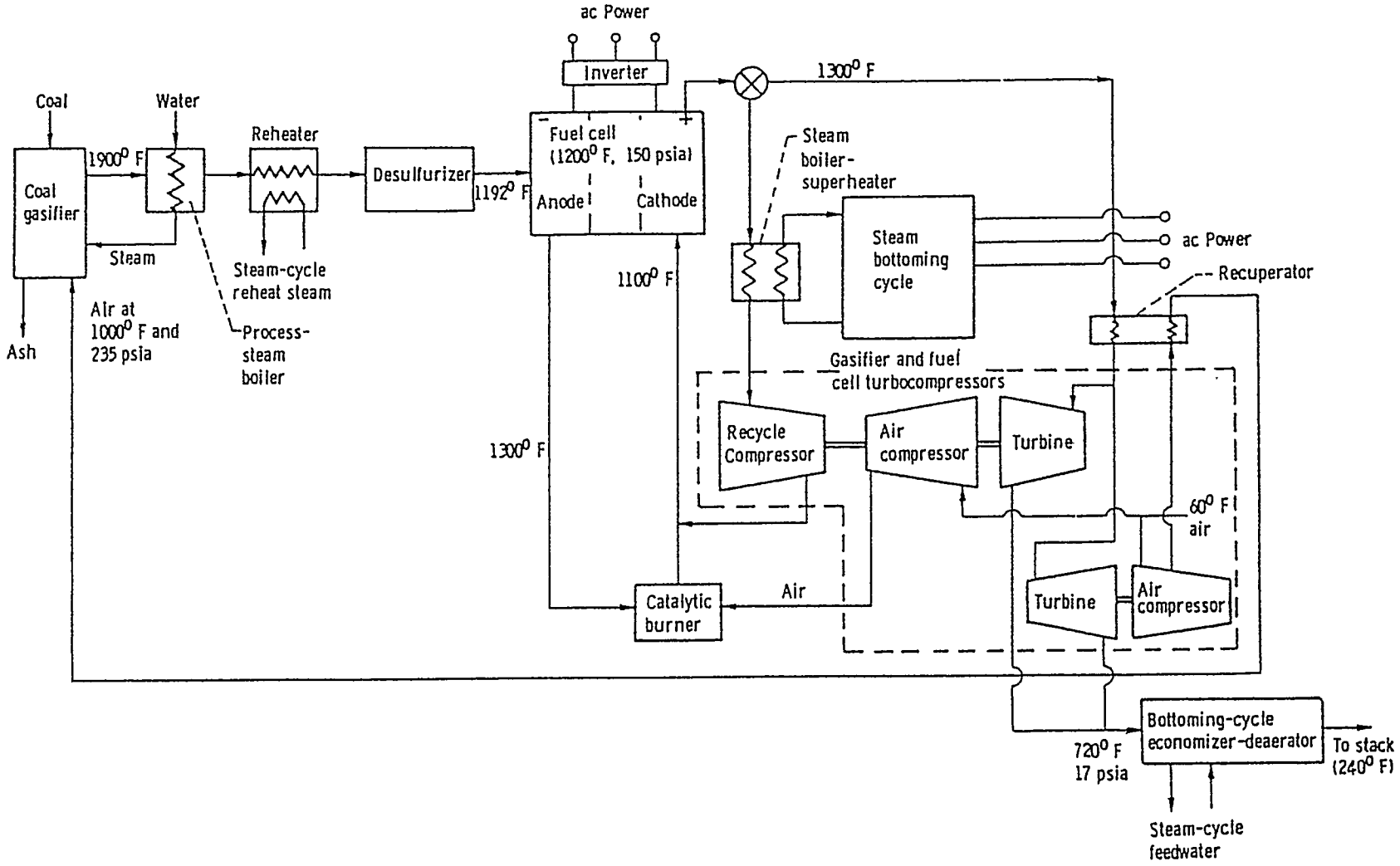

Fig. 6.2-6. Schematic of a low-BTU gasifier-MCFC-steam system.

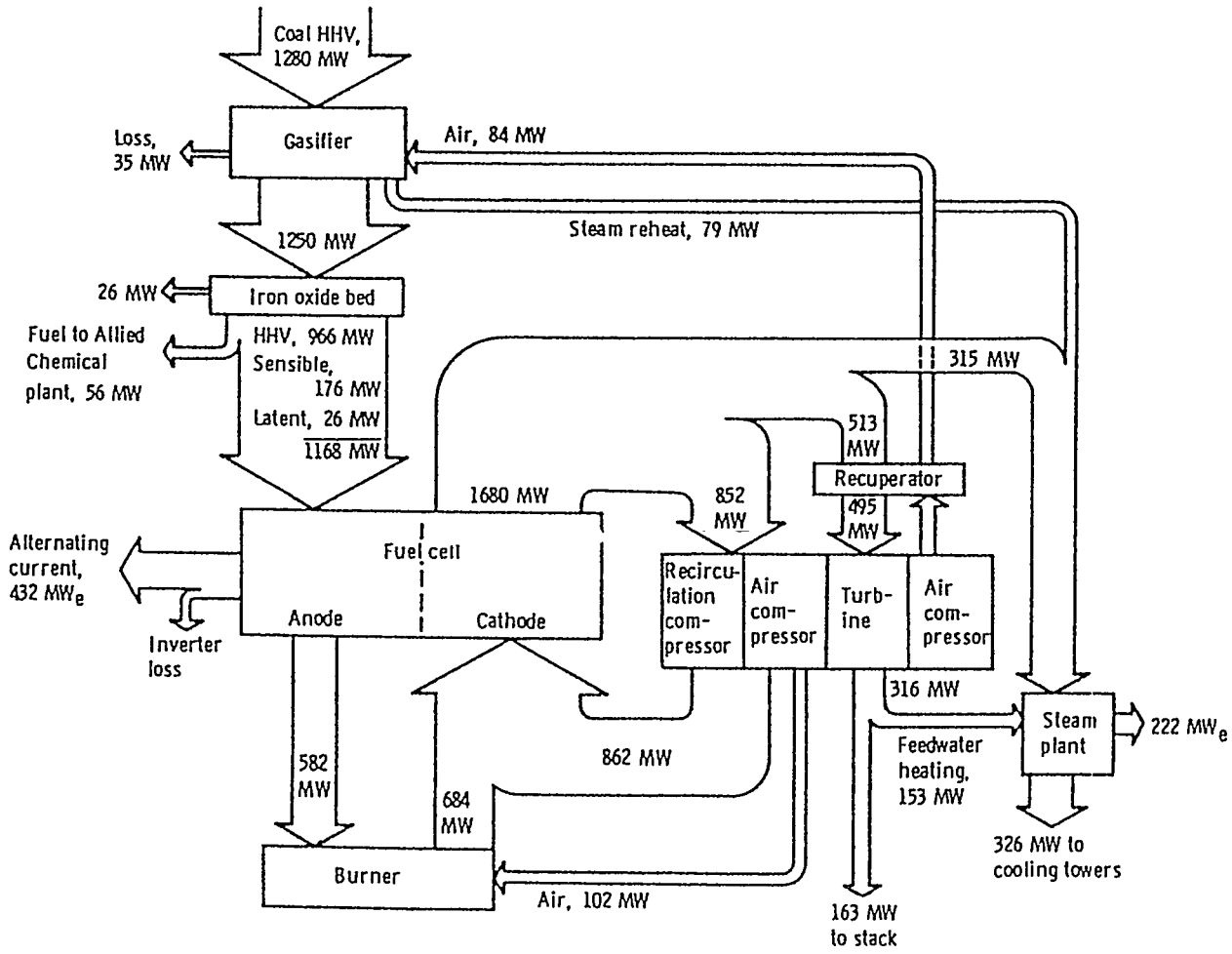

Fig. 6.2-7. Energy flow diagram for a low Btu gasifier/molten-carbonate fuel cell-MCSC-steam system. The net power output is 635 MW_e auxiliary power plus transformer losses are 19 MW_e.

6.2-4. Research Needs on Gasifier-PAFC Systems

The coal gasifier should be a modular 20-50 MW_e unit producing H_2 + CO. An atmospheric-pressure air-blown unit is acceptable but a pressurized gasifier would be preferable. The gasifier must have high reliability and be easy to operate for a wide range of coals. It should produce H_2-CO mixtures with high efficiency, yield minimal amounts of tar and oils in the raw-gas condensate, and become commercially available between the early and mid-1990s.

Candidate gasification systems include those of Shell, Texaco, Lurgi, KRW (Westinghouse), KGN, MHI, and U-GAS.

Research and development to provide one or more of these gasifiers at acceptable costs in the specified size range is recommended.

6.2-5. Other Gasifier-FC Systems

A conceptual design of a gasifier-MCFC-steam system, in which low-BTU gas is produced in the gasifier, is shown in Fig. 6.2-6. The energy-flow diagram for this unit is sketched in Fig. 6.2-7. Gasifier optimization for this system is not expected to be the pacing technology since commercial MCFC units are not likely to become available before the mid-nineties.

References

1. A. J. Appleby in Electrochemistry, p. 373, H. Bloom and F. Gutmann eds., Plenum, NY (1977).
2. S. Carnot, Reflexions sur la Puissance Motrice du Feu (1824).
3. J. Tafel, Z. Phys. Chem. 50, 641 (1905).
4. P. Van Rysselberghe in Modern Aspects of Electrochemistry, Vol. 4, p. 1, J. O'M. Bockris and B. E. Conway eds., Plenum, NY (1966).
5. J. O'M. Bockris and A. K. N. Reddy, Modern Electrochemistry, Plenum NY (1972).

6. A. J. Appleby in Modern Aspects of Electrochemistry, Vol. 9, p. 369, B. E. Conway and J. O'M. Bockris eds., Plenum, NY (1974); see also Comprehensive Treatise of Electrochemistry, Vol. 7, p. 173, B.E. Conway, J. O'M. Bockris, E. Yeager, S. U. M. Khan, and R. E. White eds., Plenum, NY (1983).
7. A. J. Appleby, J. Electrochem, Soc. 117, 641 (1970); E. Yeager, D. Scherson and B. Simic-Glavaski, Ext. Abstr. Spring Meeting Electrochem. Soc., p. 1043 (May 1983).
8. J. P. Hoare, The Electrochemistry of Oxygen, Interscience, NY (1968).
9. P. Stonehart and J. P. MacDonald, Final Report, EM-1664, Electric Power Research Institute, Palo Alto, CA (1981).
10. W. R. Grove Phil. Mag. S. 3 21, 417 (Dec. 1942).
11. H. A. Liebhafsky and E. J. Cairns, Fuel Cells and Fuel Batteries, Wiley, NY (1968).
12. M. Pourbaix, Atlas d'Equilibres Electrochimiques, Gautier-Villars, Paris (1963).
13. J. Tobler, Z. Electrochem. 39, 148 (1933).
14. F. T. Bacon in Trends in Electrochemistry, J. O'M. Bockris, D. J. Rand, and B. J. Welch eds., Plenum, NY (1977); J. Electrochem. Soc. 126, 7C (1979).
15. B. J. Crowe, "Fuel Cells, A Survey," NASA SP-5115, National Aeronautics and Space Administration, Washington, D.C. (1973).
16. D. Linden in Handbook of Batteries and Fuel Cells, p. 42-1, D. Linden ed., McGraw-Hill, NY (1984).
17. A. P. Fickett, p. 43-1 in Ref. 16.
18. J. O'M. Bockris, Energy Options, Australia and New Zealand Book Co., Sydney, Australia (1980).
19. A. T. Emergy, Ext. Abstr. National Fuel Cell Seminar, p. 98 (1983).
20. D. Bloomfield, E. Behrin, and P. N. Ross, Report LBL-14500, Lawrence Berkeley Laboratory, Berkeley, CA (1982).

21. A. J. Appleby in The ELectrochemistry of Carbon, p. 251, S. Sarangapani, J. R. Akridge and B. Schumm eds., The Electrochemical Society, Pennington, NJ (1984).
22. L. M. Handley, W. E. Houghtby, W. H. Johnson, T. G. Schiller, and H. Y. Stryker, EPRI EM-1134, Electric Power Research Institute, Palo Alto, CA (1979).
23. L. M. Handley, EPRI EM-3161, Electric Power Research Institute, Palo Alto, CA (1983).
24. M. K. Wright and L. E. VanBibber, Ext. Abstr. National Fuel Cell Seminar, P. 69 (1982).
25. P. S. Patel, EPRI EM-3307, Electric Power Research Institute, Palo Alto, CA (1983).
26. T. L. Bonds, M. H. Dawes, A. W. Schnacke, and L. W. Spradin, EPRI EM-1670, Electric Power Research Institute, Palo Alto, CA (1981).
27. E. T. ong, R. A. Donado, C. T. Li, and T. D. Claar, in "Proc. Workshop on Molten Carbonate Fuel Cells, Nov. 1978," pp. 4-18, EPRI WS-78-135, Electric Power Research Institute, Palo Alto, CA (1979).
28. W. Nernst and W. Wald, Z. Electrochem. 7, 373 (1900).
29. F. J. Rohr, Ext. Abstr. Workshop High Temp. Solid Oxide Fuel Cells, Brookhaven National Laboratory, Brookhaven, NY (1977).
30. D. C. Fee, R. K. Steunenberg, T.D. Claar, R. B. Poeppel, and J. P. Ackerman, Ext. Abstr. National Fuel Cell Seminar, p. 74 (1983).
31. C. K. Pang, S. T. Lee, K. Lee, and D. T. Imamura, EPRI EM-3205, Electric Power Research Institute, Palo Alto, CA (1983).

CHAPTER 7:
USE OF CATALYSTS DURING GASIFICATION

7.1. Selected Examples of Current Research *

7.1-1. Introduction

Catalysts play an important role in coal gasification. A list of possible uses is given in Table 7.1-1. Catalysts may be added to the feed stream just ahead of the gasifier to enhance gasification rates and improve the quality of the initial decomposition product slate. Catalysts are used for gas clean-up to facilitate efficient pollutant removal and product recovery. Processing of product gases to synthesize fuel and/or chemicals requires the appropriate use of catalysts.

This chapter deals with catalytic activity during gasification. Since in this application the catalyst material is usually added to the feed before it enters the gasifier, these are referred to as pre-gasification catalysts.

Some of the purposes of using pre-gasification catalysts are the following: to reduce gasification temperatures, pressures, and residence times; to minimize overall system sizes and costs; and improve gasifier quality and yields. Properly chosen catalysts will perform all of the specified functions and will also be sufficiently cheap to eliminate the need for complex or costly catalyst-recovery steps.

Despite extensive use and experience with catalysts, relatively little is known about the catalyst reaction mechanisms that occur in coal gasifiers. Fundamental research aimed at elucidating these functions has been an active field for research. The basic parameters governing gasification rates, such as active coal-surface area, active sites, catalyst dispersion, etc. are the proper targets of modern research. Catalytic processes

* This section has been prepared by S. S. Penner and D. F. Wiesenhahn.

are found in operating commercial plants, but few of these employed as pre-gasification catalysts. An example of efficient gasification on a nearly commercial scale is provided by the Exxon catalytic-coal-gasification process (see Sec. 7.2 for details).

The following summary is largely derived from (i) papers presented at the 1985 International Conference on Coal Science.[1-8] and (ii) information communicated to COGARN by H. Heinemann.

7.1-2. Results from the 1985 International Coal Science Conference[1-8]

The catalyst most often studied is K_2CO_3. Although the performance achieved with this and another commonly used potassium salt, KOH, has been good, they are too expensive for use as throw-away materials. For this reason, other cheaper catalysts are being examined, for example, the alkali salts $CaCO_3$, Na_2CO_3, NaOH, etc., as well as metals such as Ni. A summary of the catalysts studied in Refs. 1-8 is given in Table 7.1-2.

Basic catalyst parameters include coal-surface area,[1-3] catalyst dispersion,[1,4,7] catalyst-loading levels,[2,3,5,6,8] and coal characteristics.[3,7] Kinetic parameters were determined for assumed first-order reaction rates and an Arrhenius expression[1,5] or for rate laws corresponding to Langmuir-Hinshelwood kinetics.[6] A summary of these papers follows.

In Ref. 1, the rates and mechanisms of steam gasification of petroleum coke and activated charcoal were studied using the sodium salts listed in Table 7.1-2. For augmentation of gasification rates, the catalysts were ranked as follows: Na-lignosulfate >> EDTA-Na-salt >> Na-oxalate > Na-salicylate > Na-benzoate, Na-formate, Na-acetate > NaOH, Na_2CO_3. These results are valid at temperatures of 650 and 750°C. The reaction mechanism for EDTA-salt, Na-oxalate and others involved removal of the hetero-atom from the carbon matrix and using this atom for complexing. This procedure created edges which served as active sites for gasification. Cation exchange is the mechanism used to explain the action of the Na-lignosulfate catalyst. Active sites are formed by the exchange of sodium atom with a hetero-atom in the carbon matrix; thus, the high effectiveness of Na-lignosulfate is the result of its very high cation exchange. Dispersion effects were briefly discussed.

Table 7.1-1. Catalyst applications covering all phases of coal gasification are expected to show the listed advantages.

Increased gasification rates and reduced operating temperatures, pressures, residence times, and/or component sizes.

Improved gasifier-output quality, thus facilitating control of initial product-gas compositions and yields; reduced initial product-gas compositions and yields; reduced initial product-gas pollutant concentrations.

Easier gas clean-up for high- and low-temperature pollutant removal, product-gas purification.

Improved gas processing for the methanation of mixtures of CO, CO_2, H_2.

Improved methods for the separation of O_2 and N_2 from air.

Facilitated production of coal-derived liquids.

Table 7.1-2. Summary of catalysts for which studies were reported at the 1985 International Conference on Coal Sciences (see Refs. 1-8).

Catalyst	References(s)	Catalyst	References(s)
Na_2CO_3	1,2,5	K-Sn	2
NaOH	1	Ni	3,7
Na-acetate	1	Ni-Ca	3
Na-formate	1	Fe-Ca	3
Na-benzoate	1	KCl-NaCl	4
Na-salicylate	1	KCl-$MgCl_2$	4
Na-oxalate	1	KCl-NaCl-$MgCl_2$	4
EDTA-Na-salt	1	KCl-(mg or Ca) -(SO_4 or CO_3)	4
Na-lignosulfate	1	K_2SO_4-$FeSO_4$	4
K_2CO_3	2-7	$CaCO_3$	5
KOH	2	Na-Ca	5
$ZnCl_2$	2	Na-Ca-1	5
$SnCl_2$	2	Fe-MaII	5
$AlCl_3$	2	Na-RCl_3	5
$FeCl_3$	2	K	8
$NiCl_2$	2	Na	8
K-Zn	2	Cs	8
K-Al	2		

Gasification of Greek lignites and lignite chars with H_2 or N_2 flows was examined in Ref. 2. Catalysts were chosen in order to optimize conversion and methane yield. For methane yields, the catalysts were ranked as follows: K-Zn >> K-Sn,KOH > K-Al, Na_2CO_3 , K_2CO_3 > $FeCl_3$, $ZnCl_2$, $SnCl_2$, $AlCl_3$. The loading required to achieve effective catalytic activity for K-Zn was determined to be $\geq$ 5%. Increased loading lowered the temperature for peak methane output by approximately 100°C, with a concurrent increase in methane production. Generally, methane formation began around T-200°C and reached a plateau at about T=600°C before increasing again with temperature. Methane yield from chars were higher than from unreacted lignites. The contribution to methane production made by CH_3 radicals freed from the surface was small.

The high reactivity (in the presence of catalysts) of Blair Athol (an Australian coal) was investigated in Ref. 3. Catalysts utilized were Ni, Fe-Ca, and K_2CO_3. Other specimens tested included chars from six different coals. Pressures were 1, 10, or 30atm at 750, 850 or 900°C, while typical catalyst loadings were 1-2wt%. Mixtures of H_2O, H_2 and/or He were employed. Because it was demonstrated that the catalytic contribution was roughly proportional to the surface area divided by the crystallinity of the coal, the high reactivity of Blair Athol with Ni as catalyst was explained in terms of the great surface area of this coal. High gasification rates were obtained for the catalyst systems Ni-Ca or Fe-Ca. Tentative explanations include Ca mediating the carbon-transition metal interactions or the small amount of mineral matter found in Blair Athol coal. The influence of coal mineral matter, especially silica and alumina, on K-catalysed gasification was verified by showing that the conversion was proportional to catalyst loading only with demineralized coal. The effects of surface area, crystallinity and pore size for K-catalysed and non-catalysed coals are discussed in Ref. 3.

The goals of the authors of Ref. 4 were (i) reduction of catalyst melting points and acceleration of KCl hydrolysis by using the mixtures KCl/NaCl, KCl/$MgCl_2$, and KCl/NaCl/$MgCl_2$; (ii) formation of more active K-salts by using an <u>in situ</u> anion exchange between KCL, alkali earth sulfates, and carbonates for KCL/(Mg^{++} or Ca^{++})SO_4^{--} and KCL/(Mg^{++} or Ca^{++})CO_3^{--}; and (iii) catalytic <u>in situ</u> reduction of K_2SO_4 to K_2S using an

iron catalyst, viz., $K_2SO_4/(Fe^{++}$ or $Fe^{+++})$ $(SO_4^{--}, Cl^-$, or $O^{--})$. By monitoring CO_2 production, it was found that the temperature at which gasification begins increases with the melting temperature of the catalyst system, i.e., the catalytic system with the lowest melting point initiated CO_2 production at the lowest temperature. For this reason, the catalyst efficiencies were ranked according to catalyst melting points as follows: $KCl/NaCl/MgCl_2$(397°C) > $KCl/MgCl_2$(488°C) > KCl/NaCl(650°C) > KCl(770°C). All catalyst-containing systems showed significant improvements over uncatalysed systems. The free energy of reaction ($\Delta G_R°$) was used for the four forward and reverse reactions

$$2KCl + (Mg^{++} \text{ or } Ca^{++})SO_4^{--} \rightleftharpoons K_2SO_4 + (Mg^{++} \text{ or } Ca^{++})Cl_2^-,$$
$$2KCl + (Mg^{++} \text{ or } Ca^{++})CO_3^{--} \rightleftharpoons K_2CO_3 + (Mg^{++} \text{ or } Ca^{++})Cl_2^-,$$

and also for the anion-exchange reactions

$$2KCl + (Mg^{++} \text{ or } Ca^{++})SO_4^{--} + H_2O \rightleftharpoons K_2SO_4 + (Mg^{++} \text{ or } Ca^{++})O^{--} + 2HCl,$$
$$2KCl + (Mg^{++} \text{ or } Ca^{++})CO_3^{--} + H_2O \rightleftharpoons K_2CO_3 + (Mg^{++} \text{ or } Ca^{++})O^{--} + 2HCl.$$

It was found that the sulfate systems react more effectively with KCl than the carbonate systems. Experiments confirmed the relatively high activity of the $KCl/MgSO_4$ system, although pure KCl was more effective. Based on thermodynamic calculations, Fe was predicted to be a good catalyst for the following <u>in situ</u> reduction reactions:

$$K_2SO_4 + 4Fe \longrightarrow K_2S + 4\ FeO,$$

$$4FeO + 4(C, H_2, \text{ or } CO) \longrightarrow 4Fe + 4(CO, H_2O, \text{ or } CO_2).$$

Improved activation of K_2SO_4 by Fe was demonstrated experimentally.

The variations of conversion, gas composition, and burn-off rate with catalyst type, loading, gasification temperature, and the steam-to-carbon ratio were determined in Ref. 5. The effectiveness of catalysts, based on gasification rates, was ranked as follows: Na-Ca-I >

Na_2CO_3 > K_2CO_3 > $CaCO_3$, Na-Ca > Fe-M-I > $NaRCl_3$. Increased catalyst loadings and gasification temperatures always increased the gasification rates and conversions. Increased steam-to-carbon ratios enhanced conversion and an empirical relation was determined between these parameters. For defined ranges of steam-flow rate, temperature and carbon conversion, the gasification rates are kinetically of the first order. Resultant activation energies were calculated for an Arrhenius rate law and showed that Na-Ca-I catalysed carbon had an activation energy 90 kJ/mole lower than uncatalysed carbon. Resultant gas compositions differed as follows: uncatalysed carbon produced predominantly CO_2 with very small percentages of H_2 for $T \leq 700°C$, while the carbon catalysed with Na-Ca-I produced substantial amounts (> 54%) of H_2 for all temperatures studied ($600 \leq T,°C \leq 750$). The gas composition of Na_2CO_3-catalysed carbon was found to be insensitive to loadings for values between 2 and 5wt%, but the carbon conversion increased dramatically over this range.

The authors of Ref. 6 studied the effects of temperature, pressure, gasifying agent, and catalyst-loading levels on K_2CO_3-catalysed gasification of a low-ash char. Experimental conditions included pressures between 2 and 40 bar, temperatures between 650 and 750°C, and loadings of either 4 or 10wt%. Gasifying agents were either steam or CO_2. Gasification rates were always higher with higher catalyst loadings. Langmuir-Hinshelwood kinetics gave a good gasification and different catalyst loadings. Gasification rates increased with pressure up to about 15 bar; thereafter, the gasification rate was independent of pressure. If a single product gas is added to the gasifying agent, a dramatic decrease in gasification rate is known to occur. This effect was demonstrated by adding H_2 to the steam in K_2CO_3-catalysed gasification, although the magnitude of the rate decrease was not as large as expected. An appropriate correction was made in the kinetic expressions based on these results. Furthermore, an empirical expression relating gasification and conversion rates is given for uncatalysed gasification in the presence of hydrogen.

Thirty-four coals catalysed with K_2CO_3 or Ni were gasified in the experiments described in Ref. 7. The coals ranged from anthracite to peat and gasification was carried out with steam at 750°C and 0.06MPa. The catalyst loading was metal/coal = 10wt%. The conversion of K_2CO_3-catalysed coal was always enhanced and the degree of improvement did not appear to depend

on coal type. However, low-rank coal catalysed with Ni showed significant enhancement of conversion. Very little improvement was seen for the higher-rank coal with Ni catalyst. The critical coal characteristic was determined to be an approximate carbon content of 77wt% daf. These results were explained in terms of catalyst dispersion. Nickel has excellent dispersion only on low-rank coals, while good dispersion occurs in a steam environment for K_2CO_3 and is independent of coal rank. A proposed explanation is that, when K_2CO_3 melts, a liquid film is formed or else the K_2CO_3 decomposes to form KOC, which is dispersed on the carbon surface.

The catalytic mechanisms involving the influence of alkali carbonates on coal gasification were determined in Ref. 8 by studying the effects of alkalis on oxygen-transfer mechanisms in the reaction $C + CO_2 \longrightarrow 2CO$. For the same metal/carbon ratios, catalyst-gasification activity was ordered as follows: Cs > K > Na. This order also applies to catalyst saturation, where saturation is defined as the metal/carbon ratio above which no further improvement in gasification rate occurs. The difference in reactivity between K and Na (possibly also Cs) was explained by postulating the presence of a different number of active species. Oxygen-exchange mechanisms are believed to involve the following reactions:

$$
\begin{aligned}
* + CO_2 &\rightleftharpoons *\text{-}O + CO, \\
*\text{-}O + C_f &\longrightarrow * + C(O), \\
C(O) &\longrightarrow CO \\
C_f + CO_2 &\rightleftharpoons C(O) + CO, \\
CO &\longrightarrow C(O),
\end{aligned}
$$

where C_f is fuel carbon and the asterisk denotes an active site on the catalyst.

7.1-3. Catalytic Conversions at Reduced Temperatures[9] *

Most of the catalytic conversions discussed in Refs. 1-8 were performed at temperatures between 800 and 900°C. It is clearly desirable to

---

* The authors are greatly indebted to H. Heinemann of the Lawrence Berkeley Laboratory for required information to prepare this section, for helpful advice, and for correcting errors in the final manuscript.

search for catalysts that are effective at reduced T and p because of the associated cost reductions for capital equipment and operations. It is shown in Ref. 9 that this desirable objective is met when KOH is combined with mixtures of transition-metal oxides.

Preliminary studies have indicated that small amounts of CH_4 could be produced at very low temperatures in the presence of KOH-impregnated graphite subjected to a steam atmosphere. The rate of methane production as a function of time is shown in Fig. 7.1-1; an initially high rate of production followed by a slower rate has been attributed to agglomeration leading to large globules of KOH crystals. Results similar to those of Fig. 7.1-1 were observed for the alkali hydroxides CsOH, NaOH, and LiOH.

In similar experiments, graphite impregnated with KOH was gasified with steam at T=525°C. The resultant rate of gas production is shown in Fig. 7.1-2 and shows features similar to those in Fig. 7.1-1. Essentially the only gas produced in the portion of the curve labeled region I was H_2, while H_2 and small amounts of CO were produced in region II. The abrupt change in gas-production rate at ~ 2.5hr is caused by completion of the stoichiometric reaction:

$$2C + 2KOH \longrightarrow 2COK + H_2. \qquad (7.1\text{-}1)$$

After all of the KOH has been converted, the production of H_2 ceases. However, by raising the temperatures to ~ 1000°C, it is possible to decompose the phenolate with water, thus recovering the KOH according to the process:

$$2COK + H_2O \longrightarrow C + 2KOH + CO. \qquad (7.1\text{-}2)$$

This newly formed KOH is available to produce more H_2 according to reaction (7.1-1). It follows, therefore, that an effective conversion catalyst can catalyze reaction (7.1-2). The overall process for reactions (7.1-1) and (7.1-2) is:

$$C + H_2O \longrightarrow CO + H_2. \qquad (7.1\text{-}3)$$

It was found[9] that incorporation of a transition-metal oxide accelerates completion of reaction (7.1-2) and thus acts as a gasification

catalyst. The overall process of reaction (7.1-2) has been described by the following two sequential reactions:

$$2COK \xrightarrow{MeOx} K_2O + C + CO, \qquad (7.1\text{-}4)$$

$$K_2 + H_2O \longrightarrow 2KOH \qquad (7.1\text{-}5)$$

Conversions catalyzed by this process are illustrated in Fig. 7.1-3, which shows substantially enhanced gas-production rates at $T \geq 600°C$ for the graphite-KOH-Fe_2O_3 system. Figure 7.1-4 shows a comparison of various transition-metal oxides and indicates that NiO is the most effective oxide.

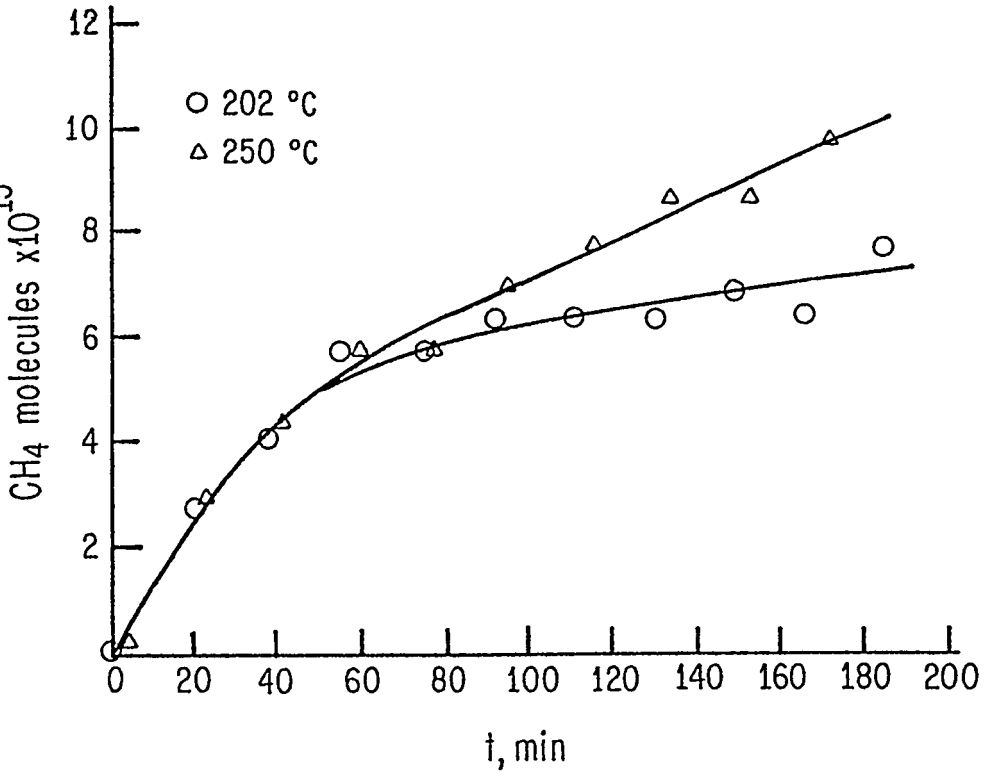

Fig. 7.1-1. Methane production at low temperatures is shown for the KOH-catalyzed steam gasification of graphite; reproduced from Ref. 9.

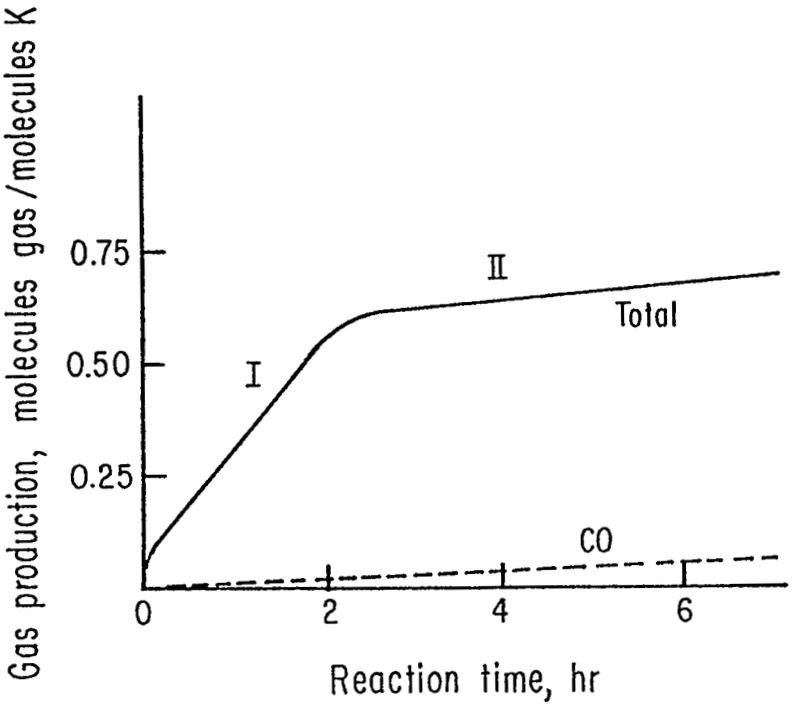

Fig. 7.1-2. The gas-production rate for KOH-catalyzed gasification of graphite; T = 525°C, (KOH)/(C) = 0.043. Roman numerals I and II refer to regimes before and after completion of the stoichiometric reaction $2C + 2KOH \rightarrow 2COK + H_2$; reproduced from Ref. 9.

Gas-production rates for NiO, KOH, and KOH and NiO used together are shown in Fig. 7.1-5 as a function of time. The characteristic rates for KOH used alone (compare Fig. 7.1-5 with Figs. 7.1-1 and 7.1-2) are not observed with KOH-NiO mixtures, and the KOH-NiO system is far more effective than KOH used alone. The high initial rate observed with NiO is consistent with the results of previous studies: the almost immediate loss of effectiveness is explained by the coating of Ni with C. The KOH-NiO system is superior to the K_2CO_3 system, as is illustrated in Fig. 7.1-6 which applies to Montana subbituminous coal.

Figure 7.1-7 shows XPS diagrams for Ni spectra and for Ni-KOH on graphite. These indicate that Ni deposited alone on graphite is not stable to at least 700°C. Similar XPS data, summarized in Fig. 7.1-8, indicate that KOH alone is not stable in the presence of water above 550°C, whereas it retains considerable stability in the presence of NiO for $T \geq 700$°C. These results suggest the formation of a compound between K and Ni oxides,

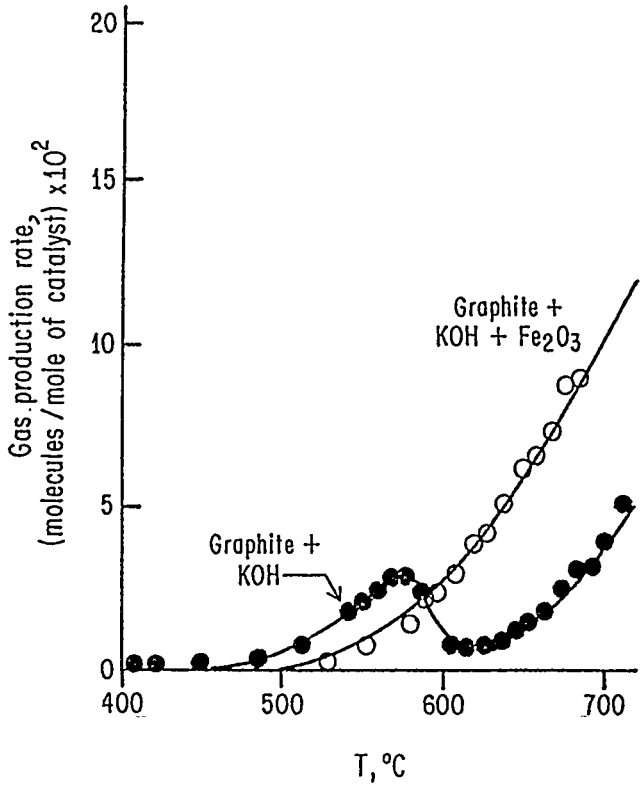

Fig. 7.1-3. Gas-production rates of the KOH- and Fe_2O_3-catalyzed gasification of graphite; reproduced from Ref. 9.

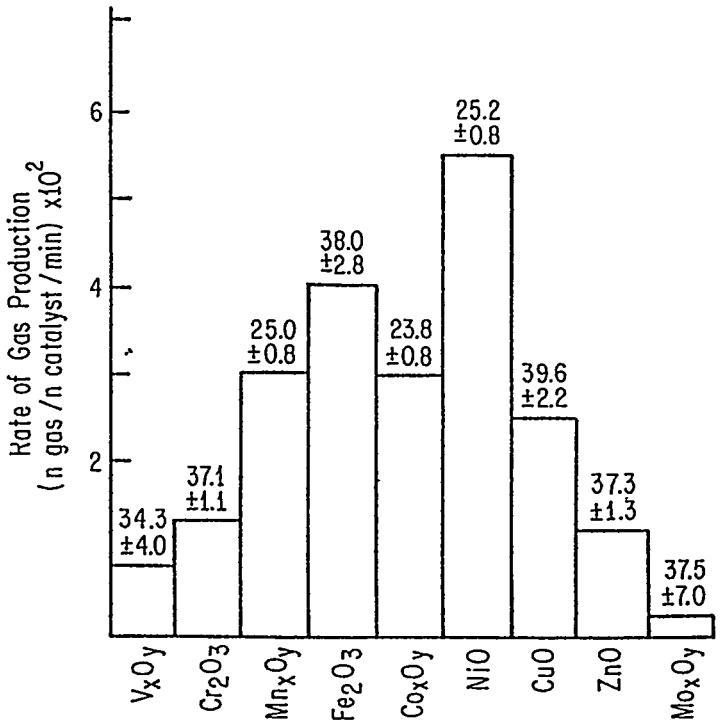

Fig. 7.1-4. Performance of various metal oxides mixed with KOH; (metal oxide)/(KOH) = 1; (KOH)/(C) = 0.04; T = 625°C; reproduced from Ref. 9. The numbers refer to the activation energies in kcal/mole of the indicated metal-oxide-KOH catalyzed system.

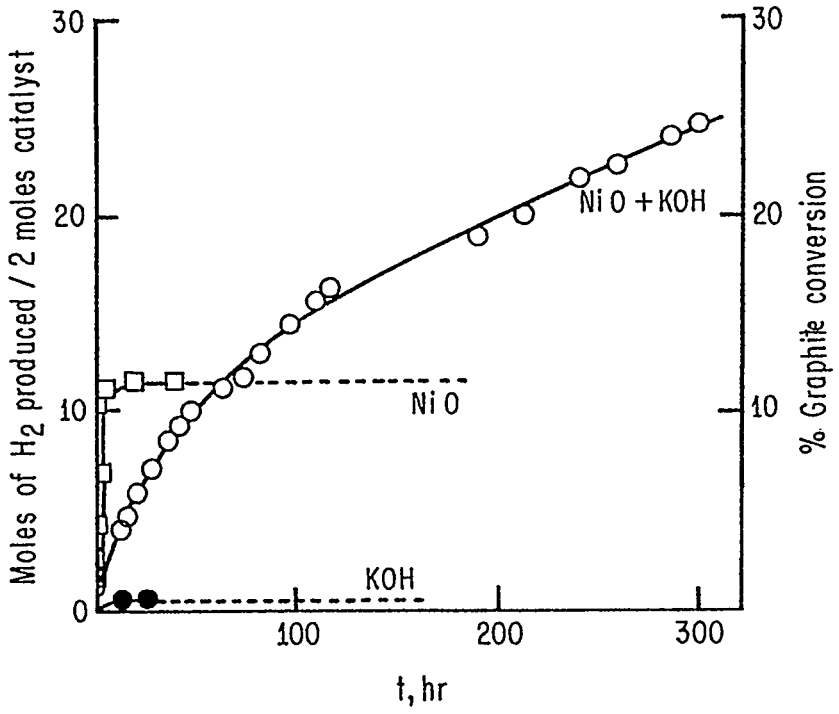

Fig. 7.1-5. Hydrogen production from graphite for the indicated catalysts at T = 527°C; reproduced from Ref. 9.

which is much more stable and is a more effective catalyst than either component alone. Recent work at LBL, performed in collaboration with workers at Exxon, has shown by electron microscopy in an environmentally controlled chamber that the mixed catalyst proceeds during gasification by edge recession at relatively good rates, while either component alone proceeds at lower rates by tunneling. The latter effect is illustrated in Fig. 7.1-9.

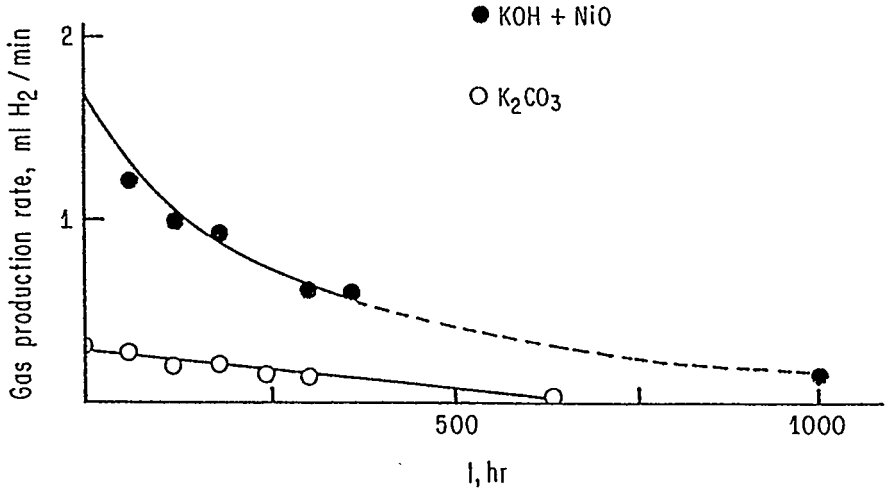

Fig. 7.1-6. Gas-production rates for Montana subbituminous coal using K_2CO_3-, KOH-, and NiO-catalyzed gasification; (K)/(C) = 0.01; (K)/(Ni) = 1.0, T = 620°C; reproduced from Ref. 9.

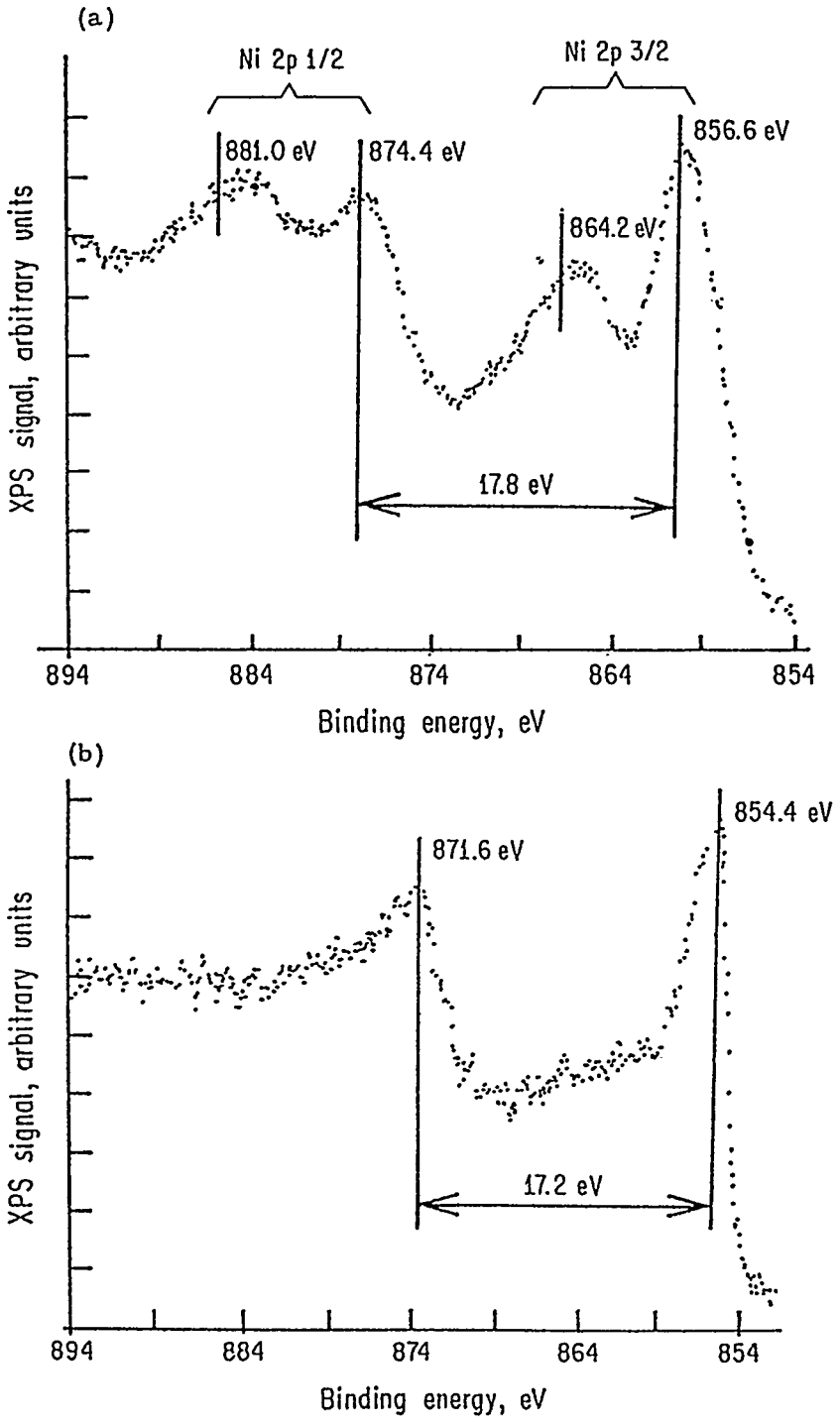

Fig. 7.1-7. The XPS diagrams for (a) Ni and (b) Ni and KOH; reproduced from Ref. 9.

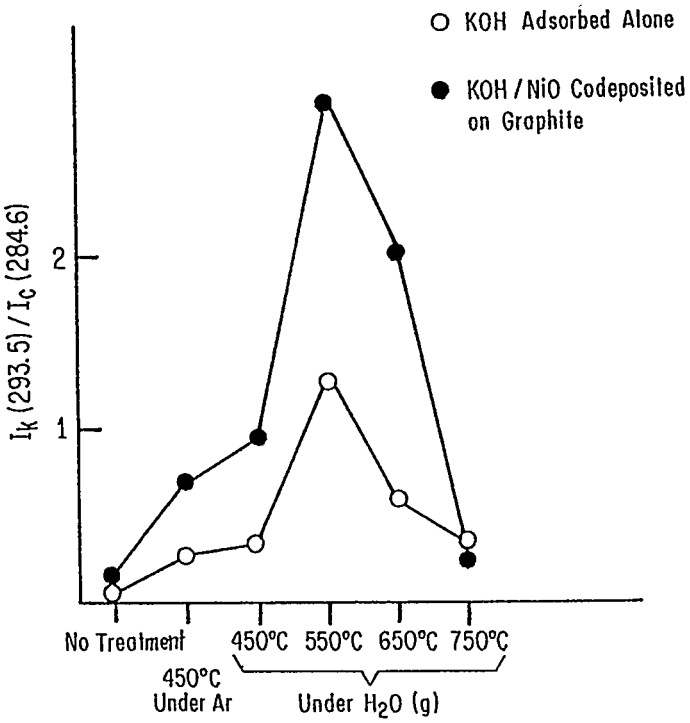

Fig. 7.1-8. The reciprocal binding energy, in terms of the ratio of the intensity at λ = 293.5 nm to the intensity at λ = 284.6 nm, is plotted as a function of temperature and in the presence of steam; reproduced from Ref. 9.

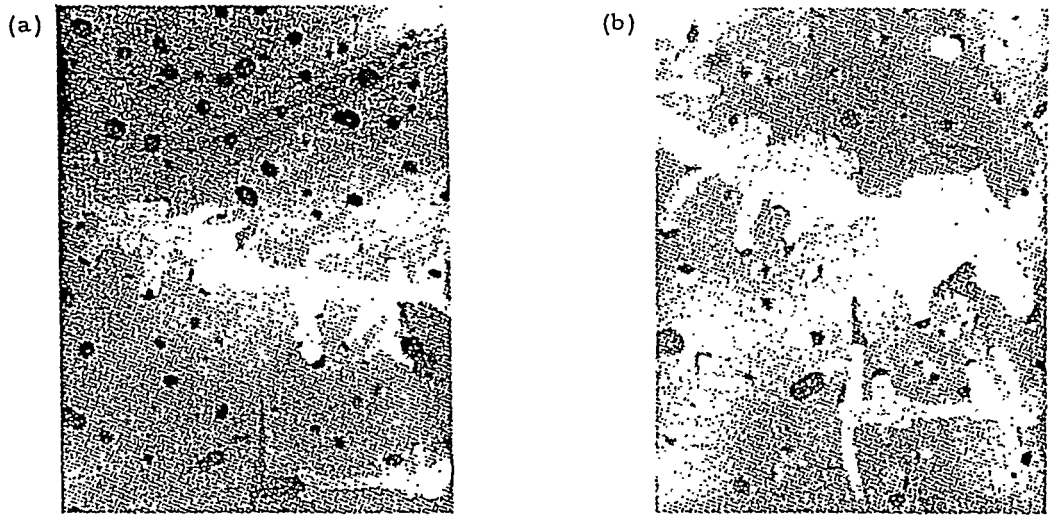

Fig. 7.1-9. Electron micrographs of KOH-catalyzed graphite; reproduced from Ref. 10; (b) was taken 11 min after (a) and shows tunneling effects induced by the catalyst.

References for Section 7.1

1. V. V. S. Revankar, A. N. Gokarn and L. K. Doraiswamy, "Catalytic Gasification of Carbon by Steam - Effect of Sodium Salts," Proceedings of the 1985 International Conference on Coal Science, pp. 249-252, Pergamon Press, NY (1985).
2. P. S. Kokorotsikos, G. G. Stavropoulos and G. P. Sakellaropoulos, "Catalytic Gasification of Greek Lignites," pp. 253-256 in Ref. 1.
3. Y. Nishiyama and T. Haga, "Peculiarity in Catalytic Gasification of an Australian Coal," pp. 257-260 in Ref. 1.
4. K. J. Hüttinger and R. Minges, "New Technical Perspectives for Catalytic Coal Gasification by Improving Activation of Low-Cost Catalyst Raw Materials," pp. 261-265 in Ref. 1.
5. M. -Z. Wei, X. -Q. Bani and K. -Q. Huang, "Effect of Several Compound Catalysts on Steam Gasification of Carbon," pp. 266-268 in Ref. 1.
6. W. Schumacher, H. J. Mühlen, K. H. van Heek, and H.Jüntgen, "Influence of Temperature, Pressure and Gasifying Agent on the K_2CO_3-Catalyzed Gasification of Char," pp. 269-272 in Ref. 1.
7. T. Takarada, Y. Tamai, and A. Tomita, "Effectiveness of K_2CO_3 and Ni Catalysts on the Steam Gasification of Thirty-Four Coals," pp. 273-276 in Ref. 1.
8. M. B. Cerfontain, R. Meijer and J. A. Moulijn, "The Difference in Reactivity of the Alkali Carbonates for the Catalyzed Carbon Gasification Interpreted with Transient Kinetic Measurements," pp. 277-280 in Ref. 1.
9. H. Heinemann, "Steam Gasification at Relatively Low Temperatures," unpublished, Lawrence Berkeley Laboratory, CA, and "Fundamental Research at UCB," pp. 309-336, Report of the Second Technical Meeting of COGARN, Feb. 25, 1986.
10. H. Heinemann and G. A. Somorjai, "Mechanism of the Catalytic Gasification and Reactivity of Graphite," pp. 401-410 in Chemical Reactions in Organic and Inorganic Constrained Systems, R. Setton, ed., D. Reidel Publishing Co., Hingham, MA (1986).

7.2. The Exxon Process for Catalytic Coal Gasification *

The Exxon Process is based on the long-known[1] discovery that potassium salts promote the gasification of coal. A single reactor process, called the Catalytic Coal Gasification (CCG) reactor, was developed at Exxon to gasify coal at a temperature of ~ 700°C.

7.2-1. Process Features

In the reaction of H_2 with CO, low temperatures strongly favor equilibrium production of CH_4 (Fig. 7.2-1). However, the gasification of coal, which must take place earlier than this methanation reaction in order to produce CO and H_2, occurs slowly at these lower temperatures ($T \leq 900°C$).

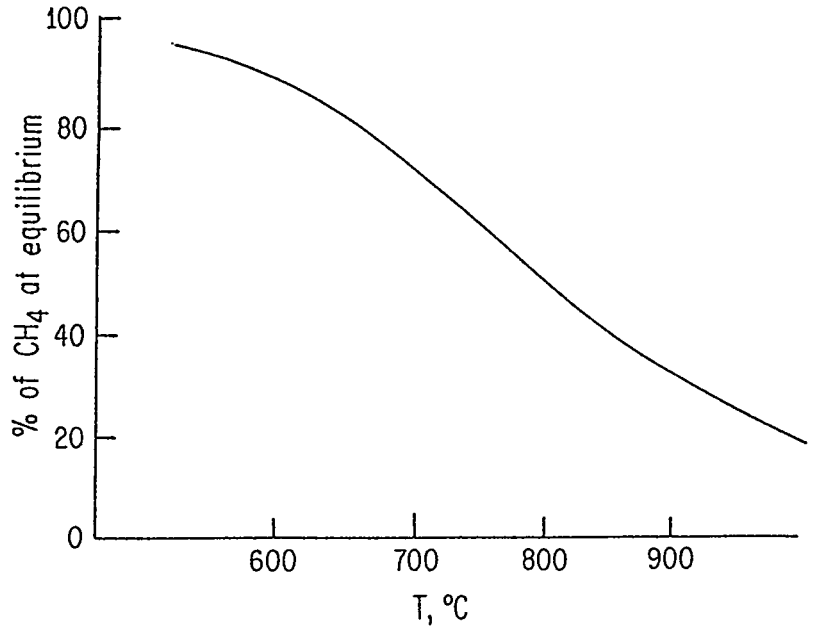

Fig. 7.2-1. Equilibrium conversion to methane according to the reaction $3H_2 + CO \rightleftarrows CH_4 + H_2O$ at 3.5 MPa as a function of temperature; reproduced from Ref. 2.

---

* Prepared by S. S. Penner and D. F. Wiesenhahn. The authors are greatly indebted to A. M. Edelman (Exxon) for supplying published information and for helpful advice.

The role of K, which is used at a level of 10 to 20% of the dry coal weight, is to accelerate the gasification of coal at lower temperatures. Workers at Exxon discovered that K on coal is a good methanation catalyst. Thus, addition of K allows both the gasification and the methanation reactions to occur at the same temperature in a single reaction vessel that is sufficiently small to be commercially acceptable. Since the overall coal-to-methane conversion is almost thermoneutral (Fig. 7.2-2), occurrence of both reactions in a single vessel requires

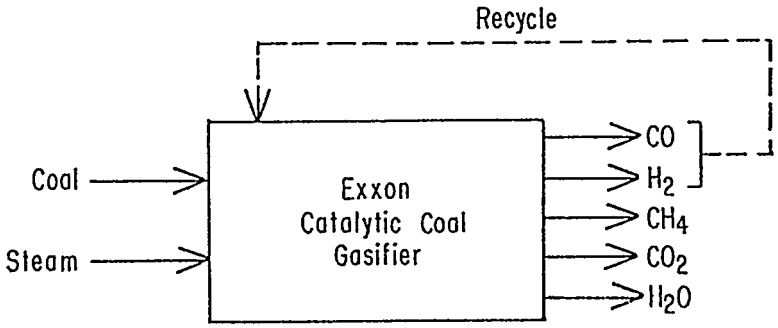

Gasification reaction: $2C + 2H_2O \longrightarrow 2CO + 2H_2$, $\Delta H_R = 268kJ$;
Shift conversion: $CO + H_2O \longrightarrow CO_2 + H_2$, $\Delta H_R = -34kJ$;
Methanation: $CO + 3H_2 \longrightarrow CH_4 + H_2O$, $\Delta H_R = -226kJ$;

Overall reaction: $2C + 2H_2O \longrightarrow CH_4 + CO_2$, $\Delta H_R = 8kJ$.

Fig. 7.2-2. Diagram showing the overall reactions occurring in the Exxon CCG.[2]

a very small heat input. This small energy deficit is made up by addition of steam and by recycling the CO and H_2 of the product gas.

A schematic diagram of the plant design is shown in Fig. 7.2-3. As received coal is crushed (1) to < 2.4-mm size, partially dried, mixed with aqueous catalyst solution, dried again to about 4% moisture (2), and fed to the gasifier through a lock hopper (3); for some caking and swelling coals, the last drying step 2 incorporates mild oxidation to reduce swell-

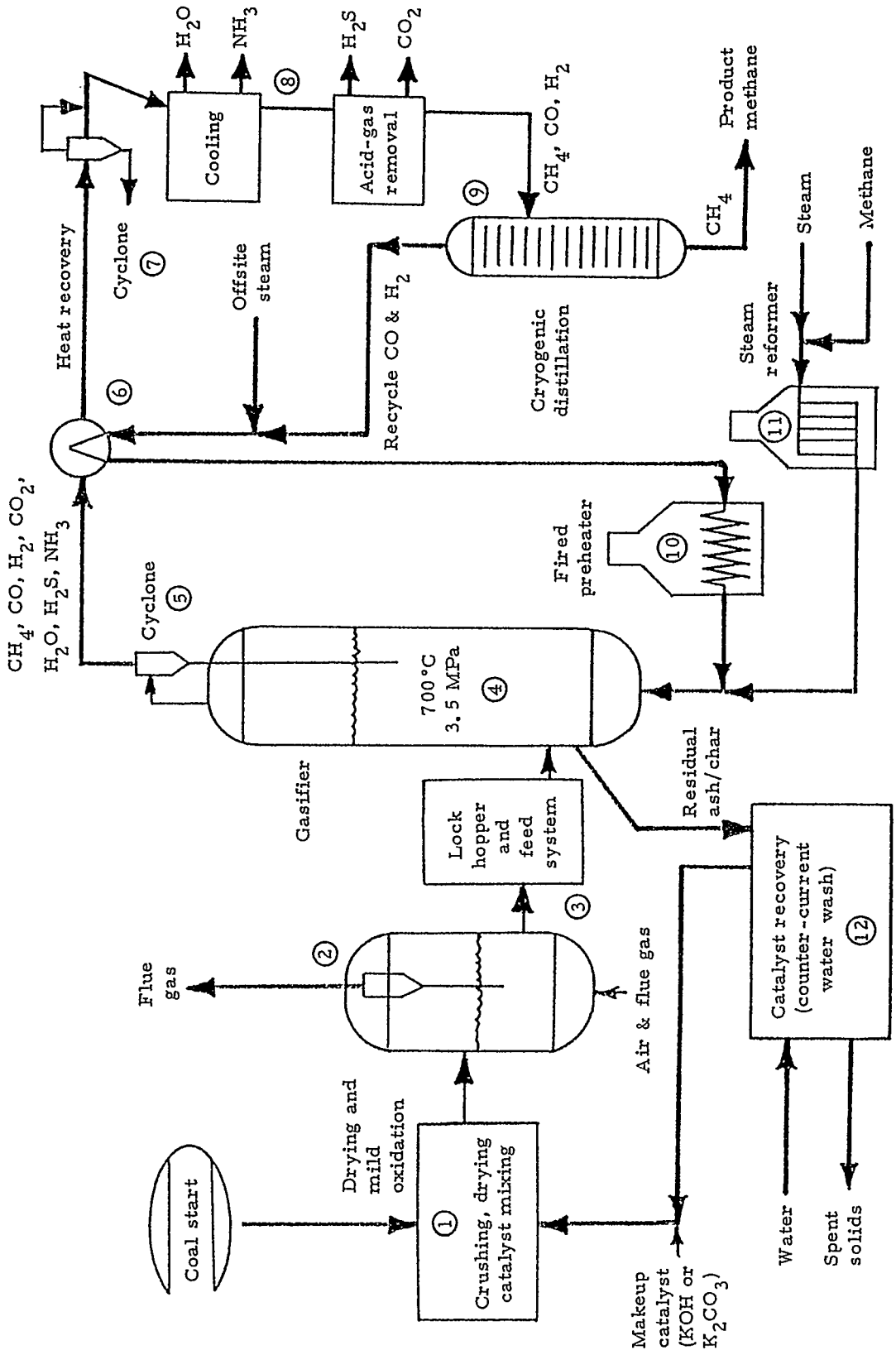

Fig. 7.2-3. Schematic plant diagram of the Exxon CCG.[2]

ing in the gasifier. The gasifier (4) operates at 700°C and 3.5 MPa. A cyclone (5) is used to return entrained fines from the effluent gases to the gasifier. After high-level heat recovery (6), the remaining fines are removed by cyclones and a venturi scrubber (7) before the unconverted steam is separated and cooling and acid-gas removal (with commercially available technology) occurs. The methane is separated from the product stream of CH_4, CO, and H_2 by cryogenic distillation (9), while CO and H_2 are recycled to the gasifier after heat recovery in (6) and additional preheating in (10). The output gases are thus CO_2, CH_4, H_2O and small amounts of NH_3 and H_2S. Some of the product methane may be reacted with steam (11) to augment the input of CO and H_2 and to increase the H_2-to-CO mole ratio. The catalyst is recovered from the residual ash/char leaving the gasifier by using a counter-current water wash (12) and is then recycled to the catalyst-mixing unit (1).

A portion of the catalyst reacts with the coal ash to form insoluble compounds, primarily potassium aluminum silicates, and cannot be recovered. The extent of catalyst removal depends on coal-ash level and composition. With Illinois No. 6 coal, about 70% of the catalyst is water-soluble, i.e., about 30% of the original potassium must be made up (as KOH or K_2CO_3).

7.2-2. Development Work

Development of CCG technology proceeded with DoE support from bench-scale research (< 20g of coal per test) between July 1976 and January 1978 at a cost of $2.4 X 10^6$, to pilot-plant testing (25 to 90 kg/day) between July 1978 and March 1981 with DoE and GRI support at a level of $6.8 X 10^6$, to a process-development unit (PDU, 1 mt/day) and engineering designs of larger plants.[2] The automated PDU at Baytown, TX, was complete with all components operational and was sufficiently large for continuous coal feed and product withdrawal.[2] The gasifier had a 0.25m diameter and was 25m long. The reactor and feed equipment were contained in a 12-story tower. Following start-up in mid-1979, the PDU was operated intermittently for about 4 years, with a 23-day demonstration run in April 1981 on Illinois No. 6 coal. Results are summarized in Table 7.2-1 and 14 material balances (with 5% closure) were completed for separate 24-hr

periods. Entrained fines were not recycled in the PDU; recycling would have further improved the carbon conversion. The somewhat low methane yield of 21% is consistent with the steam/coal ratio used.

In 1982, two bituminous and one subbituminous coal (Wyodak, a U.S. Western coal) were tested, with the bituminous coal simulating the Illinois No. 6 test results.[3-5] Coal pretreatment and performance require improvements. The Wyodak coal performance is summarized in Table 7.2-2. Comparisons of results listed in Tables 7.2-1 and 7.2-2 show that, for comparable test-bed conditions, the Wyodak coal yielded higher bed densities. Furthermore, lower overhead char was obtained presumably because Wyodak coal swells less than Illinois No. 6 coal. The high moisture content of Wyodak is expected to yield good catalyst impregnation. Carbon conversion decreased with increasing coal-feed rate and reduced gasifier-residence time, whereas the overhead entrained char remained essentially constant, i.e., fines production appeared to depend on feed-coal characteristics and not on processing conditions.[2] Of particular importance is the strong dependence of methane yield on steam/coal ratio, which was also observed for Illinois No. 6 and is claimed to be predicted from the Exxon gasifier model used for analysis.

In the 25-m long process-development unit for gasification, the bed level during operation reached 15 to 17m.[5] The highly automated PDU had a programmable controller for sequential and cyclic operations, safety interlocks and shutdown, while monitoring ~ 800 process variables concurrently with off-line data analyses.[5] Following start-up in 1979, the most serious operational problem encountered was agglomerate formation at the bottom of the gasifier at low gasifier fluidized-bed density and low CH_4 production. The agglomerates consisted of either (i) black, water-insoluble, low-conversion coal particles cemented together by hydrocarbons or (ii) light clusters that were disintegrated by water and consisted of ash particles held together by water-soluble K_2CO_3. If allowed to persist for several hours, the agglomerates accumulated at the bottom in the presence of steam and formed a plug that interfered with char withdrawal. The agglomerates were ultimately eliminated by increasing the gas velocity in the coal-feed line and thereby prevented fresh coal particles from sticking together.[5] Successful runs of 20 to 30 days and 5000 operating hours were subsequently accomplished over a period of 2 years.[5]

Table 7.2-1. Results for a 23-day PDU CCG on Illinois No.6 coal at 3.5 MPa; reproduced from Ref. 2.

Performance Parameter	Targets	Achieved
Coal plus catalyst feed rate, kg/hr	60	60
Temperature, °C	704	693
Pressure, MPa	3.45	3.45
Steam/coal ratio	1.7	1.9
Bed density, kg/m^3	> 160	256
Carbon conversion, %	> 85	85-90
Steam conversion, %	30-40	35
CH_4 in product gas, %	> 25	21
Test duration, days	14-21	23

Table 7.2-2. Results for a 27-day test of CCG for Wyodak coal at 3.5 MPa; reproduced from Ref. 2.

Performance Paramater	Coal Plus Catalyst Feed Rate, kg/hr		
	50	59	79
Temperature, °C	692	693	694
Steam/coal ratio	2.1	1.8	1.5
Solids residence time, hrs	38	27	14
Bed density, kg/m^3	480	432	320
Entrained char, %	12	16	13
Carbon conversion, %	92	85	79
Steam conversion, %	36	38	33
CH_4 in product gas, %	16	19	24

An initially obtained low fluidized-bed density (75 to 100kg/m^3) into fine particles leading to excessive fines losses. This problem was ultimately solved by mild oxidative pretreatment in the presence of catalyst in a narrow temperature range (around 200°C for some oxygen concentrations), where the coal swelling-index is very low (see Fig. 7.2-4).[5] During mild oxidation, carboxylic acid groups are added to the coal structure and the number of these added groups is greatest at the optimum temperature. With mild preoxidation, the reduction in fluidized-bed densities from an initial value of 300 kg/m^3 was strongly inhibited. Finally, it was shown[5] that preoxidation during 4 to 11 hours at 175 to 200°C yielded gasifier bed densities of 200 to 450kg/m^3. At ~ 5% incremental cost, a fluidized bed dryer may be used for both drying and preoxidation (cf. Sec. 7.2-3).

Methane production in the PDU is kinetically determined and falls well below the theoretical equilibrium curve as the steam-to-carbon mole ratio is lowered (see Fig. 7.2-5). As is evident from Fig. 7.2-5, about 27% of CH_4 was obtained in the product gas at a steam-to-carbon mole ratio of about 1.7.

Equilibrium catalyst recycle was not achieved. Instead, a theoretically predicted steady-state recycle catalyst composition was made up and tested. Process results for Illinois No. 6 coal were found to be the same with once-through and simulated recycle catalyst. However, the simulated recycle catalyst was found, in two successive trials, to produce a hole, after 10 days of operation, in the 316 stainless steel (SS) overhead line leading from the gasifier to the cyclones, filters and gas coolers. The cause of pipe failure was hot corrosion caused by molten salt fluxing of protective oxides from the metal surfaces, followed by rapid sulfidation. Bench-scale studies showed that alloys with higher Cr-contents would resist hot corrosion. The test section and results are shown in Fig. 7.2-6. The higher Ni-alloys should provide resistance to caustic stress-corrosion cracking, while 310 SS gave the best results.

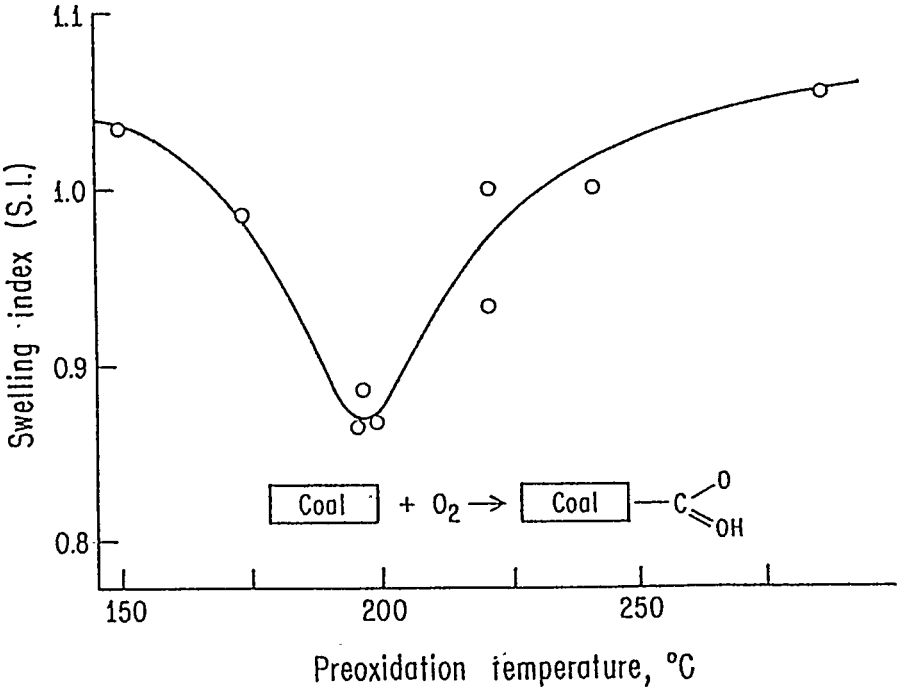

Fig. 7.2-4. The swelling index is shown as a function of coal preoxidation temperature from a bench-scale experiment with 6% O_2 in N_2 and a 6-hr residence time; the S.I. of unoxidized coal = 1.3; reproduced from Ref. 5.

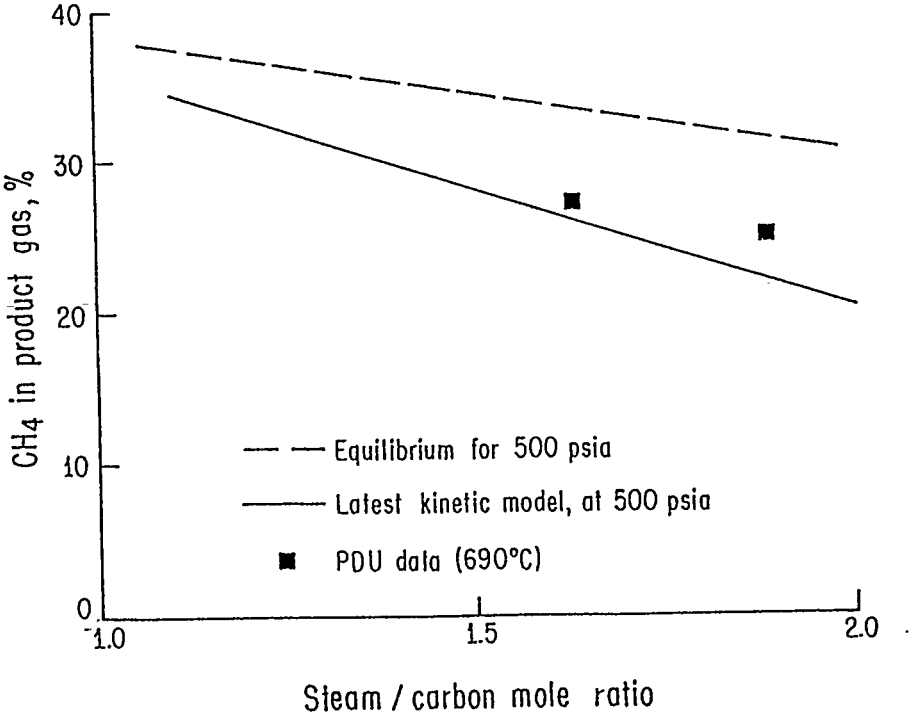

Fig. 7.2-5. The amount of methane in the product gas is shown as a function of the steam/carbon ratio at 3.5 MPa (500 psia); reproduced from Ref. 5.

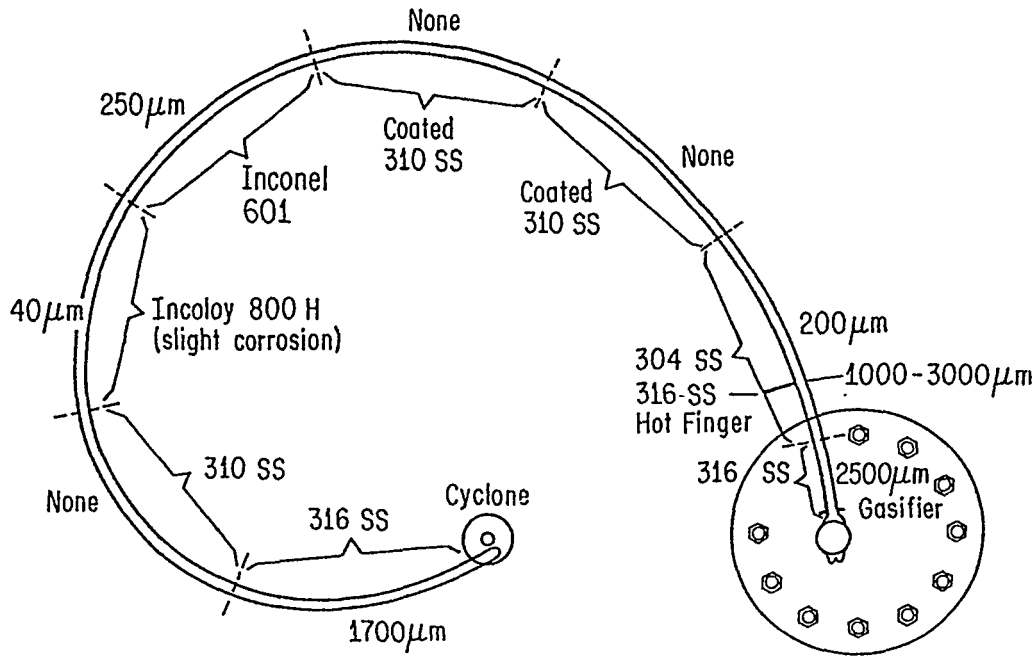

Fig. 7.2-6. Test section used for 9 days in hot-corrosion studies; the 310 SS and the coatings performed well, whereas 316 SS was heavily corroded. The thickness in μm represents approximate corrosion losses; reproduced from Ref. 2.

7.2-3. Fluid-Bed Slurry Dryer (FBSD)

The FBSD is used to recapture heat from coal drying (Fig. 7.2-7). Wet catalyzed coal slurry is fed to the unit, which operates at 4MPa and 260-425°C. Superheated steam is used to fluidize the solids and evaporate water. The steam leaving the dryer is scrubbed to remove entrained coal fines. Some of the steam leaving the scrubbers is compressed, superheated and recycled, while the remainder is fed to the gasifier. The dried coal is transferred to the gasifier in the fluidized state. The FBSD (i) recovers energy for coal drying as gasification steam and (ii) produces preheated coal for the gasifier at a higher T than can be fed through the lock-hopper system. A 2-mt/day FBSD was started up in 1983.

7.2-4. Mechanisms of Catalysis and Selection of Alternative Catalysts

The rates and reaction mechanisms involving the potassium are not understood. In fact, the label catalyst for K is a misnomer since experimental measurements (see Fig. 7.2-8) of the gasification rate as a function

of K/C mole ratio show the effective rate coefficient to be a linear function of the active K/C ratio, where the rate constant k is defined by the ratio

$$k = -[d\ln(C)/dt]/[(H_2O)/(H_2)]. \qquad (7.2\text{-}1)$$

The fact that (compare Fig. 7.2-8)

$$-d(C)/dt = k(C)(H_2O)/(H_2) \cong 7.5x(K_{active})(H_2O/(H_2) \qquad (7.2\text{-}2)$$

suggests a complex reaction mechanism with K as an active participant and the possibility of finding alternative chemicals that may be more effective than K in gasification. In Fig. 7.2-8 and in Eq. (7.2-2), (K_{active}) is the total molar K concentration less the molar K concentration bound in ash minerals. The precise form of C is seen to have little effect on gasification activity (compare Fig. 7.2-8). The method of introduction used for K was also found to be unimportant, since substantially equivalent results were obtained for carbon compounds impregnated with aqueous K_2CO_3 or KOH or dry K_2CO_3 in powdered form.

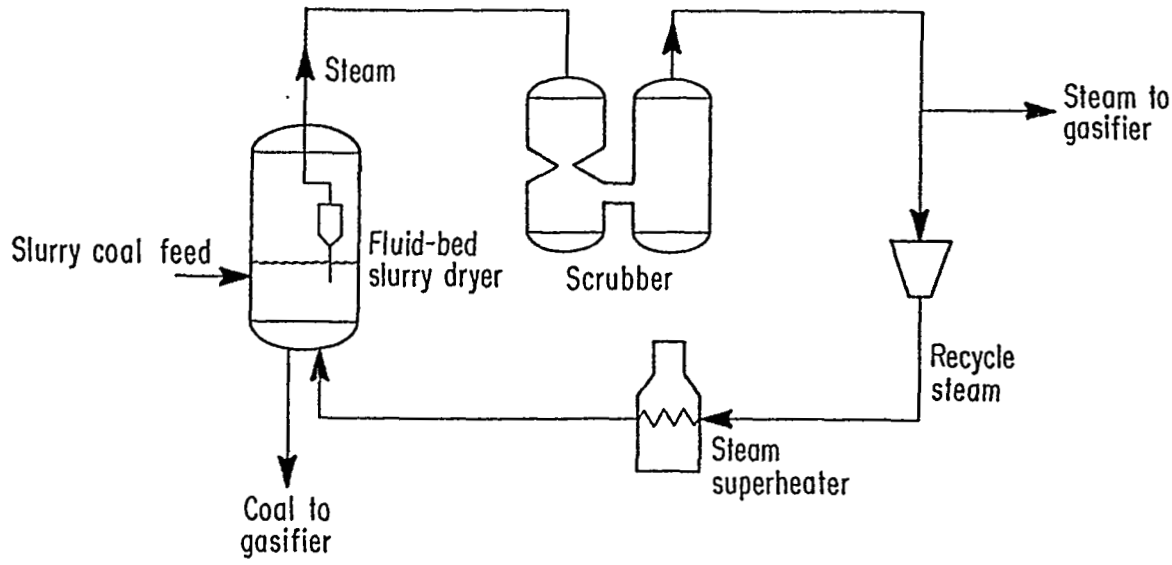

Fig. 7.2-7. Schematic diagram of the FBSD; reproduced from Ref. 2.

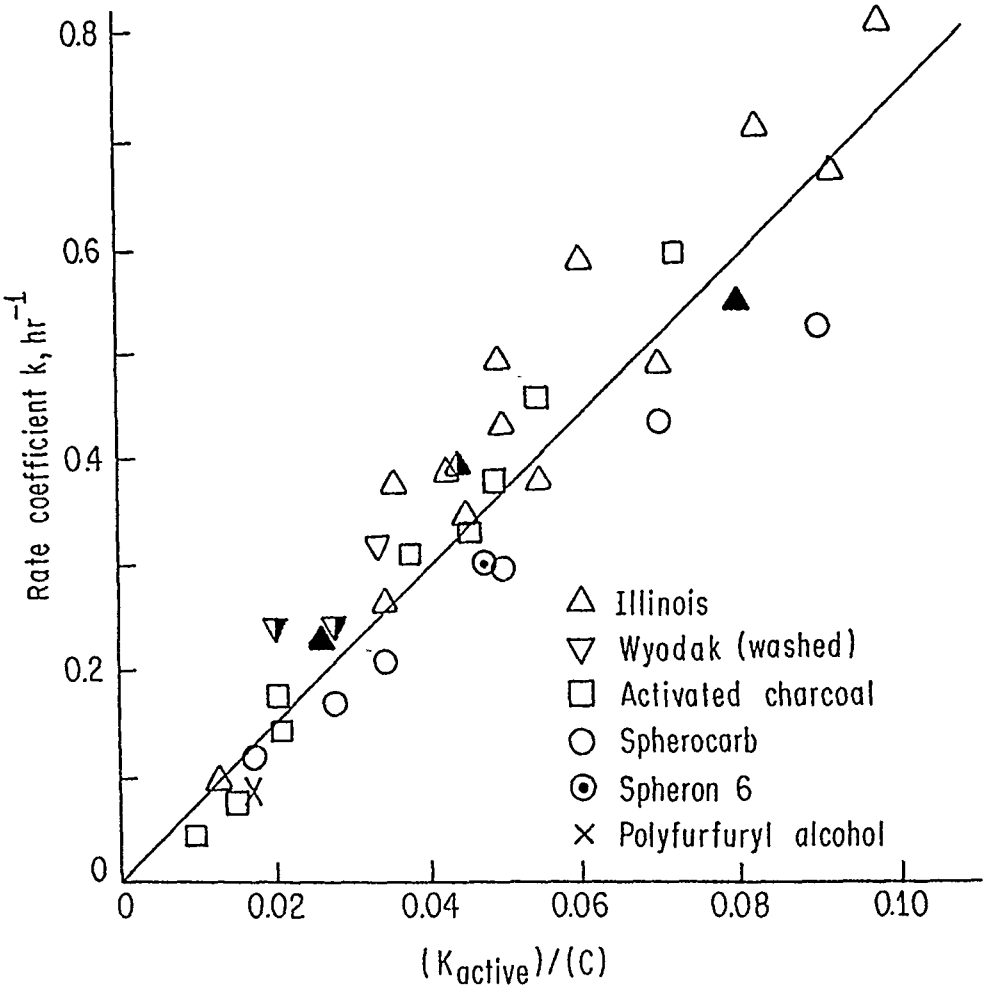

Fig. 7.2-8. The rate coefficient k observed in a small flow reactor as a function of the molar ratio of K to C for a variety of carbonaceous materials at 1 atm; reproduced from Ref. 5. Open symbols refer to K introduced as aqueous K_2CO_3 or KOH, whereas filled-in symbols refer to K added as dry K_2CO_3 powder; the half-open symbols refer to K introduced by ion-exchange.

The results were interpreted[5] to show that active sites form on the coal surface by combination of K_2CO_3 with char, leading to the release of CO_2. This mechanism was verified by C-14 labeling of some of the C in K_2CO_3, which was observed to be released when reacted with coal. Furthermore, X-ray diffraction also showed the disappearance of K_2CO_3 as it interacted with the coal. Using isotope tracers, rapid water decomposition and surface oxide formation were observed at the active sites, whereas the rate was inhibited by oxide reduction with H_2. The final rate-determining

step leads to CO formation and involves the critical surface oxide.[5] The following are believed[5] to be critical reaction steps in the gasification mechanism:

$$\text{char} + K_2CO_3 \longrightarrow \text{K-char} + CO_2 \quad \text{(complex formation)}, \quad (7.2\text{-}3)$$

$$\text{K-char} + H_2O \longrightarrow \text{K-char-O} + H_2 \quad \text{(water activation)}, \quad (7.2\text{-}4)$$

$$\text{K-char-O} \longrightarrow \text{K-char} + CO \quad \text{(gasification)}. \quad (7.2\text{-}5)$$

This reaction model was usefully employed in the design of the gasification reactor.[6,4]

The observed approach to the equilibrium curve of Fig. 7.2-1, at fixed pressure and catalyst loading, is strongly dependent on T. For 20wt%

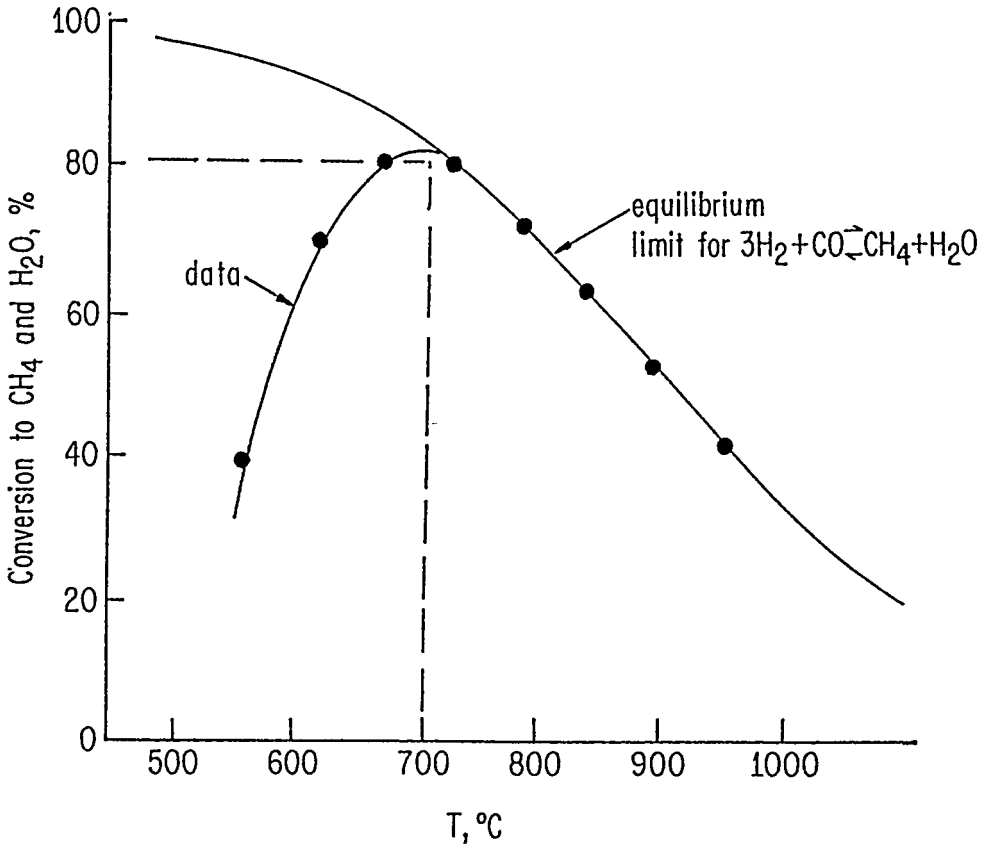

Fig. 7.2-9. Conversion to methane as a function of temperature for 20wt% K_2CO_3, 80wt% char, at 3.5MPa and a space velocity of 2300 volumes of reactants per hour per volume of gasified bed; reproduced from Ref. 5.

K_2CO_3, 3.5MPa, and a space velocity of 2300 volumes of reactants/hr per volume of gasifier bed, the equilibrium composition was observed in experimental studies (see Fig. 7.2-9) down to about 700°C. Below T = 700°C, a sharp drop-off in percentage conversion to CH_4 occurred from ~ 82% at 700°C to ~ 40% at 540°C. An ideal catalyst would allow conversion to CH_4 to follow the equilibrium curve to substantially lower temperatures (~ 300-500°C).

Alternative catalysts should be so inexpensive that catalyst recovery is not necessary and so effective that reduced process temperatures may be used, while the methane content of the product gas is sufficiently high to eliminate the need for cryogenic separation (compare Fig. 7.2-3) and recycle to CO and H_2. A promising candidate for a throw-away catalyst is Ca, which was shown in bench-scale tests on Illinois No. 6 coal to yield nearly the same gasification rates as K at 700°C. The requirement of a somewhat higher operating T with Ca is a detriment. In general, a small reduction in methane yield and the greater difficulty of catalyst impregnation with Ca must be weighed against elimination of the catalyst-recovery unit and the use of lower cost materials. Hot corrosion and caustic stresses associated with K may also be reduced with Ca.

7.2-5. Environmental Aspects of CCG

Applicable environmental standards will be met with CCG, using conventional technology such as a Claus plant to convert H_2S to S_x and biological oxidation and/or carbon absorption for wastewater treatment. Tar or heavy oil by-products are not produced in normal CCG operation. At 90% carbon conversion, the wet char, after catalyst recovery, will contain 10-15% of carbon and 7 to 10% of K as insoluble salts; for long-term disposal, this material must be processed, e.g., by combustion to remove residual carbon while raising steam and forming stable aggregates.

The char has not shown genetic activity or carcinogenicity in short-term tests; long-term dermal tests remain to be completed. Leaching of toxic material met applicable standards of the US Resources Conservation and Recovery Act for nonhazardous wastes.

7.2-6. Large Pilot Plant

Long-term process and equipment performance data on a large pilot plant are needed before scale-up to commercial plant sizes. Also needed are results for a variety of coals. Environmentally acceptable performance over a long period of time remains to be demonstrated.

References for Section 7.2

1. H. S. Taylor and H. A. Neville, JACS 43, 2065 (1921).
2. R. A. Cardello, R. A. Reitz and F. C. R. M. Smits, "Catalytic Coal Gasification Development," Discussion No. 5, 11th World Petroleum Congress, London, England (August 1983).
3. R. R. Lessard and R. A. Reitz, "Catalytic Coal Gasification: An Emerging Technology for SNG," presented at the 9th Energy Technology Conference, Washington, D.C. (February 1982).
4. C. A. Euker, Jr., and R. D. Wesselhoft, "Catalytic Coal Gasification-Process Development Unit Operations," presented at the 90th AIChE National Meeting, Houston, TX (April 1981).
5. R. L. Hirsch, J. E. Gallagher, Jr., R. R. Lessard, and R. D. Wesselhoft, Science 215, 121 (1982).
6. J. M. Eakman, R. D. Wesselhoft, J. J. Dunkleman, and D. J. Vadovic, Coal Processing Technology, Vol 6, pp. 146-158, AIChE, New York (1980).

7.3 Recommended Research for Syngas Production from Coal

The following items 1 to 6 are viewed as high-priority and item 7 as a possible research area, which would be pursued at Exxon if the project were still active:

1. Definitions of optimal coal-pretreatment conditions for different coals and catalysts.
2. Studies of rates and mechanisms of salts leaching from coal ash during counter-current washing for catalyst recovery; studies to reduce costs of the recycle system.

3. Long-term, hot-corrosion testing under steady-state operating conditions and laboratory studies to define mechanisms and rates of hot corrosion.
4. Identification of lower-cost, throw-away catalysts.
5. Identification of catalysts for operation at reduced T.
6. Research to assure long-term leaching stability of coal ash.
7. Improvement of the quantitative gasifier model.

The 1 mt/day PDU project was terminated in late 1983. Exxon believes that its 1978 cost estimates are generally valid but that the fossil-fuel market conditions changed to such an extent that adequate return on investment could not be assured in the foreseeable future with syngas production.

Laboratory research should focus on development catalysts that hold the promise of improving operating conditions (e.g., lowering required temperatures, residence times, pressures, system sizes) or improving the initial gas composition (lowering pollutant levels, increasing methane yields, etc.). Many different approaches and catalysts are being studied empirically (Sec. 7.1-1). A useful theoretical interpretation and classification of research results in terms of systems promise remains to be worked out and should be supported by DoE.

CHAPTER 8:
GAS-CLEANING PROCESSES FOR COAL GASIFICATION*

8.1. Introduction

Gas-cleaning systems are incorporated in the process design of coal-gasification facilities for the purpose of converting the raw gas exiting the gasification reactor into a gas which meets end-use specifications. Thus, the design and structure of the gas-cleaning system (Fig. 8.1-1) depend on both the characteristics of the gasification process, which determines raw-gas composition, and on end-use specifications. Potential end uses for the gaseous products from coal gasification include fuel for on-site boilers, turbines or fuel cells and synthesis gas for the production of methane (SNG), ammonia, methanol, or other HC products. The gas composition and purity specifications vary widely for these applications, as is illustrated in Table 8.1-1.

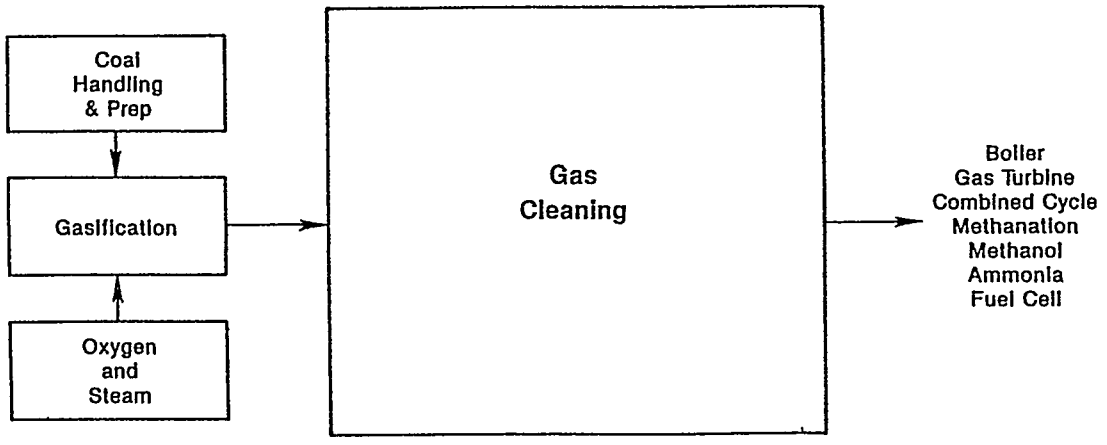

Fig. 8.1-1. Role of gas cleaning in coal gasification.

* This chapter has been written by Robert A. Magee (Radian Corp.). An Appendix to this chapter by J.F. Elliott (M.I.T.) deals with the use of slag for in-bed sulfur removal.

Table 8.1-1. Example of gas cleanup requirements.

Parameter	Boiler combustion	Gas turbine	Fuel cells	Methanation, methanol
Particulates	0.03 lb/10^6 BTU (0.07 g/SCF at at 350 BTU/SCF)	0.025 g/SCF (<3 μm) 0.03 g/SCF (3-5 μm) 0.0036 g/SCF (>5 μm)		
S	1.2 lb/10^6 BTU (2500 ppm)	500 ppm	5 ppm	0.2 ppm
Cl			1.0 ppm	
NH_3			0.1 ppm	
Metals (ppm, w/w)				
V		0.5		
Na + K		0.5		
Ca		10		
Pb		2		
Cu		0.2		

The parameters listed in Table 8.1-1 represent some of the fuel specifications for boilers, turbines or fuel cells and for methanol production. Some of these specifications, such as those for boiler fuels, reflect environmental limitations that are imposed on the resulting emissions through end-use applications. Other specifications are based on operational requirements relating to the end-use process, for example, the avoidance of catalyst poisoning in methanation or the production of methanol.

8.2. Gas Cleanup Systems

Current design approaches for gas cleaning consist of the serial application of a number of gas-cleaning processes, each of which is designed to remove one or more contaminant species, as illustrated in Fig. 8.2-1. The contaminant species of interest for most combinations of gasification and end-use applications are aerosols (both particles and liquid droplets), sulfur compounds, inorganic compounds, alkali and heavy metals, and organic chemicals. The capital cost for these processes is a significant portion of the total cost of the facility. The 1979 data shown in Table 8.2-1 still constitute a relatively accurate presentation of the impact of major elements of a coal-gasification facility on the total capital cost of the facility.[2] The data apply to two of the primary types of coal-gasification

systems that are commercially available [i.e., pressurized, fixed-bed (Lurgi) and pressurized, entrained-bed (Texaco) systems] when these are applied in combination with two of the most economically viable end uses

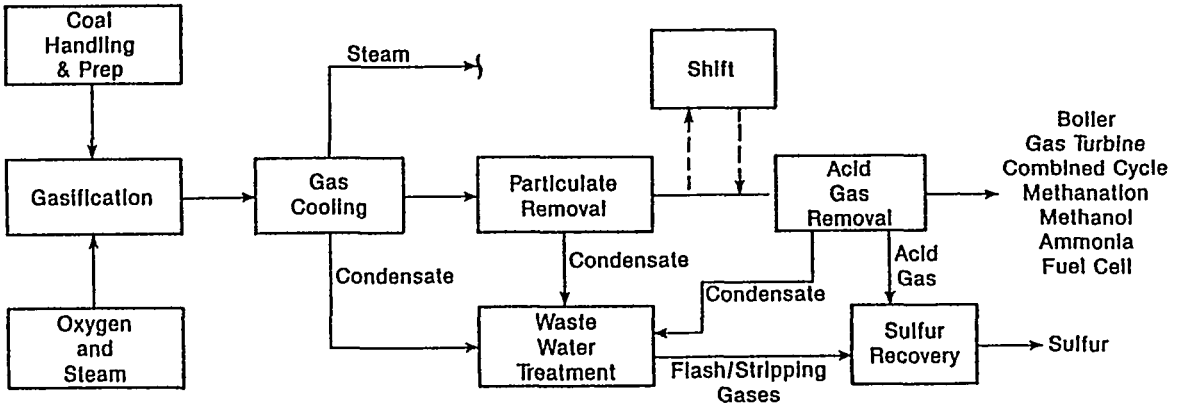

Fig. 8.2-1. Major coal-gasification process units.

Table 8.2-1. Plant investment breakdown; reproduced from Ref. 2.

Process	Percent of Total Plant			
	Lurgi SNG		Texaco IGCC	
Coal handling and preparation	1.0		3.7	
Oxygen and steam	29.3		18.7	
Gasification and ash handling	18.3		3.8	
Gas cooling and condensate treatment	10.5		13.6	
Shift	2.5	= 31.9	--	= 23.7
Acid-gas removal	15.6		8.1	
Sulfur recovery	3.3		2.0	
Methanation and SNG handling	11.7		--	
Combined-cycle system	--		42.8	
Support facilities	7.8		7.3	
Total	100.0		100.0	
$\frac{\Sigma \text{ Gas cleaning}}{\text{gas plant}}$	36.1		41.4	

(production of SNG and IGCC for electric power generation). Since 1979, these process configurations have been constructed and operated on a commercial scale and the relative capital costs listed in Table 8.2-1 have been demonstrated to apply to the US.

Based on the generally accepted design approach for serial applications of species-specific processes, the most probable means for reducing significantly the capital investment required for the gas-cleaning portion of a coal-gasification facility is the drastic simplification of the elimination of one or more process units in the gas-cleaning system. With this objective in mind, the approaches and processes available to remove contaminants from the process gas were reviewed and examined for opportunities to achieve simplification or elimination of units through additional research and development. The process components reviewed were (i) quenching, cooling and heat recovery; (ii) removal of particles, aerosols, and inorganic compounds; and (iii) acid-gas removal and sulfur recovery.

8.3. Quenching, Cooling and Heat Recovery

These processes may be grouped into two broad generic categories: direct and indirect.

Direct processes involve intimate contact between the gas and the cooling or quenching medium (usually water) and are generally accomplished in a scrubber system, which also removes at least a portion of the aerosols and inorganic contaminants. The direct contact processes are distinguished by their mechanical configuration or mode of forced mixing and contact between the gas and the scrubbing medium. Configurations include spray towers, venturi and packed-bed scrubbers and simple dip-tube quench-chambers. Although these vary widely in contact efficiency, they suffer from common problems and limitations. The liquid-phase build-up of dis-solved or suspended components that are removed from the gas results in deposits or plugging if it is not reduced by blowdown. This blowdown must be treated prior to discharge or recycle to the process. In all configura-tions, the contact efficiency between gas and liquid is proportional to the energy expended in the contacting process. Minimization of the slope of this energy-efficiency relation has been the objective of years of research in gas-liquid contractor design.

Indirect processes involve the transfer of heat through an intermediate from the gas to the cooling or quenching medium. Indirect contact configurations include shell-and-tube and water-wall boiler designs, as well as gas-recycling schemes. The transfer of heat from the gas to the cooling

medium involves not only the characteristics of the medium and the gas but also those of the transfer medium and the contact configuration. Thus, the efficiency may be enhanced through materials research and refinement and through development of techniques which predict the heat-transfer properties and longevity of the transfer medium. Research on heat transfer, tube fouling and waste-heat boilers and models may be expected to contribute to this predictability and, therefore, to the design efficiency of future systems. For example, the radiant heat boiler at the Cool Water Gasification Project is significantly over-designed in order to provide adequate contingencies for uncertainties in boiler-design parameters and the unpredictability of the impact of ash and metals deposition on tubes and other heat-transfer surfaces.

8.4. Removal of Particles, Aerosols and Inorganic Compounds

Processes for the removal of particles and aerosols may be broadly grouped as wet and dry processes. Dry processes rely on filtration, as well as on aerodynamic momentum or electrostatic forces to impact and collect solid or liquid aerosols entrained in the flowing gas streams. High-temperature filtration developments have included applications of ceramic materials to the removal of fine particles from process-gas streams. Confident design and operation of dry aerosol-removal processes requires detailed understanding of solid-gas transport phenomena at gasification temperatures and pressures. Fluid dynamic data for complex mixtures at these conditions increase the design reliabilities and operating efficiencies of cyclones and similar aerodynamic collection devices.

Wet-collection processes are similar to the specified direct cooling and quenching processes. Many of the same design and operation considerations apply. In particular, gas-liquid mass-transfer models and parameters for NH_3, CO_2, H_2S, HCN, HCl, and other inorganic gasification products for the range of mixtures encountered for these components, are required to predict the performance of gas-scrubbing processes. Operation of these systems is often limited by precipitation or scale formation from dissolved components, in particular, carbonates and silicates. In addition, blowdown from these processes must be treated prior to discharge or recycle.

The construction of treatment processes requires similar gas-liquid mass-transfer data for the design of flash and stripping processes.

8.5. Acid-Gas Removal and Sulfur Recovery

Acid-gas removal and sulfur recovery are currently the most complex portions of the gas-cleaning train. A wide variety of collection media and contact configurations have been employed to enhance efficiency and reduce the costs of these processes. The commercially available processes may be grouped into five categories, depending on the collection media and chemical or physical processes involved: (i) chemisorption (mildly alkaline chemicals); (ii) physical absorption (organic solvents with high CO_2 and H_2S solubilities); (iii) hybrid systems (mixtures of mildly alkaline chemicals and organic solvents); (iv) solid sorbents; and (v) sulfur conversion (solutions or reactors which oxidize sulfide to elemental sulfur or sulfur oxides).

Each of these collections media and process types has distinctive characteristics, which lead to advantages and disadvantages for various applications. A summary description of the commercially available sulfur and acid-gas removal and recovery processes, their operating characteristics, and normal equipment configurations is presented in Ref. 3. Table 8.5-1 is a summary of example processes and characteristics for each major process type.

A great deal of industry-funded and proprietary development has contributed to the availability of a variety of liquid sorbent-based systems for acid-gas removal from process-gas petroleum-refining industries. All of the chemisorption and physical sorption processes require cooling of the gas prior to treatment and an additional process unit to treat the concentrated acid gases in order to recover sulfur components that are removed from the process gas. Significant economic advantages would be gained if cooling could be eliminated or removal and sulfur recovery accomplished in a single step. Solid sorbents offer the potential for elimination of the cooling requirement. Redox sulfur-conversion processes allow collection and conversion of sulfur components in a single process unit. The status of these two process types will now be described in greater detail.

Table 8.5-1. Examples of acid-gas removal and sulfur-recovery processes.

Examples	Characteristics
Chemisorption Processes	
Alkanoamines MEA DEA DGA (Fluor) DIP (Shell)	Relatively low-pressure operation; rapid sorption (short towers); low H_2S/CO_2 selectivity; high utility requirements, low efficiency for organic sulfur; production of nonregenerables with COS
Alkaline salt solutions Carl Still (NH_4OH) Catacarb (K_2CO_3) Benfield (K_2CO_3) Alkazid (amino acids)	Low solvent costs; COS hydrolysis; gas-cooling is minimized; carbon steel construction is required; low solvent losses; operation at moderate pressures; low H_2S in the acid gas; formation of formates from CO; low H_2S/CO_2 selectivity (except alkazid)
Physical Absorption Processes	
Selexol (DMEPED) Rectisol (methanol) Fluor (propylene carbonate) Purisol (N-methyl pyrrollidine)	Minimum utility requirements; high H_2S/CO_2 selectivity; low corrosion; high operating pressures; relatively slower absorption (tall towers); HC losses; low COS absorption
Mixed Solvents	
Sulfinol (sulfolane and DIPA), Shell Amisol (methanol and DGA), Lurgi	Compromises between physical and chemisorption
Solid Sorbents	
Zinc oxide Molecular sieve Iron oxide Lime Activated C	Low outlet H_2S; high H_2S/CO_2 selectivity; removal of organic S species; low utility costs; low capacity; high ΔP; treatment of regeneration gases; sorbent costs
Zinc ferrite Solid supported molten salts	High-temperature operation; developmental
In-bed sulfur capture	Low-cost sorbents required; waste-disposal considerations; ash-handling load increased
Sulfur Conversion	
Claus	High-purity sulfur product; low-pressure operation; high exit-sulfur concentration; requires high inlet-sulfur concentration; ammonia combustion problems
Sulfur Redox Stretford/Lo-Cat Thylox	Single AGR/S recovery process step; high H_2S efficiency; high H_2S/CO_2 selectivity; wide tolerance of inlet H_2S level; low COS and organic sulfur efficiency; complex process chemistry and control; solvent degradation and disposal; sulfur contamination

8.5-1. Solid Sorbents and In-Bed Desulfurization

The fundamental reactions involved in the removal of gas-phase sulfur with solid-sorbent reactors and the absorption of sulfur from coal by using solid additives in the gasification reactor are essentially the same.

Although operating conditions in terms of temperature, pressure and gas composition are somewhat different, similarities are nevertheless sufficiently great to allow a combined discussion. The reaction of reduced sulfur compounds, particularly H_2S, with oxides of metals and alkali metals has been utilized for decades to desulfurize process gases. Common absorbents are oxides of Fe, Zn, Ca and Mg or carbonates of calcium and/or magnesium (limestone or dolomite). In most previous applications, the sulfurized solid was disposed of after complete reaction. In some cases, the reactions are reversible, thus allowing reuse of the sorbent until physical degradation requires replacement.

Recent research supported by DoE[4] has demonstrated that mixed oxides of Zn and Fe (zinc ferrites) are effective sorbents of reduced sulfur compounds at temperatures which allow elimination of much of the cooling of gasification-product gas. These sorbents have been regenerated through contact with air and steam to allow reuse of the sorbent materials. Product gas at 800-1200°F and 4000-9000 ppm sulfur may be cleaned to levels containing 2-4 ppm sulfur. The sulfurized solid sorbent may then be regenerated with with air and steam at less than 1500°F, thus producing an exhaust stream of steam, sulfur dioxide and nitrogen. Advantages of the zinc ferrite sorbent process are: (i) extremely high sulfur capture by removing H_2S, COS and CS_2; (ii) operating temperatures applicable to gas-turbine systems; (iii) a dry, inexpensive, regenerable sorbent material: (iv) sharp reaction profiles, allowing for reactor-design flexibility; (v) reasonable operating pressure drops; and (vi) sorbent resistant to sintering because of the high melting points of zinc oxide/sulfide compounds.

The process has been tested on side-streams of product gases from both fixed- and fluidized-bed gasifiers. The results of these tests have shown the capability of reducing the sulfur contents, while demonstrating regenerability through multiple absorption-regeneration cycles. Current plans are to evaluate the process at the pilot scale through operation at a fluidized bed gasification-pilot facility. Remaining uncertainties for the process include: (i)sorbent durability; (ii) solid phase equilibrium boundaries; (iii) solid sulfate formation during regeneration; (iv) zinc evaporation; (v) sorbent structural changes; (vi) treatment or disposal of regeneration exhaust gases; (vii) control of product gas ammonia content; and (viii) process economics.